Stony Brook University

Mitigation of Bone Loss and Augment of Anabolic Adaptation by Physiological Dynamic Fluid Flow Stimulation

A Dissertation Presented

by

Minyi Hu

to

The Graduate School

in Partial Fulfillment of the

Requirements

for the Degree of

Doctor of Philosophy

in

Physiology and Biophysics

Stony Brook University

December 2012

Stony Brook University

The Graduate School

Minyi Hu

We, the dissertation committee for the above candidate for the

Doctor of Philosophy degree, hereby recommend

acceptance of this dissertation.

Yi-Xian Qin – Dissertation Advisor
Professor, Department of Biomedical Engineering,
Department of Physiology and Biophysics

Thomas W. White - Chairperson of Defense
Professor, Department of Physiology and Biophysics

Raafat El-Maghrabi
Research Associate Professor, Department of Physiology and Biophysics

Hui (Herb) B. Sun – External Member
Associate Professor, Department of Orthopaedic Surgery and Radiation Oncology
Albert Einstein College of Medicine/Montefiore Medical Center

This dissertation is accepted by the Graduate School

Charles Taber
Interim Dean of the Graduate School

Abstract of the Dissertation

Mitigation of Bone Loss and Augment of Anabolic Adaptation by Physiological Dynamic Fluid Flow Stimulation

by

Minyi Hu

Doctor of Philosophy

in

Physiology and Biophysics

Stony Brook University

December 2012

Novel modalities with strong translational potential to prevent osteoporosis are urgently called for, as osteoporosis strikes the society with high incidences of disease-related fractures and excessive medical costs. While bone fluid flow (BFF) regulates bone adaptation, intramedullary pressure (ImP) can initiate BFF and influence osteogenic signals. To establish the translational potential, a non-invasive intervention with direct ImP-coupled BFF can help develop new non-pharmaceutical treatments for osteopenia/osteoporosis.

The overall objective of this dissertation was to investigate the effects of a novel, non-invasive dynamic hydraulic stimulation (DHS) on skeletal regulatory responses at the tissue, cellular, and molecular levels. The global hypothesis was that DHS mediates ImP-induced regulation of BFF and promotes osteogenic adaptation, which in turn mitigates bone deterioration under disuse condition. This hypothesis was tested with four specific aims: 1) to investigate the ability of DHS to induce ImP with minimal bone strain as a loading dependence matter, and to determine the optimized DHS in bone, 2) to evaluate the effects of optimized DHS

on skeletal tissue adaptation under functional disuse condition, 3) to evaluate the effects of optimized DHS on bone marrow mesenchymal stem cell (MSC) population, 4) to elucidate the alterations of the gene expressions of osteogenic growth factors and transcription factors in response to DHS.

Immediate ImP induction was observed in the *in vivo* rat tibiae in response to DHS. Induced ImP (peak-to-peak) values were in a nonlinear fashion over the loading frequencies (1~10 Hz), which peaked at 2 Hz. Oscillatory DHS at various loading frequencies generated minimal bone strain. Furthermore, trabecular bone quantities and microstructural properties, as well as dynamic remodeling processes of the loaded tibiae in hindlimb suspended rats were evaluated using μCT and histomorphometry analyses. Significant improvements by oscillatory DHS on trabecular bone structural properties and bone formation indices were shown. These data strongly suggest that oscillatory DHS may regulate the tissue fluid dynamics, which serves critically in bone adaptation. Finally, longitudinal evaluations of bone marrow MSC population and osteogenic gene expressions demonstrated the effects of DHS on bone at the cellular and molecular levels, as well as their contributions to mitigate phenotypic disuse bone loss. These results clearly imply the ability of DHS as an effective, non-invasive intervention for potential osteopenia and osteoporosis treatments.

Table of Contents

Abstract……...……iii

Table of Contents……v

List of Figures……...viii

List of Tables……..……..xiv

List of Abbreviations…….xv

Chapter 1 – Introduction and Background…….……..…1

1.1. Research Significance…..……..2

1.2. Skeletal Physiology.……...….……..3

Skeletal Functions and Bone Anatomy……3

Bone Remodeling…….5

Blood Circulation in Bone……...6

1.3. Pathology of Disuse Osteoporosis ……..**.....**7

1.4. Hindlimb Suspension as a Functional Disuse Model……...8

1.5. Mechanical Loading as a Countermeasure for Osteoporosis……9

1.6. Bone Fluid flow as a Mediator for Skeletal Adaptation…….10

1.7. Mesenchymal Stem Cell and Skeletal Phenotype Biasing…….**.....**12

1.8. Load-induced Gene Expressions of Growth Factors and Transcription Factors…**....**13

1.9. Summary……..……**...**15

Chapter 2 - Hypothesis and Specific Aims……....17

Chapter 3 – The Ability of Oscillatory Dynamic Hydraulic Stimulation to Induce Intramedullary Pressure with Minimal Bone Strain…..**...**……21

Abstract……..22

Introduction……23

Materials and Methods……...25

Results……27

Discussion……..28

Figures……...……32

Chapter 4 – The Effects of Dynamic Hydraulic Stimulation on Mitigation of Trabecular Bone Loss in a Rat Functional Disuse Model…….....35

Abstract……..36

Introduction……37

Materials and Methods……...40

Results……43

Discussion……..44

Figures and Tables……50

Chapter 5 – The Effects of Dynamic Hydraulic Stimulation on Bone Marrow Mesenchymal Stem Cell Population……...58

Abstract……..59

Introduction……60

Materials and Methods…….....62

Results……64

Discussion……..65

Figures…….....……69

Chapter 6 – The Alterations of the Gene Expressions of Osteogenic Growth Factors and Transcription Factors in Response to Dynamic Hydraulic Stimulation…..……..74

Abstract……..75

Introduction……76

Materials and Methods…….....78

Results…….....81

Discussion……..……82

Figures…….....87

Chapter 7 - Overall Discussion……...……..….92

References……...……..……..……101

List of Figures

Figure 1.1……4

Basic bone anatomy of a long bone. A long bone is composed of cortical bone and trabecular bone. It can be regionally divided into epiphysis, metaphysis, and diaphysis. Each individual bone tissue unit is called osteon [1], (image adapted from [2]).

Figure 1.2……5

Bone remodeling cycle. The remodeling cycle of bone is composed of sequential phases including the activation of precursor cells, bone resorption by osteoclasts, bone formation by osteoblasts after reversal, and mineralization. The osteoblasts that are buried within the newly formed matrix become osteocytes. Other osteoblasts that rest on the bone surface become bone lining cells [3], (image adapted from [4, 5]).

Figure 1.3……..11

Bone fluid flow (BFF) mechanism. Image showing the lacunarcanalicular system within bone forms an extensive interconnected fluid network. Upon cyclic mechanical loading, interstitial fluid drains from the lacunarcanalicular system into and out of the vascular porosity [6], (image adapted from [7]).

Figure 1.4……..12

Muscle pump theory. Muscle contraction compresses the blood vessels in skeletal muscles, which generates a vessel pressure gradient that leads to increased hydraulic pressure in the capillary bed and amplified capillary filtration in bone [8-10]. Increased vessel pressure can directly increase the ImP that further drives BFF [11].

Figure 1.5……..15

Mechanical stimulation activates intracellular signaling pathways that converge with growth factors to activate transcription factors, which promotes bone formation (image adapted from [111]).

Figure 3.1……..32

Surgical setup. For the ImP measurements, a micro-cardiovascular pressure transducer was inserted into each of the tibial and femoral bone marrow cavities. For bone strain measurements, a single element strain gauge was firmly attached to the flat surface of each of the same tibia and femur over the mid-diaphyseal regions. Simultaneous ImP and bone strain were then measured in the operated tibia and femur under DHS on the tibia.

Figure 3.2……..33

Representative traces of ImP measurements from DHS-loading at various frequencies over time. (A) Representative traces of ImP measurements – raw data. (B) Fast Fourier Transform (FFT) analysis of the ImP measurements.

Figure 3.3……..34

Graph shows mean±SD values of the tibial ImP measurements. ImP in the tibia increased significantly with DHS loading frequencies of 1.5 Hz, 2 Hz, 2.5 Hz, 3 Hz, 3.5 Hz, 4 Hz, and 5 Hz. In the loading frequency spectrum from 0.5 Hz to 10 Hz, a maximal ImP of 14.48±3.10 mmHg was observed at 2 Hz, which was around 7 folds higher than at 0.5 Hz (1.98±1.57 mmHg). [a] $p<0.01$ vs. baseline ImP; [b] $p<0.05$ vs. baseline ImP.

Figure 4.1……..50

Experimental setup. DHS is achieved through a costumer design inflatable cuff. The stimulation cuff is connected to an oscillatory actuator-driven syringe, a force-controlled syringe, and a pressure sensor.

Figure 4.2……..51

Representative 3D μCT images of proximal tibial trabecular bone. The proximal metaphysis of the tibiae were scanned for trabecular bone morphology using a high resolution μCT scanner with a spatial resolution of 30 μm. A 1500 μm region of trabeculae was analyzed in the proximal metaphysis, starting from 1800 μm distal to the growth plate.

Figure 4.3……..52

Graphs show mean±SD values for bone volume fraction (BV/TV, %). DHS at 2 Hz produced a significant change, compared with values obtained in 4-week HLS. *p<0.05; ***p<0.001.

Figure 4.4……..53

Graphs show mean±SD values for connectivity density (Conn.D, 1/mm^3). DHS at 2 Hz produced a significant change, compared with values obtained in 4-week HLS. *p<0.05; **p<0.01; ***p<0.001.

Figure 4.5……..54

Graphs show mean±SD values for trabecular number (Tb.N, 1/mm). DHS at 2 Hz produced a significant change, compared with values obtained in 4-week HLS. *p<0.05; **p<0.01.

Figure 4.6……..55

Graphs show mean±SD values for separation (Tb.Sp, mm). DHS at 2 Hz produced a significant change, compared with values obtained in 4-week HLS. *p<0.05; ** p<0.01.

Figure 4.7……..57

Representative 2D images of calcein (green) labeled trabecular bone histomorphometry in the proximal metaphyseal region of the tibia. The calcein (green marker) labeled the mineralizing bone surfaces. Trabecular bone formation was clearly indicated by the double calcein labels in the HLS+DHS group.

Figure 5.1……..69

Bone marrow MSC population – day 3. Graphs show mean±SD. HLS reduced the total MSC number in the bone marrow, although it was not statistically significant ($p>0.05$). At this stage, DHS did not have any effect on the bone marrow MSC population under disuse condition.

Figure 5.2……..70

Bone marrow MSC population – day 7. Graphs show mean±SD. HLS significantly reduced the total bone marrow MSCs compared to age-matched control ($p<0.01$). By this day, DHS started to elevate the MSC number within the bone marrow ($p>0.05$). *$p<0.05$ vs. age-matched; **$p<0.01$ vs. age-matched.

Figure 5.3……..71

Bone marrow MSC population – day 14. Graphs show mean±SD. HLS greatly reduced the bone marrow MSCs compared to age-matched control ($p>0.05$). The increase of MSC number of the DHS-treated group became more apparent compared to HLS ($p>0.05$).

Figure 5.4……..72

Bone marrow MSC population – day 21. Graphs show mean±SD. HLS continued to reduce the bone marrow MSC number ($p<0.001$). The previous elevated bone marrow MSC number by DHS in conjunction with HLS was diminished. Significant reduction of the MSCs within the

bone marrow was again observed in the DHS-treated group compared to age-matched control (p<0.001). ***p<0.001 vs. age-matched.

Figure 5.5……..73

Summary of bone marrow MSC numbers of age-matched, HLS and HLS+DHS groups over 3 days, 7 days, 14 days, and 21 days. Normalized to age-matched, MSC numbers of HLS and HLS+DHS groups had similar trends of reductions, which the MSC numbers were greatly reduced by day 7, peaked on day 14, and diminished by 21 days. Compared to HLS, the induction of the MSC number in response to DHS gradually increased between 7 to 14 days. [a]p<0.01 vs. HLS – Day 3; [b]p<0.01 vs. HLS – Day 14; [c]p<0.001 vs. HLS – Day 3; [d]p<0.05 vs. HLS+DHS – Day 7; [e]p<0.01 vs. HLS+DHS – Day 3; [f]p<0.001 vs. HLS+DHS – Day 14.

Figure 6.1……..87

mRNA levels in the tibiae – day 3. Graphs show mean±SE. HLS greatly reduced the mRNA levels of all the selected genes compared to age-matched controls. The effect of DHS was not obvious, where the mRNA levels in the DHS-treated group were similar to the HLS group for most of the selected genes, except for runx2.

Figure 6.2……..88

mRNA levels in the tibiae – day 7. Graphs show mean±SE. The overall reductions of the mRNA levels in the HLS group compared to age-matched controls were lower than day-3's data. Interestingly, the mRNA levels of DHS-treated group of all the selected genes remained low. *p<0.05 vs. HLS.

Figure 6.3……..89

mRNA levels in the tibiae – day 14. Graphs show mean±SE. The selected genes in the DHS-treated group were greatly upregulated. For instance, the fold changes of the DHS-treated group

were 3.0 (runx2), 4.5 (β-catenin), 3.5 (osteopontin), 3.5 (VEGF), 3.7 (BMP2), 4.6 (IGF-1), and 3.2 (TGF-β).

Figure 6.4……..90

mRNA levels in the tibiae – day 21. Graphs show mean±SE. The elevated mRNA levels of the DHS-treated group were slightly less pronounced compared to day-14's data. Specifically, the DHS-driven fold changes were 1.2 (runx2), 2.4 (β-catenin), 1.8 (osteopontin), 1.9 (VEGF), 2.5 (BMP2), 2.2 (IGF-1), and 2.4 (TGF-β).

Figure 6.5……..91

Summary of mRNA fold changes of the selected osteogenesis-related genes over the 21-day time course. In general, the mRNA levels of the selected genes in the HLS groups attempted to catch up to the according age-matched levels. However, the mRNA levels of these genes in the HLS+DHS groups did not elevate until day 14.

List of Tables

Table 4.1……56

Proximal tibia metaphysic histomorphometry. Trabecular bone histomorphological analyses on age-matched control, HLS, HLS+static, and HLS+DHS. Values are mean±SD. BV/TV, bone volume/tissue volume; MS/BS, mineralized surface/bone surface; MAR, mineral apposition rate; BFR/BS, bone formation rate/bone surface. *p<0.05 vs. age-matched; $^{\#}p$<0.05 vs. HLS; **p<0.001 vs. age-matched; $^{\#\#}p$<0.001 vs. HLS; ^{a}p<0.05 vs. HLS+static.

List of Abbreviations

BFF	Bone Fluid Flow
BFR	Bone Formation Rate
BMD	Bone Mineral Density
BMP-2	Bone Morphogenetic Protein-2
BV/TV	Bone Volume Fraction
BV/TV-Histo	Histomorphometric Bone Volume Fraction
Conn.D	Connectivity Density
DHS	Dynamic Hydraulic Stimulation
DXA	Dual-energy X-ray Absorptiometry
FFT	Fast Fourier Transform
HLS	Hindlimb Suspension
HSC	Hematopoetic Stem Cell
IGF	Insulin-like Growth Factor
ImP	Intramedullary Pressure
MAR	Mineral Apposition Rate
MS	Muscle Stimulation
MS/BS	Mineralizing Surface/Bone Surface
MSC	Mesenchymal Stem Cell
SCI	Spinal Cord Injury
Tb.N	Trabecular Number
Tb.Sp	Trabecular Spacing
Tb.Th	Trabecular Thickness
TGF-β	Transforming Growth Factor-β
VEGF	Vascular Endothelial Growth Factor

Chapter 1 – Introduction and Background

1.1. Research Significance

Osteoporosis is a bone disease characterized by low bone mass and microstructural deterioration of the skeleton, leading to weaker bones with higher risks of chronic and traumatic fractures [12]. As a major public health problem, osteoporosis affects over 200 million people worldwide, in which 44 million of these are Americans [13, 14]. The occurrence of osteoporosis is expected to continue rising with the increasing elderly population [14]. Subsequent health complications associated with the physiological and/or pathophysiological changes in the skeleton, such as increased risks of falls and fractures, often require long-term recovery. Osteoporosis-associated fractures have been estimated for approximately 1.5 million incidences annually within the United States. Key skeletal sites that are susceptible to fractures include the hip, spine, wrist, and other limb sites [15]. The increased fracture risks further lead to morbidity and mortality of the affected individuals, which greatly reduce their quality of life. Moreover, these associated complications of osteoporosis impact the society with a substantial financial burden, primarily from health services including hospitalization and nursing home duties [14, 16]. In the United States, these direct medical costs are estimated at 17 ~ 20 billion dollars each year and continue increasing [17].

Daily physical activities rely on the quantity and quality of bone. Physical exercise is essential for the maintenance and enhancement of bone mass and strength [18]. On the other hand, functional disuse causes bone loss and has been classified as secondary osteoporosis [19]. Common targets of disuse osteoporosis include patients subjected to prolonged immobility or bed-rest (e.g., due to spinal cord injury), as well as astronauts who participate in long-duration spaceflight missions [19]. Detailed mechanisms of the etiology, pathophysiology and the resulting pathology of disuse osteoporosis are not fully understood [19]. The currently state-of-

the-art diagnostic technique for osteoporosis is to use dual-energy x-ray absorptiometry (DXA) to measure bone mineral density (BMD) before the first fracture occurs. Results of DXA BMD usually present standardized values such as T-scores. Based on the classification by the World Health Organization of BMD, a T-score of -2.5 or less is defined as osteoporosis while a T-score between -1.0 and -2.5 is defined as osteopenia [20]. Osteopenia is an earlier stage of bone loss progression towards osteoporosis [21, 22]. To develop preventative methods for osteoporosis, animal models with osteopenia have been used in many *in vivo* studies. Current treatments for osteoporosis include anti-resorptive and anabolic pharmacological agents. However, pharmacological interventions often require high costs and long-duration therapies, and easily give rise to adverse side effects [23]. On the other hand, non-pharmacological mechanical interventions provide a non-invasive alternate approach toward such disease to initiate and regulate the remodeling process of skeletal tissue [24-27]. Based on the benefits of mechanical loading as a primary natural factor for bone strength, it provides an insightful strategy to develop novel modalities with strong translational potential to prevent osteoporosis.

1.2. Skeletal Physiology

Skeletal Functions and Bone Anatomy

The primary functions of the skeleton are to provide structural support for the rest of the body and to protect internal organs. A variety of other functions include assisting locomotion and movements, maintaining homeostasis and acid-base balance, as well as providing the environment for growth factors, cytokines, and hematopoiesis [1].

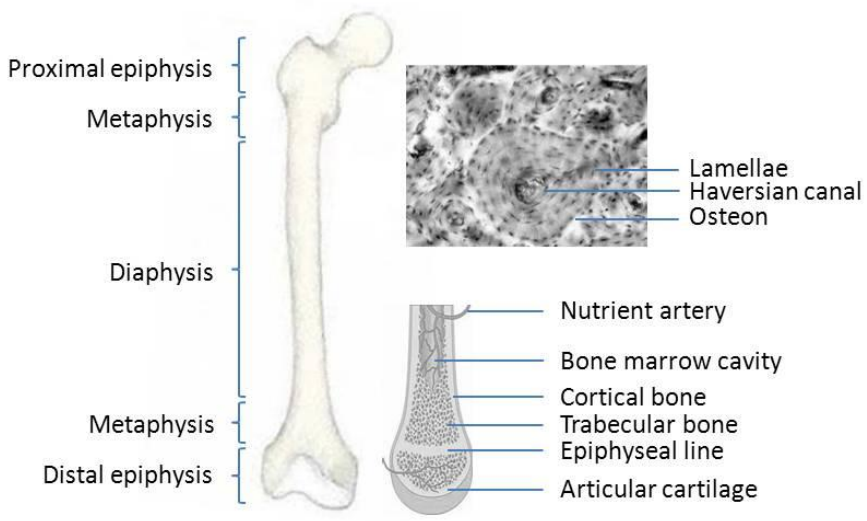

Figure 1.1. Basic bone anatomy of a long bone. A long bone is composed of cortical bone and trabecular bone. It can be regionally divided into epiphysis, metaphysis, and diaphysis. Each individual bone tissue unit is called osteon [1], (image adapted from [2]).

Using a long bone as an example, a long bone is regionally divided into epiphysis, metaphysis, and diaphysis (Figure 1.1). There are two types of bone tissues, cortical (compact) bone and trabecular (cancellous) bone, where cortical bone is dense and solid while trabecular bone is a spongy-like network of trabeculae. Cortical bone surrounds the bone marrow cavity space, and trabecular bone intersperses in the marrow compartment and constitutes the metaphyseal and epiphyseal regions [1]. Osteons are individual bone units in both cortical and trabecular bone. Cortical osteons, referred as Haversian systems, are cylindrical structured, and their walls are made of concentric lamellae. Trabecular osteons are shaped of semilunar and composed of concentric lamellae. A lamellar pattern is normally seen in the formation of cortical bone and trabecular bone, in which collagen fibrils are oriented alternatively as they are laid down. The cortical bone's outer-most layer is called periosteum and its inner-most layer is called endosteum. The periosteal surface is mainly active for appositional growth and fracture repair, whereas the endosteal surface has a higher remodeling activity [1]. At the tissue level, cortical

bone and trabecular bone modify their structure in response to hormonal influences, mechanical stimuli, immobilization, etc. [28-32]. Bone adapts its external shape and internal structure in responds to functional demands and mechanical loading [33]. Thus, understanding the skeletal biology and the mechanically regulated bone adaptation becomes an interesting research focus.

Bone Remodeling

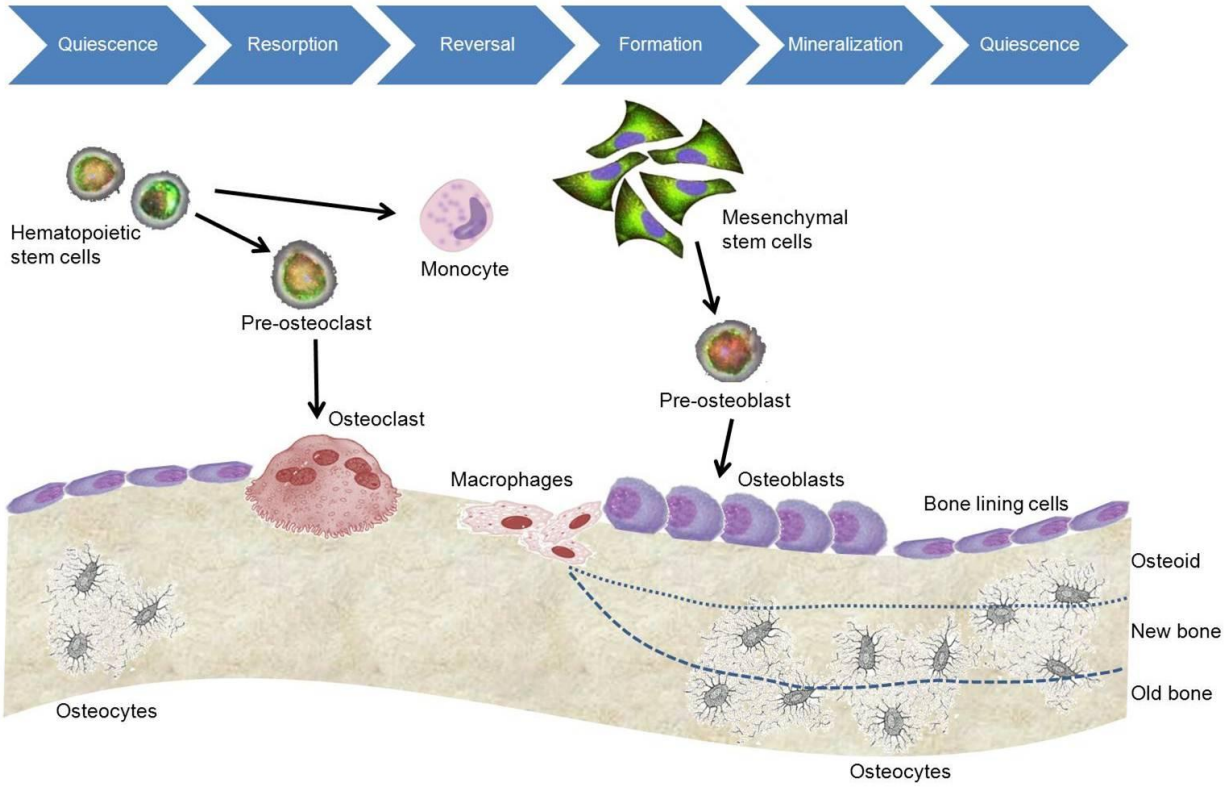

Figure 1.2. Bone remodeling cycle. The remodeling cycle of bone is composed of sequential phases including the activation of precursor cells, bone resorption by osteoclasts, bone formation by osteoblasts after reversal, and mineralization. The osteoblasts that are buried within the newly formed matrix become osteocytes. Other osteoblasts that rest on the bone surface become bone lining cells [3], (image adapted from [4, 5]).

Throughout one's lifetime, bone remodeling is the process by which bone is renewed to maintain bone strength and mineral homeostasis. Through the balanced functions of various types of bone cells (osteoblasts and osteoclasts), the bone remodeling process erodes old bone, followed by the replacement of newly synthesized matrix and subsequent mineralization to form

new bone. This process ensures the prevention of bone microdamage accumulation. The sequential phases composing the remodeling cycle include the activation of precursor cells, bone resorption by osteoclasts, bone formation by osteoblasts after reversal, and mineralization (Figure 1.2). The osteoblasts that are surrounded and buried within the matrix become osteocytes, which are the most abundant cell type in bone and have been suggested as bone mechanical sensors [3].

Blood Circulation in Bone

Blood supply to bone is essential to maintain bone health. The first recognized function of the skeletal vascular system is to provide nutrients to bone and marrow, and to remove wastes from these sites. Disruption of blood circulation in bone, e.g., due to skeletal injuries, can interfere the normal healing process in bone tissue [9]. Knowledge of the distribution of blood supply in bone can help us better understand its role in bone physiology. Similar characteristics of the vasculature organization have been observed in all bones, including a centrally located nutrient artery followed by small nutrient arteries in the periphery, a capillary bed within the bone tissue, and profuse sinusoids in the marrow [34]. There are three basic blood supplies in the long bones: the nutrient vessels, the metaphyseal and epiphyseal vessels, and the periosteal vessels [35]. As the main blood supply in the diaphysis, the nutrient artery penetrates the cortex and branches toward opposite directions along the cortex within the marrow cavity, becoming medullary arteries. A centrifugal flow goes through the cortical bone, allowing exchange vessels within the Haversian canals drain to venules on the periosteum. This functionally important vascular organization may contribute to the intramedullary pressure-mediated interstitial fluid movement in bone [34].

Recent research has pointed out the key relationship between angiogenesis and osteogenesis. Some of which have argued that the endothelial cells within the bone vasculature network should be included into the study of the bone-cell communication network as well as their involvement in bone formation and bone resorption coupling [36, 37]. In particular, cell diffusion studies in rats have indicated the positive effects of endothelial cells and calvarial cells on mineralization and alkaline phosphatase activity [38]. Cell-culture studies have demonstrated that vascular endothelial growth factor plays a critical role in controlling mineralization during endochondral bone formation [39].

1.3. Pathology of Disuse Osteoporosis

The removal of mechanical loading generates skeletal decrements, resulting disuse osteoporosis [19]. Immobilizations and the reduction of ground forces reaction are severe outcomes of paralysis caused by spinal cord injury (SCI), which can lead to atrophic responses in the skeleton [40]. Significantly higher incidences of post-injury fractures are often seen in SCI patients [41, 42]. As indicated in quantitative bone structural measurements of SCI patients, their overall bone quantities were decreased exponentially over time after the injury. The study demonstrated that between 2 months to 50 years of paralysis, SCI led to 25~35% of decreases in mean cortical thickness in tibial and femoral diaphysis at steady state compared to the mobilization controls [43]. Decreases of 25% and 31%, respectively to these regions, were observed in the section moduli due to the thinner cortical bone. Results from another study using peripheral quantitative computed tomography also showed a 14~16% of lower mean trabecular density and a 7% decrease of average cortical density in the tibia 1 year after SCI [44]. SCI-induced osteopenia and/or osteoporosis can lead to a higher frequency of fractures, by up to 34%

[41, 45-47]. Similarly, exposure to microgravity also results in bone loss due to reduced weight-bearing and ground reaction forces [19]. A reduction of 1~2% bone mass per month in microgravity occurs in astronauts and results in osteopenia [48, 49]. Analysis from 6-month space missions showed an average loss of total bone mass of approximately 11% in the proximal femur region, in which trabecular bone mass and density declined by 14.4~16.5% [50]. Cortical density in the femur and tibia was decreased by about 2% after 6 months of spaceflight; whereas about 5% and 12% of the trabecular density was reduced in distal tibia and proximal femur, respectively [49, 51]. The quantitative bone losses in humans subjected to SCI and microgravity are comparable, yet different mechanisms may be involved [19]. Site-specific bone mass may be restored upon re-loading but complete return to normal quantity and quality may not be achieved [49, 52, 53]. Furthermore, observations in postmenopausal women with fractures showed altered cortical and trabecular architecture. Decreases by 12% and 19% in cortical thickness and trabecular bone volume fraction were measured respectively. Therefore, effective interventions are continuously being developed to investigate the underlying mechanisms and potential treatments for disuse osteoporosis.

1.4. Hindlimb Suspension as a Functional Disuse Model

Hindlimb suspension rodent models were first designed by NASA to mimic the response of bone to microgravity [54, 55]. It is a well-developed disuse model, where animal hindlimbs are unloaded for the duration of the study, eliminating weight-bearing, ground reaction forces, and muscle contractions during locomotion. Skeletal adaptive outcomes from hindlimb suspension are comparable to the exposure to microgravity. Reduced trabecular number and thickness, bone mineral density, and increased bone resorption occurred in rodents on Cosmos

spaceflights over 14~40 days [56-58], while ground-based hindlimb suspended rodents included as controls showed to coincide with the atrophic changes in bone [59]. Site-specific bone loss of hindlimb suspended rodents is similar to human after space missions, which the bone loss was mainly in the metaphysis and epiphysis regions of the lower extremities [52, 60]. Up to 20% of reduced trabecular BMD in the femoral neck and proximal tibia resulted from the hindlimb suspension treatment on skeletally mature adult rats [61, 62]. Two weeks of hindlimb suspension in adult female rats showed a 15% decrease in bone volume fraction (BV/TV), a 2.3% decrease in trabecular number (Tb.N), a 22% decrease in connectivity density (Conn.D), and a 5% decrease in trabecular thickness (Tb.Th). Hindlimb suspension also negatively affected the cellular activities in bone [63]. Other studies of histomorphometric analyses in hindlimb suspension experiments demonstrated decreases of 34% [64], 65~88% [62, 65], and 19% [61], in the tibio-fibular junction, on the periosteal surface of the tibial mid-diaphysis, and on the metaphyseal trabecular bone surface in the distal femur, respectively.

1.5. Mechanical Loading as a Countermeasure for Osteoporosis

The importance of biomechanical signals to bone morphology and strength has long been recognized [18]. Bone adapts its external shape and internal microarchitecture in response to mechanical forces [33]. As a natural form of short and repetitive mechanical loading, exercise governs bone strength and reduces osteoporosis [18]. In particular, exercise leads to greater bone density and bone mineral contents in children, as well as maintenance of bone mass in adults. In converse, absence of weight-bearing activities or disuse of bone could reduce bone formation on periosteal surfaces, and increase bone turnover and resorption on endocortical and trabecular surfaces, which together lead to rapid bone loss [33]. The response of skeletal tissues to

mechanical stimuli depends on factors including the magnitude, duration, and rate of the stimuli. Dynamic or cyclic stimuli seem to be more anabolic to bone compared to static stimuli. Because bone cells will accommodate to routine loading, rest periods between cycles of mechanical loading should be inserted to restore bone's mechanosensitivity [18, 33].

Based on the benefits of mechanical loading as a primary natural factor for bone strength, various modalities have been designed as countermeasures for osteoporosis. Load-driven strain from *in vivo* four-point bending [66, 67] and axial loading [68-70] can lead to bone formation. Low-magnitude, high-frequency vibrations are also anabolic to both human [27] and animal [26] skeletons. Joint loading is a recently developed unique modality that has the effects of stimulating trabecular and cortical bone formations [71-74]. Previous *in vivo* studies from our group using dynamic electrical muscle stimulation (MS) demonstrated that muscle contractions can successfully mitigate bone loss in a rat hindlimb suspension model [75].

1.6. Bone Fluid Flow as a Mediator for Skeletal Adaptation

As a potent regulator in bone adaptation, bone interstitial fluid flow with altered velocity or pressure acts as a communication media between an external load and the bone cells, which then regulate bone remodeling (Figure 1.3) [76-81]. In converse, discontinuous fluid flow can initiate bone turnover and result in osteopenia [8, 9, 26, 82]. Physical signals such as intramedullary pressure (ImP) have been suggested to initiate bone fluid flow (BFF) and influence the osteogenic signals within bone [82]. Several studies have shown that intramedullary bone fluid flow alone, in the absence of mechanical strain, can initiate and regulate bone remodeling. Application of a direct ImP to an isolated turkey ulna without bone deformation was shown to increase bone formation in response to the applied pressure [82]. In a

recent study introducing a novel microfluidic system for generating dynamic ImP and BFF within the femurs of alert mice, osteogenic responses were induced [83].

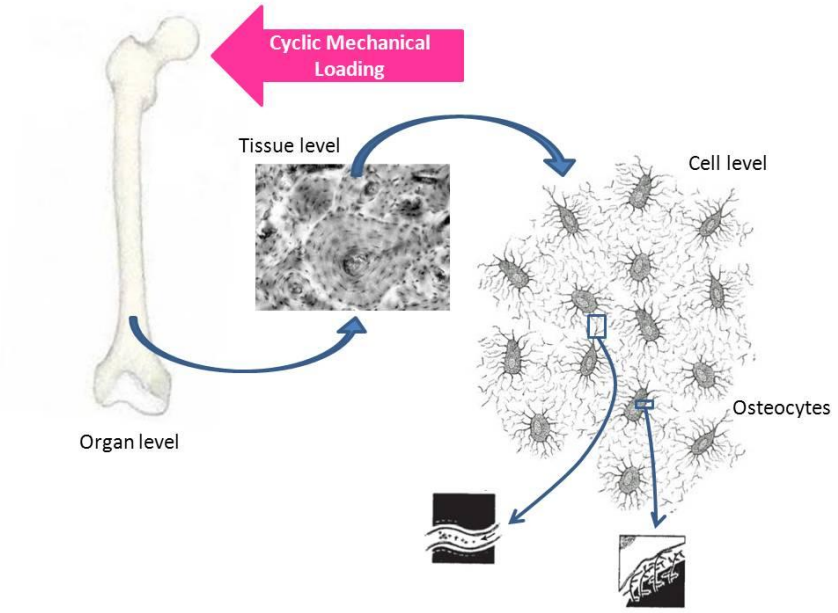

Figure 1.3. Bone fluid flow (BFF) mechanism. Image showing the lacunarcanalicular system within bone forms an extensive interconnected fluid network. Upon cyclic mechanical loading, interstitial fluid drains from the lacunarcanalicular system into and out of the vascular porosity [6], (image adapted from [7]).

ImP-induced BFF provides a great potential to develop novel mechanical stimuli as countermeasures for disuse bone loss. Previous *in vivo* study using dynamic electrical stimulation in a rat hindlimb suspension model demonstrated that dynamic muscle contraction can generate ImP to mitigate disuse osteopenia [75, 84]. Based on the muscle pump theory (Figure 1.4), it is thought that muscle contraction compresses the blood vessels in skeletal muscles, which generates an arteriovenous pressure gradient that further increases the hydraulic pressure in skeletal nutrient vessels and amplifies the capillary filtration in bone [8-10]. Increased vessel pressure can directly increase the ImP that further drives BFF [11]. In order to establish the translational potential of ImP based on the muscle pump theory, a novel and non-invasive method that directly couples an external load and internal BFF is a must.

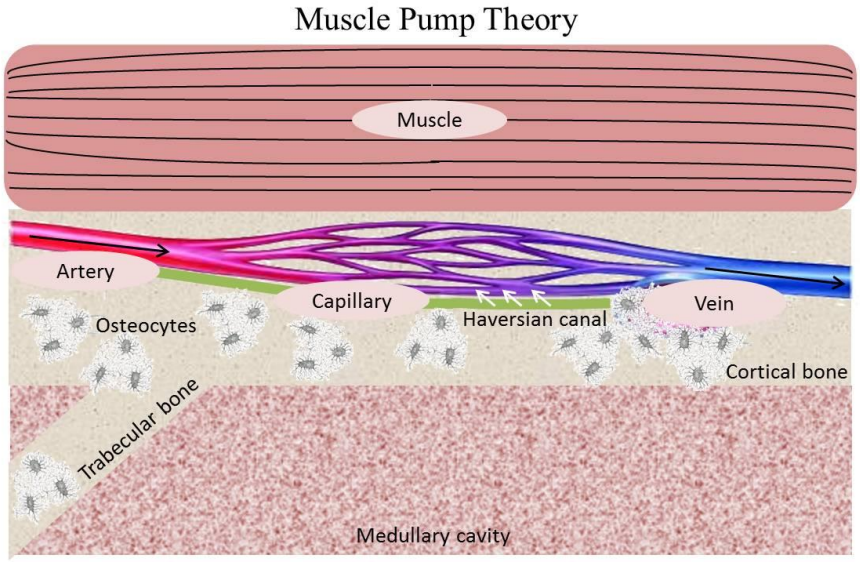

Figure 1.4. Muscle pump theory. Muscle contraction compresses the blood vessels in skeletal muscles, which generates a vessel pressure gradient that leads to increased hydraulic pressure in the capillary bed and amplified capillary filtration in bone [8-10]. Increased vessel pressure can directly increase the ImP that further drives BFF [11].

1.7. Mesenchymal Stem Cell and Skeletal Phenotype Biasing

Mesenchymal stem cells (MSCs) are pluripotent cells defined by their abilities of self-renewal and potential differentiations into cells that form tissues such as bone [85]. Osteoblasts are derived from MSCs, and bone formation begins with stem cell proliferation and condensation [86, 87]. Rather than targeting the resident bone cell population, new strategies for encountering osteoporosis have directed to the design to control the fate of MSCs for skeletal phenotype [88-91]. Pharmacological agents, e.g., statins, have been shown to increase bone marrow osteogenesis [92]. On the other hand, a great amount of published work has pointed out that external mechanical signals are able to regulate osteogenesis of MSCs. The ability of different types of macro-level mechanical loading (e.g., fluid flow, tension, compression, hydrostatic pressure, etc.) to alter the differentiation patterns of MSCs biasing toward osteogenesis and

chondrogenesis has been studied [87, 93]. Moreover, more complex 3D systems have been used by tissue engineers to explore the role of mechanical forces in MSC adhesion and differentiation, as well as the promotion of the growth of both bone and cartilage [94-100]. *In vivo* studies using mechanical stimulation, such as whole body vibration, have also demonstrated its effects on MSC proliferation and differentiation toward osteogenesis [101-103].

While mechanical signals direct MSCs toward osteoblastogenesis and are anabolic to bone, reduction in physical impacts on bone leads to adverse outcomes. *In vitro* simulated microgravity conditions, mimicking the reduced mechanical stress occurring in spaceflight and in hindlimb suspension, alter the differentiation-associated genes in osteoblast and preosteoblasts [104-108]. *Ex-vivo* studies of hindlimb suspension treatment in mice demonstrated a net consequence in suppressing the osteogenic gene expressions [108]. A similar study of hindlimb suspension treatment in rats showed that 28 days of hindlimb suspension negatively affected the growth potential of MSCs, but this adverse effect was removed upon recovery of normal gravity. Decreased osteogenic potential of MSCs was resulted from hindlimb suspension even under an *in vitro* osteogenic induction condition. Low levels of osteoblast gene markers were observed in the cells induced from the MSCs of the hindlimb suspended rats, which eventually led to a decrease of bone mass. However, re-exposure to normal gravity or centrifugal force was able to reverse such changes [109].

1.8. Load-induced Gene Expressions of Growth Factors and Transcription Factors

Mechanical stimulation plays an important role in the maintenance and enhancement of skeletal mass and strength. This functional process is performed through mechanotransduction, which requires the perception of extracellular stimuli and their conversion into downstream

intracellular biochemical responses. This in turn transmits load-induced signals to the nucleus, and then expresses osteogenic genes that further regulate bone metabolism [110-113]. Augmented mechanical stimulation gives rise to signals that directly activate molecular pathways, which in turn trigger the osteoblastic differentiation and proliferation, resulting in bone formation [114, 115]. A complex array of growth factors and mechanical cues that act via interconnected signaling networks, resulting in the activation of specific transcription factors and then their target genes, determines the coordinated function of skeletal cells [116].

Mechanical stimulation triggers bone regeneration through secretion of growth factors, including some of the most potent ones being the transforming growth factor-β (TGF-β), the insulin-like growth factors (IGFs), the bone morphogenetic protein-2 (BMP-2) [116, 117], and vascular endothelial growth factor (VEGF) [116, 118]. TGF-β is suggested to enhance proliferation of osteoprogenitor cells and osteoblasts during bone regeneration [117, 119]. IGFs are involved in marrow stromal cells-regulated osteoblast proliferation and osteoblastogenesis [117, 120]. BMP-2 has been shown to facilitate the differentiation of MSCs to osteochondroblastic lineage [119, 121]. VEGF is known to promote the differentiation of osteoblasts and increase the mineralization of regenerated bone [118].

Upon mechanical stimulation, intracellular signaling pathways are activated and then converge with growth factors to activate transcription factors that promote bone formation (Figure 1.5) [116]. Osteoblasts differentiate from committed osteoprogenitor cells from MSCs, which then express phenotypic osteoblastic genes once become mature and functional [122]. Runx2 is a principal transcription factor regulating osteoblast differentiation [123]. Other transcription factors downstream of runx2, such as β-catenin, contribute to the control of

osteoblastogenesis [124]. Osteopontin modulates both osteoblastic and osteoclastic functions in response to cytokines and mechanical signals [125].

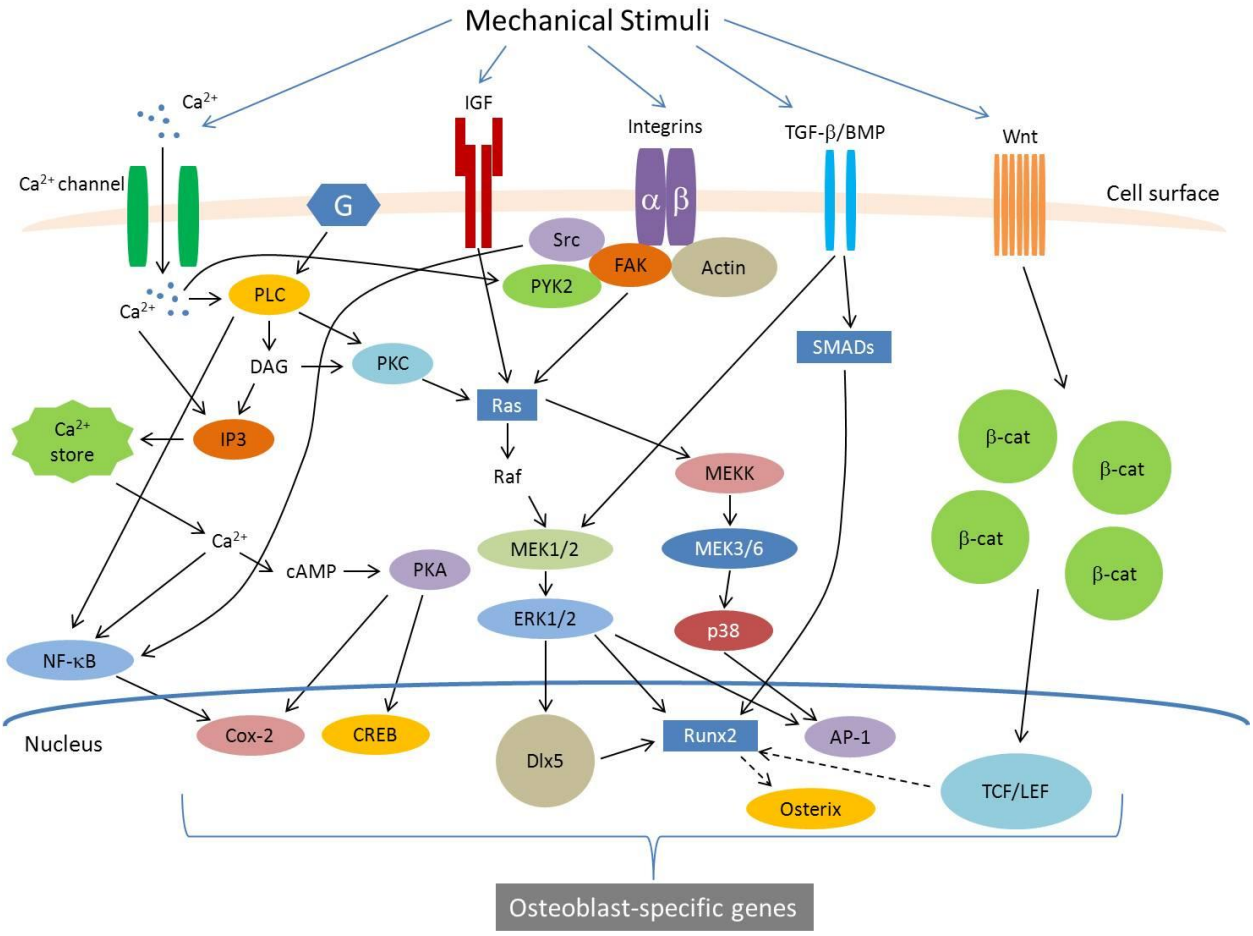

Figure 1.5. Mechanical stimulation activates intracellular signaling pathways that converge with growth factors to activate transcription factors, which promotes bone formation (image adapted from [111]).

1.9. Summary

Changes in the mechanical environment due to disuse, can lead to severe detrimental effects in bone. As osteoporosis strikes the society with high incidences of disease-related fractures and excessive medical costs, novel modalities with strong translational potential to

prevent osteoporosis are urgently called for. Due to the great anabolic potential of mechanical loading as a natural factor that plays a key role in maintaining bone strength, understanding the mechanisms of mechanical forces on skeletal adaptation is a major step in developing a better intervention for such condition. BFF has been demonstrated as a critical regulator in mechanotransductive signaling and bone adaptation. ImP is suggested to initiate BFF and influence the osteogenic signals within bone. In order to establish the translational potentials of ImP, a non-invasive intervention with direct BFF coupling is necessary to develop new non-pharmacological treatments for osteopenia/osteoporosis. While an in-depth knowledge is required to understand how mechanical signals are delivered to bone cells and how bone cells respond to such signals, it would be particularly attractive to utilize a novel tool to study the bone biomechanical regulations at the tissue, cellular, and molecular levels.

Chapter 2 - Hypothesis and Specific Aims

As a natural determinant, mechanical loading gives rise to strong anabolic potential in maintaining bone strength. Increasing fluid perfusion in the skeletal organization during cyclic mechanical loading has the potential to initiate skeletal responsive adaptation. Changes in the physiological and/or mechanical environments, e.g., exposure to microgravity, can influence skeletal mass and cellular functions. These alterations subsequently lead to associated health complications such as osteoporosis and osteopenia, which affect millions of individuals worldwide. In particular, disuse osteoporosis often occurs in elderly, long-term bed-rest patients (e.g., due to spinal cord injury), and astronauts who participate in long-duration spaceflight missions. Furthermore, osteoporosis-related fractures give rise to medical concerns and decreased life quality that critically affect the patients. Therefore, an effective intervention with clinically applicable potentials is in great need to treat disuse osteoporosis.

A growing number of evidence has pointed to bone fluid flow (BFF) as a critical regulator in mechanotransductive signaling and bone adaptation. Intramedullary pressure (ImP) is a key mediator for BFF initiation; and it can influence the osteogenic signals within bone. The potential ImP-induced BFF then triggers bone adaptation. Thus, a non-invasive intervention with direct ImP-coupled BFF stimulation serves great translational potentials to help develop new non-pharmacological treatments for osteopenia/osteoporosis. Moreover, if successful, the novel intervention can become a valuable tool to investigate the anabolic and/or anti-resportive potentials of ImP-induced BFF, including its role in regulating skeletal mechanotransductive mechanisms.

This dissertation introduces a novel, non-invasive dynamic hydraulic stimulation (DHS) as a potential countermeasure for osteoporotic bone loss. Its enhancement of ImP-coupled BFF to elicit skeletal adaptive responses was the main focus of this dissertation. DHS provides direct

external pressure compressions on the skeletal muscles, creating an arteriovenous pressure gradient to bone, which may increase ImP that further drives BFF. The effects of DHS on skeletal regulatory responses at the tissue, cellular and molecular levels were examined. Such stimulation was evaluated via four specific aims (S.A.) and the corresponding sub-hypotheses.

Hypothesis: DHS mediates ImP-induced regulation of BFF and promotes osteogenic adaptation, which in turn mitigates bone deterioration under disuse condition.

Objective: To investigate the effects of a novel, non-invasive DHS on skeletal regulatory responses at the tissue, cellular, and molecular levels.

S.A.1. To investigate the ability of DHS to induce ImP with minimal bone strain as a loading dependence matter, and to determine the optimized DHS in bone.

Sub-hypothesis 1. Oscillatory DHS induces ImP with minimal bone strain, which is frequency/rate dependent.

- Insert a micro-cardiovascular pressure transducer into the bone marrow cavity of the stimulated tibia of an experimental rat.
- Firmly attach a single element strain gauge onto the surface of the same tibia in the mid-diaphyseal region.
- Apply DHS over a range of frequencies, while measuring the ImP and bone strain simultaneously.

S.A.2. To evaluate the effects of optimized DHS on skeletal tissue adaptation under functional disuse condition.

Sub-hypothesis 2. BFF induced by DHS can regulate adaptive responses in skeletal tissue, inhibiting bone loss due to functional disuse.

- Apply DHS to the stimulated tibiae using a 4-week hindlimb suspension (HLS) rat model.
- Evaluate the trabecular bone quantities and the microstructural properties of the stimulated tibiae using μCT.
- Evaluate the dynamic remodeling processes of the trabecular bone tissue of the stimulated tibiae using fluorescent histomorphometric analysis.

S.A.3. To evaluate the effects of optimized DHS on bone marrow mesenchymal stem cell (MSC) population.

Sub-hypothesis 3. Bone marrow MSC quantity is enhanced in response to DHS, which may lead to further osteogenic activities.

- Apply DHS to the stimulated tibiae using a HLS rat model for a time course of 21 days.
- Extract bone marrow from the stimulated and control tibiae, and then isolate the MSCs using specific cell surface markers.
- Evaluate the MSC quantification using flow cytometry analysis.

S.A.4. To elucidate the alterations of the gene expressions of osteogenic growth factors and transcription factors in response to DHS.

Sub-hypothesis 4. DHS activates the gene expressions of osteogenic growth factors and transcription factors that are involved in mechanotransduction and bone metabolism.

- Apply DHS to the stimulated tibiae using a HLS rat model for a time course of 21 days.
- Isolate RNA from the stimulated tibiae.
- Evaluate the expressions of selected osteogenic genes using quantitative real time PCR.

Chapter 3 – The Ability of Oscillatory Dynamic Hydraulic Stimulation to Induce Intramedullary Pressure with Minimal Bone Strain

Abstract

Physical signals within bone, i.e., generated from mechanical loading, have the potential to initiate skeletal adaptation. In particular, strong evidence has pointed to bone fluid flow (BFF) as a communication media between an external load and bone cells, in which its changes in velocity and pressure can ultimately initiate and regulate the mechanotransductive signaling as well as the remodeling process within bone. Load-induced BFF can be altered by factors such as intramedullary pressure (ImP) and/or matrix deformation (bone strain), mediating bone adaptation under normal and disuse conditions. Several studies have shown that BFF altered by ImP alone, in the absence of bone strain, can drive bone remodeling. However, isolating the ImP factor from the bone strain factor using a non-invasive *in vivo* method still remains challenging. To apply ImP alterations as a means for regulating BFF, it was hypothesized that the recently developed non-invasive dynamic hydraulic stimulation (DHS) can induce local ImP with minimal bone strain to potentially elicit osteogenic adaptive responses. To test this hypothesis, we evaluated the immediate effects of oscillatory DHS on local and distant ImP and bone strain in response to a range of loading frequencies. Simultaneous femoral and tibial ImP and bone strain values were measured during DHS loading on the tibia with frequencies of 1 Hz to 10 Hz. Demonstrating in three 15-month-old female Sprague Dawley rats, oscillatory DHS showed noticeable effects on ImP induction in the stimulated tibia. The observed ImP (peak-to-peak) values were in a nonlinear fashion in response to DHS over the range of loading frequencies, which peaked at 2 Hz. Oscillatory DHS at various loading frequencies generated minimal bone strain in the tibiae. Maximal bone strain measured at all loading frequencies was less than 8 με. No detectable induction of ImP or bone strain was observed in the un-stimulated femur. Results from this study strongly suggest that oscillatory DHS may regulate the local environmental fluid

dynamics with minimal mechanical strain in bone, which serves critically in bone adaptation. These results clearly imply DHS's potential as an effective, non-invasive intervention for osteopenia and osteoporosis treatments.

Introduction

Aging or functional disuse of bone can subsequently create a number of physiological or pathophysiological changes in the skeletons of the affected subjects (e.g., elderly, long-term bed-rest patients, and astronauts who participate in long-duration spaceflight missions), leading to conditions such as osteopenia [19]. Studies of mechanobiology and novel modalities of mechanical loading have demonstrated their abilities in regulating bone strength [66, 67, 70-72, 74, 75, 126]. However, the underlying mechanotransductive mechanisms, namely, how mechanical signals are delivered to bone cells and how bone cells respond to such signals, remain unclear.

As a potent regulator in bone adaptation, bone fluid flow (BFF) with altered velocity or pressure acts as a communication media between an external load and bone cells, which then regulates bone remodeling [76-81]. In converse, discontinuous BFF can initiate bone turnover and result in osteopenia [8, 9, 26, 82]. Physical signals such as intramedullary pressure (ImP) have been suggested to initiate BFF and to influence the osteogenic signals within bone [82]. A few studies using surgical methods on animal models have shown that *in vivo* BFF can be altered by ImP without bone deformation; and ImP alone is sufficient to induce potent adaptive responses in bone. Qin et al. applied a direct ImP to an isolated turkey ulna without deforming the bone tissue and found increased bone formation in response to the applied pressure [82].

Similarly, a more recent study introduced a novel microfluidic system for generating dynamic ImP and BFF within the femurs of alert mice to induce osteogenic responses [83].

Therefore, ImP-induced BFF provides a great potential to develop novel mechanical stimuli as countermeasures for disuse bone loss. Previous *in vivo* study using oscillatory electrical muscle stimulation (MS) in a hindlimb suspension (HLS) functional disuse rat model has demonstrated that oscillatory MS-induced muscle contraction can generate ImP and bone strain to mitigate disuse osteopenia [75, 84]. However, to non-invasively isolate the ImP factor from the bone strain factor *in vivo* still remains challenging. Furthermore, in order to establish the translational potential of ImP, a novel and non-invasive method that directly couples an external load and internal BFF would be an attractive intervention. To reach this goal, our group has recently developed a novel, non-invasive dynamic hydraulic stimulation (DHS). Its promising effects on mitigating disuse bone loss have been shown via a 4-week rat HLS study followed by μCT and histomorphometry analyses [127]. The results indicated a great potential of DHS to become a novel countermeasure for osteoporosis/osteopenia.

Identifying the stimulation parameters within an optimal loading regimen, e.g., frequency, is important to maximize the effectiveness of the stimulation and to generate beneficial adaptive responses in bone. As an important determinant of bone adaptation to mechanical loading, loading frequency has been shown with a positive correlation to the improved bone quality in various studies [128-130]. Interestingly, effective loading frequencies seem to differ among various loading modalities [69, 74, 128, 129]. Whole-body vibrations are known to be more effective at high frequencies (>30 Hz). On the other hand, an ulna axial loading study in mice reported a higher effect at lower loading frequencies (5 Hz and 10 Hz) as opposed to higher frequencies (20 Hz or 30 Hz) [69]. Related to ImP and BFF loading theory,

relatively lower frequencies (5 Hz and 10 Hz) were reported to be more effective in bone adaptation in the femur [83] and tibia [74], respectively.

To test the hypothesis that non-invasive oscillatory DHS can induce local ImP with minimal strain to potentially elicit osteogenic adaptive responses, the objective of this study was to evaluate the immediate effects on femoral and tibial ImP and bone strain induced by oscillatory DHS over the tibia within a broad range of loading frequencies.

Materials and Methods

Animals

All surgical and experimental procedures were approved by the Institutional Animal Care and Use Committee (IACUC) at Stony Brook University. Surgical experiments were performed on three 15-month old female Sprague Dawley virgin rats (Charles River, MA; body mass 426±36 g) to measure the ImP and bone strain simultaneously during DHS loading.

ImP Measurements

Each animal was anesthetized through standard isoflurane inhalation. An approximately 1 cm incision was made in the anterior knee region of the animal's right leg to expose the distal femur and proximal tibia. From the distal end of the femur and the proximal end of the tibia, a 1 mm hole was carefully drilled into each of the right femoral and tibial bone marrow cavities, respectively. Guided by a 16-gauge catheter, a micro-cardiovascular pressure transducer (Millar Instruments, SPR-524, Houston, TX) was inserted into each of the femoral and tibial bone marrow cavities (Figure 3.1). The catheter and the pressure transducer apparatus were sealed tightly within the drilled holes.

Bone Strain Measurements

Similar to the above surgical procedures, a 2 cm incision was made on the anterior side of the right tibia and the lateral side of the right femur. A linear single element strain gauge (120Ω, factor 2.06, Kenkyojo Co., Tokyo) was firmly attached to the flat surface of each of the same tibia and femur within the mid-diaphyseal regions (Figure 3.1). The exposed muscles underwent minimal disruption, and the open skin was sutured before applying DHS.

DHS Loading

DHS was achieved through a costume-made inflatable cuff placed around the right tibia, with the similar setup in our recently published study [127]. Briefly, the inflation and deflation of the cuff was driven by a syringe pump with the loading magnitudes and frequencies delivered by a programmable waveform/signal generator (HP33120A, Hewlett-Packard, Palo Alto, CA). A pressure sensor was included to monitor the stimulation amplitudes throughout the entire stimulation process. The pressure stimulation was achieved by 40 mmHg static pressure + the peak-to-peak dynamic pressures given by the function generator that was set at 1.5 V of constant voltage. To start the experiment, DHS was applied to the operated tibia by placing the stimulation cuff around the mid-tibial region and loaded at frequencies of 0.5 Hz, 1 Hz, 1.5 Hz, 2 Hz, 2.5 Hz, 3 Hz, 3.5 Hz, 4 Hz, 5 Hz, 6 Hz, 7 Hz, 8 Hz, 9 Hz, and 10 Hz. Measurements of ImP and bone strain values of the stimulated right tibia and un-stimulated right femur were recorded simultaneously using a strain gauge amplifier (National Instrument). For each animal, the entire frequency spectrum was repeated for at least three times.

Fast Fourier Transform (FFT) Analysis

Each run of data recording was put through a FFT analysis using Matlab. The random noise was removed by zeroing any values in each power spectrum that were below a threshold.

This threshold was defined as the middle point between the lowest peak of the signal and the average of the random noise. Once the noise was removed, each frequency step was analyzed individually. Each step was divided into twenty intervals. The difference between the maximum and minimum values was calculated and averaged over all intervals for that particular frequency step. This was taken as the peak-to-peak value for the according loading frequency (Figure 3.2).

Statistical Analysis

The values of ImP measurements were reported as mean±SD. The effects of treatments were evaluated using a Kruskal-Wallis one-way ANOVA on ranks and Dunn's pairwise comparison post-hoc test using GraphPad Prism 3.0 Software (GraphPad Software Inc., La Jolla, CA). The level of significance was established at $p<0.05$.

Results

Tibial and Femoral ImP Induced by DHS

Approximately 1 mmHg tibial ImP and 5 mmHg femoral ImP within the bone marrow cavities were generated by normal heart beat. Oscillatory DHS over the tibial region of each rat's right hindlimb, loaded at various frequencies, generated additional fluid pressures in the tibial bone marrow cavity but not in the femoral bone marrow cavity. Tibial ImP generated by oscillatory DHS at each frequency was plotted and shown in Figure 3.3. The observed responding trend of the ImP (peak-to-peak) values against frequency was induced in a nonlinear fashion during the DHS loading. The induced ImP values (peak-to-peak) were in the order of 1.98±1.57 mmHg at 0.5 Hz ($p>0.05$), 9.20±4.58 mmHg at 1 Hz ($p>0.05$), 13.98±3.23 mmHg at 1.5 Hz ($p<0.01$), 14.48±3.10 mmHg at 2 Hz ($p<0.01$), 13.99±2.58 mmHg at 2.5 Hz ($p<0.01$), 13.18±2.07 mmHg at 3 Hz ($p<0.01$), 12.52±2.08 mmHg at 3.5 Hz ($p<0.01$), 12.09±2.18 mmHg

at 4 Hz (p<0.05), 11.52±2.48 mmHg at 5 Hz (p<0.05), 10.56±2.67 mmHg at 6 Hz (p>0.05), 9.59±3.21 mmHg at 7 Hz (p>0.05), 8.55±2.97 mmHg at 8 Hz (p>0.05), 7.76±3.70 mmHg at 9 Hz (p>0.05), and 7.28±4.85 mmHg at 10 Hz (p>0.05). The ImP reached the peak at 2 Hz.

Effects of DHS on Tibial and Femoral Bone Strains

Oscillatory DHS over the tibial region of the rats' hindlimbs at various loading frequencies generated minimal bone strains within the tibia. Maximal bone strain measured at all loading frequencies was smaller than 8με. Similar to the femoral ImP measurements, no detectable induction of bone strain was observed in the un-stimulated femur.

Discussion

For the first time, this study demonstrated a non-invasive method that can be applied to an *in vivo* rodent model to isolate ImP and bone deformation, which are the two key determinants for BFF. The promising results from this study indicated that oscillatory DHS was able to generate local fluid pressure in bone with simultaneously minimal bone strain. Oscillatory DHS over the rat tibia induced a peak of tibial ImP at 2 Hz. While the observed tibial bone strain over the range of loading frequencies was smaller than 8 με, relatively high ImP values were observed as a function of loading frequency. Tibial ImP measurements between 1.5 Hz and 5 Hz of loading showed significant increases compared to the baseline level. These results suggested that DHS could potentially produce high fluid pressure gradients within the local bone marrow cavity. As a key determinant of BFF, loading generated fluid pressure in bone may have strong potentials in attenuating disuse bone loss, if loaded at proper frequencies.

The results from this study coincided with one of our recently published *in vivo* experiment, in which DHS loading at frequency of 2 Hz was shown to have mitigation effect on

disuse trabecular bone loss in a rat HLS functional disuse model [127]. For example, trabecular bone volume fraction (BV/TV) in the stimulated tibia was increased by 83% when a DHS protocol at 2 Hz was applied for four weeks in conjunction with HLS. The high surface area of the trabecular network allows it to expose to the rapid change in fluid pressure, leading to the pronounced effects of DHS observed in the trabecular bone. The DHS stimulation was designed as dynamic circular compressions around the diaphysis region of the loaded bone, which does not provide direct physical contact over the metaphyseal region. However, the anabolic/anti-catabolic effects of DHS on disuse trabecular bone strongly support the ImP-induced BFF mechanism. According to the beneficial role of mechanotransduction in triggering bone remodeling [131, 132], strong evidence has suggested that interstitial fluid flow in bone can be altered by external muscular activities through various mechanisms [133, 134]. Based on the muscle pump theory, it is thought that muscle contraction compresses the blood vessels in muscle, which generates an arteriovenous pressure gradient that further increases the hydraulic pressure in the skeletal nutrient vessels and amplifies the capillary filtration in bone [8-10]. Increased vessel pressure can directly increase the ImP that further drives BFF [11]. Direct circular compressions provided by DHS over the surrounding muscles have demonstrated its ability in ImP induction and potential in attenuating disused bone loss [127].

The observed ImP inductions have indicated a nonlinear response to the DHS loading spectrum between 0.5 Hz and 10 Hz, in which peaked at 2 Hz. This response to the loading frequency range is different from our previous observations using electrical muscle stimulation (MS), in which oscillatory MS induced the maximal ImP at 20 Hz. Based on the characteristics of the tissue material, e.g., the viscoelastic nature of the surrounding muscle tissue, the loads at high frequencies could be quickly damped. Due to the different physical orientations of how

oscillatory MS and DHS contact the loaded tissue, as well as the different material densities and viscosities within hard and soft tissues, maximal DHS-induced ImP may result at relatively lower loading frequencies compared to MS. This also suggests that direct hydraulic coupling may influence bone adaptation in a more physiological frequency range, where normal heart rate is about 360 times per minute. Furthermore, the mechanotransductive sequence through different connective tissues during DHS may attenuate the high frequency response in bone, e.g., via the connective pathway from the contacted muscle vs. tendon to bone, resulting a peaked ImP at a different frequency compared to MS. To further reveal this complex mechanism, future investigation may need to focus on muscle kinetics and BFF generation.

Previous studies from our group have shown that BFF can be altered by ImP with minimal bone strain, and that ImP alone is sufficient to induce bone adaptation. A loss of cortical bone by 5.7% was resulted in a disuse avian ulna [82]. An increase in cortical bone mass by 18% was shown with a direct physiological fluid loading into the ulna at 20 Hz for 4 weeks. Moreover, the study also observed a strong correlation between the transcortical fluid pressure gradient and the total bone formation. Similarly, generation of dynamic ImP and BFF within the femurs of HLS mice using a novel microfluidic system significantly reduced the disuse bone mass loss in both trabecular bone and cortical bone [83]. Our present study demonstrated DHS's ability in ImP induction, which strongly suggested its potential in attenuating disuse bone loss. The working hypothesis is further supported by the mitigation effect of DHS at 2 Hz, indicated in our recent publication [127]. Interesting, DHS on the tibia only affected the tibial ImP but not the femoral ImP, indicating the local effect of DHS. This is suggesting that the function of DHS may be site-specific. More detailed *in vivo* experiments are needed to validate this observation.

In summary, oscillatory DHS can generate local ImP as a function of stimulation frequency with minimal strain, in which the induced dynamic ImP may subsequently enhance BFF. DHS, if applied at an optimal frequency, has strong potential in preventing and attenuating bone loss under disuse osteopenia condition. Results from this study provide evidence that may facilitate the development of a biomechanical based intervention for osteoporosis prevention and treatment, which provide great insights for future clinical applications.

Figures

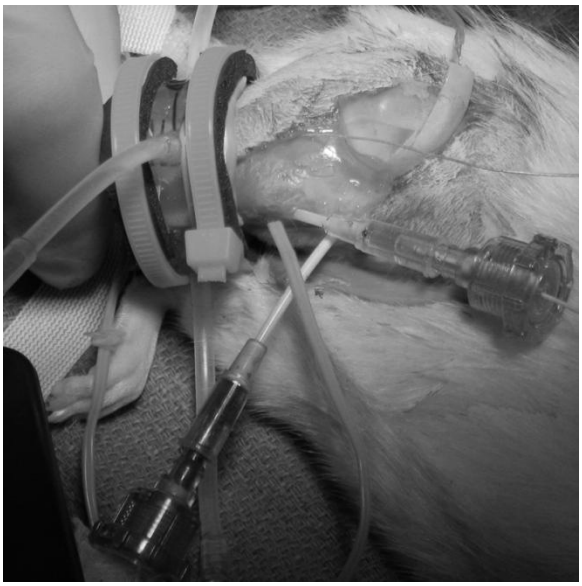

Figure 3.1. Surgical setup. For the ImP measurements, a micro-cardiovascular pressure transducer was inserted into each of the tibial and femoral bone marrow cavities. For bone strain measurements, a single element strain gauge was firmly attached to the flat surface of each of the same tibia and femur over the mid-diaphyseal regions. Simultaneous ImP and bone strain were then measured in the operated tibia and femur under DHS on the tibia.

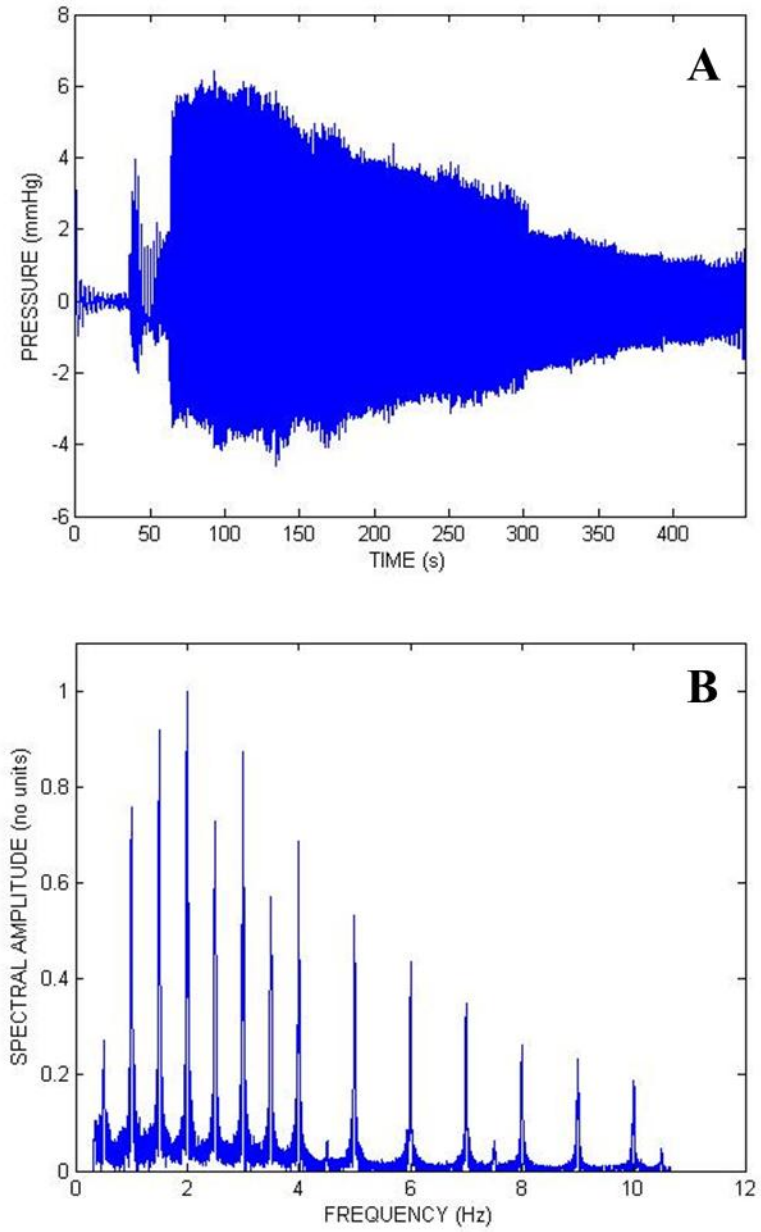

Figure 3.2. Representative traces of ImP measurements from DHS-loading at various frequencies over time. (A) Representative traces of ImP measurements – raw data. (B) Fast Fourier Transform (FFT) analysis of the ImP measurements.

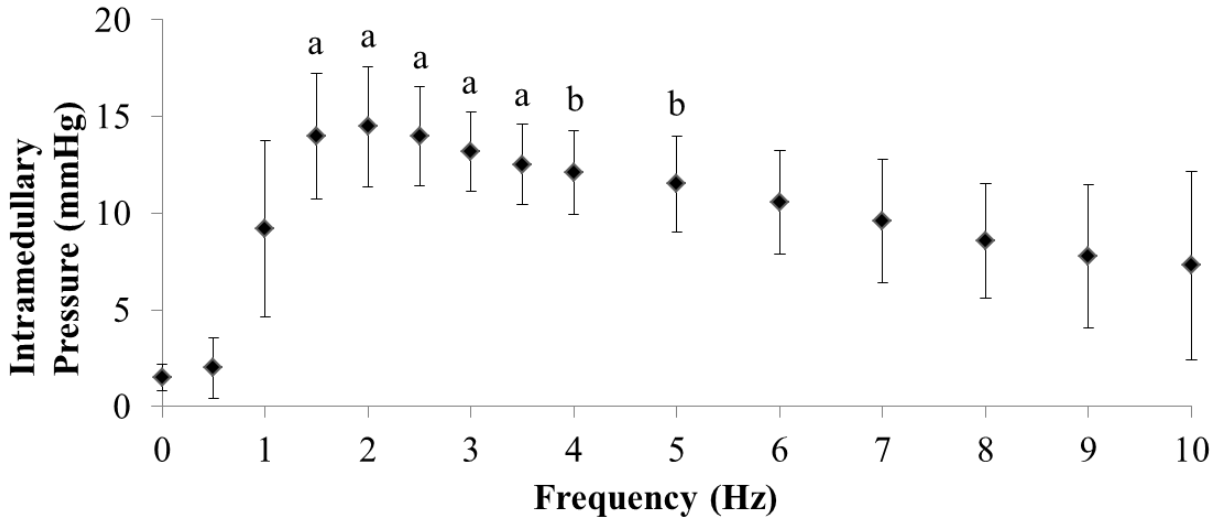

Figure 3.3. Graph shows mean±SD values of the tibial ImP measurements. ImP in the tibia increased significantly with DHS loading frequencies of 1.5 Hz, 2 Hz, 2.5 Hz, 3 Hz, 3.5 Hz, 4 Hz, and 5 Hz. In the loading frequency spectrum from 0.5 Hz to 10 Hz, a maximal ImP of 14.48±3.10 mmHg was observed at 2 Hz, which was around 7 folds higher than at 0.5 Hz (1.98±1.57 mmHg). [a] $p<0.01$ vs. baseline ImP; [b] $p<0.05$ vs. baseline ImP.

Chapter 4 – The Effects of Dynamic Hydraulic Stimulation on Mitigation of Trabecular Bone Loss in a Rat Functional Disuse Model

*This chapter is reprinted from Hu M., Cheng J., Qin YX., *Dynamic hydraulic flow stimulation on mitigation of trabecular bone loss in a rat functional disuse model*, Bone, 2012. Oct; 51(4):819-25.

Abstract

Bone fluid flow (BFF) has been demonstrated as a critical regulator in mechanotransductive signaling and bone adaptation. Intramedullary pressure (ImP) and matrix strain have been identified as potential generators to regulate BFF. To elevate *in vivo* oscillatory BFF using ImP, a dynamic hydraulic stimulation (DHS) approach was developed. The objective of this study was to evaluate the effects of DHS on mitigation of bone loss and structural alteration in a rat hindlimb suspension (HLS) functional disuse model. Sixty-one 5-month old female Sprague Dawley rats were divided into five groups: 1) baseline control, 2) age-matched control, 3) HLS, 4) HLS+static loading, and 5) HLS+DHS. Hydraulic flow stimulation was carried out daily on a "10 min on–5 min off–10 min on" loading regime, 5 days/week, for a total of 4 weeks in the tibial region. The metaphyseal trabecular regions of the proximal tibiae were analyzed using μCT and histomorphometry. Four weeks of HLS resulted in a significant loss of trabecular bone, leading to structural deterioration. HLS with static loading alone was not sufficient to attenuate the bone loss. Bone quantity and microarchitecture were significantly improved by applying DHS loading, resulting increase of 83% in bone volume fraction, 25% in trabecular number and mitigation of 26% in trabecular separation compared to HLS control. Histomorphometry analysis on trabecular mineralization coincided with the μCT analysis, in which DHS loading yielded increases of 34% in histomorphometric BV/TV, 121% in MS/BS, 190% in BFR/BS and 146% in BFR/BV, compared to the HLS control. Overall, the data demonstrated that dynamic hydraulic flow loading has potentials to provide regulatory signals for mitigating bone loss induced by functional disuse. This approach may provide a new alternative mechanical intervention for future clinical treatment for osteoporosis.

Introduction

Complications associated osteopenia and osteoporosis, whether generated by aging or disuse, are commonly referred to low bone mass and microstructural deterioration of the skeleton, leading to fragile bones that are more susceptible for fractures. Common targets of disuse osteoporosis include patients subjected to prolonged immobility or bed-rest (e.g., due to spinal cord injury), astronauts who participate in long-duration spaceflight missions, and the aged population [19]. Effective and clinically applicable interventions are greatly needed to prevent such skeletal deterioration and to enhance bone structural quality.

Paralysis caused by spinal cord injury (SCI) outlines severe immobilizations and atrophic responses in musculoskeleton [40], and that SCI patients have significantly higher incidences of post-injury fractures [41, 42]. Studies of quantitative bone structural measurements have been performed in SCI patients. In a pQCT study of SCI patients, overall bone quantity decreased exponentially with time after injury. Between 2 months to 50 years of paralysis, SCI leads to 25~35% of decreases in mean cortical thickness at tibial and femoral diaphysis at steady state compared to the controls with mobile ability [43]. Because of the thinner cortical bone, the section moduli also decreased by 25% and 31%, respectively to these regions. Another study also showed that 1 year after SCI, decreases of 14~16% mean trabecular density and 7% average cortical density resulted in the tibia [44]. Studies have reported that SCI-induced osteopenia and/or osteoporosis can lead to up to 34% of fracture frequency [41, 46]. Similarly, analysis from space missions of 6 months has demonstrated an average loss of total bone mass of approximately 11% in the proximal femur region, in which trabecular bone mass and density declined by 14.4~16.5% [50]. Femoral and tibial cortical density decreased by about 2% after 6 months of spaceflight [49, 51]; while approximately 5% and 12% of trabecular density

reductions were observed at the distal tibia and proximal femur, respectively. Furthermore, altered cortical and trabecular architecture have been observed in postmenopausal women with fractures; showing 12% and 19% decreases in cortical thickness and trabecular bone volume fraction [135].

Current treatments for osteoporosis include anti-resorptive and anabolic pharmacotherapies with noticeable benefits in clinic. Pharmacological interventions often require high costs and long-duration therapy, and easily give rise to adverse side effects (e.g., atypical fracture) [23]. Recent developments of non-pharmacological mechanical interventions, on the other hand, provide a non-invasive alternate approach. Mechanobiology and novel mechanical stimulations have been investigated for their abilities to regulate bone health. Bone adapts its overall shape and internal architecture in response to the applied mechanical stimuli [136]. Responsive skeletal adaptation to mechanical loading has been demonstrated with various modalities in the past research. In vivo studies have shown that load-driven strain from four-point bending [66, 67] and axial loading [70] can lead to bone formation. Low-magnitude, high-frequency vibrations have also been shown to be anabolic in both human [137] and animal [126] skeletons. Joint loading has recently been shown as a unique modality to stimulate trabecular and cortical bone formations [71, 72, 74]. Previous in vivo studies from our group demonstrated that dynamic electrical muscle stimulation successfully mitigated bone loss in a rat hindlimb suspension (HLS) model [75]. While increases of physical activities result in increased bone mass [138-140], removal of functional loads can result in bone mass reduction [141, 142]. Reduced trabecular number and thickness, bone mineral density, and increased bone resorption occurred in rodents on Cosmos spaceflights over 14~40 day periods [56-58]. Ground-based HLS

rodent models were included in the Cosmos 2044 mission as controls and coincided the atrophic changes in bone with the ones on flight [59].

Due to the anabolic potential of mechanical loading as a natural determinant in maintaining bone strength [143], a biomechanical intervention based on the skeletal mechanotransduction pathway is proposed as an alternative and potential approach for osteopenia and osteoporosis treatments. This requires an in-depth understanding of how mechanical signals are delivered to bone cells and how bone cells respond to such signals. A growing body of evidence has pointed bone fluid flow (BFF) as a communication media, bridging an external load and the bone cells, thereby regulating the bone remodeling process [77-81]. Thus, BFF has been a contributing mechanism through which mechanical stimulations act. Previous studies have shown that intramedullary bone fluid flow alone, in the absence of mechanical strain, can drive bone remodeling. Qin et al. applied a direct intramedullary pressure (ImP) to an isolated turkey ulna without deforming the bone tissue and found increased bone formation in response to the applied pressure [82]. Similarly, a recent study introduced a novel microfluidic system for generating dynamic ImP and interstitial fluid flow within the femurs of alert mice to induce osteogenic responses [83]. The observations from these in vivo studies clearly determined that BFF can be altered by ImP with minimal strain.

As a practical translational potential of ImP, a non-invasive method that directly couples an external stimulation and internal bone fluid flow is in great need. Here, we hypothesized that daily non-invasive dynamic hydraulic stimulation (DHS) induced bone fluid flow can initiate adaptive responses in vivo to elicit osteogenic activity during a 4-week study using a functional disuse model. To evaluate the potential of DHS mediated fluid flow on the skeletal system, the

objective of the study was to demonstrate the effects of dynamic external pressure stimuli on trabecular bone structural properties in a rat hindlimb suspension model.

Materials and Methods

Experimental Design

All experimental procedures were approved by the Institutional Animal Care and Use Committee (IACUC) at Stony Brook University. Sixty-one 5-month old female Sprague Dawley virgin rats (Charles River, MA) were used to investigate the effects of DHS on skeletal adaptation under disuse conditions. Animals were provided with standard rodent chow and water ad libitum, and housed in 18″×18″×24″ (L×W×H) stainless steel HLS cages. The animal room was temperature-controlled and had a 12:12 hour light:dark cycle. Animals were randomly assigned into five groups: baseline control (n=15), age-matched control (n=12), hindlimb suspended (HLS, n=10), HLS+static pressure (n=10), and HLS+DHS (n=14). Functional disuse in the rat hindlimbs was introduced via the HLS procedure, similar to the setup from Lam's study [75]. Briefly, an animal's tail was lightly coated with tincture of benzoin after being cleaned with 70% alcohol. A piece of surgical tape was then attached to the dried and sticky tail, forming a loop close to the end of the tail. The surgical tape was secured with three strips of elastic adhesive bandage along the surgical tape that was placed on the tail. The loop formed from the surgical tape was attached to a tail harness apparatus and a swivel hook suspended from the top of the cage. The animal was suspended with an approximately 30° head down tilt, having the hindlimbs about 2 cm above the cage bottom. Full access to the entire cage bottom was allowed for the animal's forelimbs. Animals' body weights and overall health were carefully monitored throughout the entire study.

Dynamic Hydraulic Stimulation Protocol

For the stimulated animals, daily DHS was applied in conjunction with HLS for the 4-week study. DHS was achieved through a customer design inflatable cuff placed around the right hindlimb of the tibia. The stimulation cuff was connected to an oscillatory actuator-driven syringe, a force-controlled syringe, and a pressure sensor (Figure 4.1). The inflation and deflation of the cuff was driven by the actuator-driven syringe controlled by a programmable waveform/signal generator (HP33120A, Hewlett-Packard, Palo Alto, CA). The force-controlled syringe was included to maintain the static pressure, and the pressure sensor was used to monitor the hydraulic pressure throughout the procedure to maintain baseline static pressure. The magnitudes of the pressure stimulation were 30 mm Hg static pressure + 30 mm Hg (peak-to-peak) dynamic pressure, with a stimulation frequency of 2 Hz. The daily stimulation of "10 min on - 5 min off - 10 min on" was applied to each stimulated animal while under anesthesia (isoflurane inhalation) 5 days/week, for 4 weeks. The static pressure was released during the 5 min break. The rats were euthanized at study's end, and the right tibiae were obtained and preserved with 70% ethanol.

μCT Evaluation

The proximal metaphyseal portions of the tibiae were scanned for trabecular bone morphology using a high resolution μCT scanner (μCT-40, SCANCO Medical AG, Bassersdorf, Switzerland) with a spatial resolution of 30 μm. For image smoothing purposes and to define the desired analyzed objects, all images were evaluated using a Gaussian filter, with specific sigma, support and threshold values of 0.3, 1, and 320, respectively. A 1500 μm region of trabecular bone was analyzed in the proximal metaphysis, starting from 1800 μm distal to the growth plate. Values for bone volume fraction (BV/TV, given as %), connectivity density (Conn.D, $1/mm^3$),

trabecular number (Tb.N, 1/mm), and trabecular separation (Tb.Sp, mm) were evaluated for each metaphyseal trabecular region.

Static and Dynamic Histomorphometry

Two doses of calcein (10 mg/kg) were given to the animals through intraperitoneal injections on days 2 and 16 prior to euthanasia. After the μCT scans, the proximal portions of the tibiae were kept and dehydrated with isopropanol. The samples were then infiltrated and embedded with the mixture of methyl methacrylate, n-butyl phthalate, and benzoyl peroxide. The samples were sectioned to 8 μm slices longitudinally using a microtome (Leica 2165, Wetzlar, Germany). Osteomeasure software (OsteoMetrics Inc., Decatur, GA) was used to perform histomorphometric measurements by tracing calcein labels in the trabecular bone in the metaphyseal region (5 mm^2×3 mm^2). Histomorphometric bone volume fraction (BV/TV-Histo, %), mineralizing surface/bone surface (MS/BS, %), mineral apposition rate (MAR, μm/day), and bone formation rate (BFR/BS, $\mu m^3/\mu m^2$/day; BFR/BV, $\mu m^3/\mu m^3$/day) were calculated by the software from the single- and double-label values.

Statistical Analyses

The statistical analysis of all results is reported as mean±SD. Differences between groups were determined using GraphPad Prism 3.0 Software (GraphPad Software Inc., La Jolla, CA) for body weight measurements, bone structural analysis, and static and dynamic histomorphometric analysis. One-way ANOVA with Tukey's post-hoc test was performed on the μCT and histomorphometry data with normal equal variance to determine the differences among groups. The level of significance was established at $p<0.05$.

Results

Body Weight

The animals' body weights were carefully monitored for 5 times per week throughout the entire experimental period. The body weights were not significantly different between groups at the beginning of the study, with an average of 305±16 g. Age-matched control animals were able to maintain a steady body weight throughout the study, with only a +4.7% difference between the start and end dates. Animals subjected to 4-week functional disuse, including HLS control and stimulated groups, lost a great amount of body mass. These weight reductions were similar in HLS, HLS+static, and HLS+DHS groups, with -5% for HLS ($p>0.05$), -7% for HLS+static ($p<0.0001$), and -5% for HLS+DHS ($p<0.05$).

μCT — Trabecular Bone

Results of μCT analysis with representative scanned images are shown in Figure 4.2 for the tibial proximal metaphyseal region. The lack of weight-bearing activity for 4 weeks significantly reduced trabecular bone quantity and quality, demonstrated by a 41% decrease in BV/TV ($p<0.05$) (Figure 4.3), a 47% decrease in Conn.D ($p<0.01$) (Figure 4.4), a 17% decrease in Tb.N ($p<0.05$) (Figure 4.5), and a 27% increase in Tb.Sp ($p<0.05$) (Figure 4.6) compared with the age-matched group. Animals with static pressure pre-load alone showed slight improvements in microarchitecture although it's not statistically significant. HLS+static animals showed an increase of 20% in BV/TV (Figure 4.3), an increase of 30% in Conn.D (Figure 4.4), an increase of 11% in Tb.N (Figure 4.5), and a decrease of 19% in Tb.Sp compared with age-matched group ($p>0.05$) (Figure 4.6). Trabecular BV/TV in DHS treated animals was significantly greater than that of disused bone. Animals with DHS at 2 Hz showed an increase in BV/TV by 83% ($p<0.001$). Measures of Conn.D, Tb.N, and Tb.Sp were also significantly affected by DHS at

2 Hz. There were up to 102% (p<0.001) and 25% (p < 0.01) increases for Conn.D and Tb.N; and up to a 26% (p<0.01) decrease for trabecular separation (Figures 4.3 – 4.6). When compared to HLS+static animals, HLS+2 Hz DHS animals showed 36% (p>0.05), 54% (p<0.05), and 17% (p>0.05) increases for BV/TV, Conn.D, and Tb.N; and up to a 21% decrease for trabecular separation (p>0.05) (Figures 4.3 – 4.6).

Static and Dynamic Histomorphometry

The static and dynamic histomorphometry data showed significant improvements in the histomorphometric BV/TV and other bone formation parameters in response to DHS (Table 4.1 and Figure 4.7). HLS significantly reduced BV/TV, MS/BS, MAR, BFR/BS and BFR/BV compared to age-matched controls by 29% (p<0.05), 62% (p<0.001), 28% (p<0.05), 73% (p<0.001), and 67% (p<0.001), respectively. HLS+static pressure alone did not show significant difference compared to HLS, except for MS/BS. However, HLS + 2 Hz DHS-treated rats showed significant increases in BV/TV and all other bone formation parameters, except for MAR. HLS+DHS had increases compared to the age-matched group by 34% in BV/TV (p<0.05), 121% in MS/BS (p<0.001), 34% in MAR (p>0.05), 190% in BFR/BS (p<0.001), and 146% in BFR/BV (p<0.001).

Discussion

In the present study, a non-invasive dynamic hydraulic stimulation was developed to successfully mitigate bone loss and detrimental changes to trabecular architecture induced by a lack of daily weight bearing activities, with only 4-week of loading. Specifically, 20-min bouts of daily DHS at low magnitude onto the hindlimb suspended rats increased trabecular bone volume fraction and microarchitecture, which critically contribute to a stronger skeleton. With

the idea of direct coupling with oscillatory marrow fluid pressure, DHS serves as low-magnitude loads that are applied to the tibial diaphysis and potentially alters pressure in the intramedullary cavity, leading to influences in interstitial fluid flow and further bone adaptation. Moreover, DHS makes itself a valuable tool to investigate the anabolic and/or anti-resorptive potentials of interstitial fluid flow and its role in regulating skeletal mechanotransduction mechanisms. The promising data may ultimately offer some insights into future potential clinical applications.

Mechanical signaling has long been recognized for its importance in skeletal health, playing a critical role in strong anabolic potential and naturally gauging bone strength [18]. A good understanding on the mechanism of how bone cells sense physical signals is needed to further develop the therapeutic potential of mechanical signals. Factors including strain and ImP-induced bone fluid flow are potential determinants of bone mass and morphology. While early investigations had indicated strain magnitude as a dominant factor for osteogenic responses, dynamic or cyclic stimuli were shown in the later studies as being more anabolic to bone than static stimuli [144]. Since bone will accommodate to prolonged routine loading, rest periods between bouts of mechanical loading are needed to reinstate bone's mechanosensitivity [18]. In our present study, a rest period of 5 min was inserted in between two bouts of 10-min DHS. Yet, static loading alone, even with the rest period and constant loading magnitude, was not effective in attenuating bone loss. From our data, we concluded that the effectiveness of DHS was greatly dependent on the dynamic components that were superimposed to the static pre-load. While static loading was unsuccessful in preventing osteopenia, 2 Hz DHS applied to the tibia was able to maintain trabecular bone mass. Strain information has also been hypothesized to accumulate and integrate over time [145], suggesting that low-magnitude mechanical strain induced by DHS, if any, may propagate in the skeleton and initiate osteogenic responses. Low-magnitude stimuli,

such as vibration, have been shown in previous research to mediate bone formation and to enhance bone morphology and bone strength [126, 146]. Responsiveness to mechanical signals has been observed at the cellular level in bone, e.g. osteoblasts and osteocytes. Growth hormones and cytokines activated from subsequent mechanotransduction-induced signaling cascades can play a role in the balance of bone formation and resorption [33, 147-149].

Another crucial factor, bone fluid flow induced by ImP, has also been proposed to account for adaptive bone response [150]. Murine femoral ImP measurements showed a 23% drop in ImP upon HLS and a 25% increase upon femoral vein ligation, strongly supporting the hypothesis that hindlimb disuse leads to decreased pressure gradients and subsequent reductions in interstitial fluid flow, which can be re-built by femoral vein ligation [133]. Previous *in vivo* study from our group demonstrated that muscle contraction using dynamic electrical stimulation was able to induce ImP, and this change was strongly correlated with the bone structural adaptive effects [75, 84]. Aimed at decoupling the matrix deformation factor from interstitial fluid flow, Qin et al. applied a direct ImP to the isolated turkey ulna without deforming the bone tissue and found increased bone formation in response to the applied pressure [82]. Similarly, a recent study introduced a novel microfluidic system for generating dynamic ImP and interstitial fluid flow within the femurs of alert mice to induce osteogenic responses [83]. The observations from these *in vivo* studies clearly determined that fluid flow can be altered by ImP alone. Moreover, modulation potential in bone remodeling through autocrine and paracrine signaling cascades may occur with changes in the fluid environment [133, 151, 152]. Interestingly, trabecular bone growth in the proximal tibia could result from the direct compression by DHS on the diaphysis. The linkage between the site of pressure application and the site of bone formation may be an

ImP gradient that influences the magnitude of mechanotransductory signals on the trabecular bone that is exposed in the marrow cavity.

Current limitations in this field involve either the lack of ability to isolate the matrix strain and ImP, or using highly invasive methods to decouple these two factors. Directly related to translational potentials of ImP, a non-invasive method that couples external stimulation and internal bone fluid flow has been a challenge. As a direct circular compression with low magnitude pressure on surrounding soft tissues, DHS provides an excellent method to eliminate matrix deformation, i.e. axial compression or torsion, bending, or shear stress. As suggested in the theory of muscle pump, veins within skeletal muscle are compressed upon DHS and thus increasing the arteriovenous pressure gradient and promoting blood flow to the capillary bed [8-10]. The pressure gradient in the muscle vasculature may be relayed to the nutrient vessels in bone, further increasing ImP and inducing fluid flow in bone [11]. Based on this theory, this pilot study of DHS first investigated 30 mmHg as the dynamic loading magnitude. The reason behind it is this magnitude is large enough to temporarily block venous blood flow, while still allowing the arterial blood flow for pressure build-up.

Loading frequency is an important determinant of bone adaptation to mechanical loading. A positive correlation has been demonstrated repeatedly in various studies [128-130]. Mechanical stimulation with various loading frequencies forms a nonlinear relationship with femoral strain measured at the mid-diaphysis [145, 146, 153, 154]. However, effective loading frequency has also been shown to differ among various loading modalities [74, 128, 129]. Higher frequencies (>30 Hz) in whole-body vibration are known to be more effective. On the contrary, lower frequencies (5 Hz and 10 Hz) were reported to be more effective over higher frequencies (20 Hz or 30 Hz) in an ulna axial loading study in mice [69]. In recent studies based on

ImP/interstitial fluid flow loading theory, relatively lower frequencies 5 Hz and/or 10 Hz were effective in bone adaptation in the femur [83] and tibia [74], respectively. In our present study, functional disuse for 4 weeks significantly reduced the metaphyseal bone volume fraction, mainly via a decrease in trabecular number, thereby reducing its connectivity and augmenting the marrow space. DHS with 2 Hz proved capable of preserving bone mass, trabecular number, and connectivity. The promising histomorphometry data further verified and coincided with the μCT analysis, in which DHS treatment had significant increases in histomorphometric BV/TV and other bone formation parameters compared to HLS. The precise mechanisms of how a potential cause of differential frequency responses in the skeletal tissue are not yet identified. Though, our finding implies that direct hydraulic coupling may influence adaptation in a more physiologic frequency range. In addition to strain, nonlinear ImP profile with loading frequencies has also been observed during dynamic mechanical stimulation [84].

Selecting an optimal loading regimen with the appropriate magnitude, frequency and duration is important to maximize the effectiveness of DHS. One limitation of this study is that we did not test a wide range of these parameters to determine their combinational effects in skeletal adaptive responses. Future studies will extend the investigation into various loading regimes. Further, while DHS has been shown to significantly improve the structural quality of the disuse bone, DHS can be likely to act through increased bone formation and/or decreased bone resorption. Our *ex vivo* methodology of the tibias precluded analysis that requires cellule markers. Therefore, future studies will also incorporate cellular assays, such as TRAP and ALP staining, to further determine this process.

In summary, dynamic hydraulic pressure stimulus, applied externally and non-invasively, provides a physiological fluid flow intervention to attenuate trabecular bone loss in a functional

disuse rat HLS model. The results of this study suggested that low magnitude, 2~3 Hz short duration, external hydraulic fluid flow loading is able to provide sufficient mechanotransductive signals to attenuate disuse osteopenia, showing improvements on bone structural quality. The skeletal adaptive responses induced by fluid flow are highly depended on its dynamic components such as loading frequency and duration. The underlying mechanism may involve regulation of oscillatory marrow fluid pressure to initiate adaptation. Although we only focused on indices of bone structural morphology, it is likely that this structural change may be adapted through integrated improved bone formation and inhibition of bone resorption activities. Applied fluid pressure significantly mitigated bone loss with only 20 min of daily loading at low magnitude. This will provide significant insights for future clinical applications.

Figures and Tables

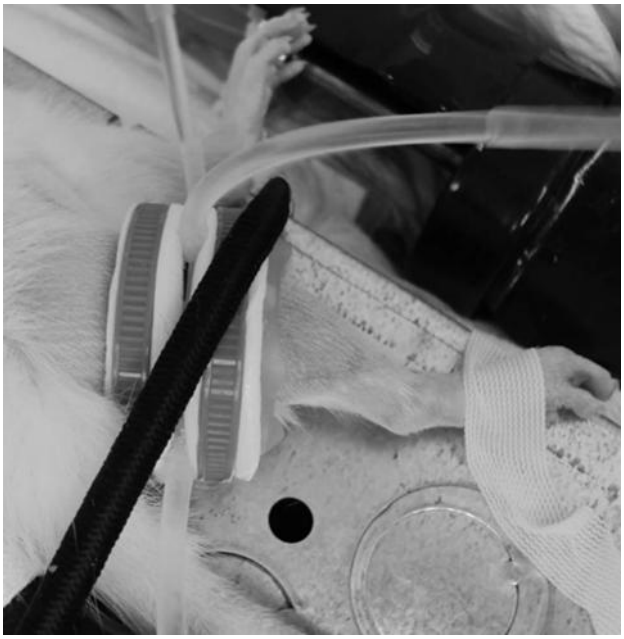

Figure 4.1. Experimental setup. DHS is achieved through a costumer design inflatable cuff. The stimulation cuff is connected to an oscillatory actuator-driven syringe, a force-controlled syringe, and a pressure sensor.

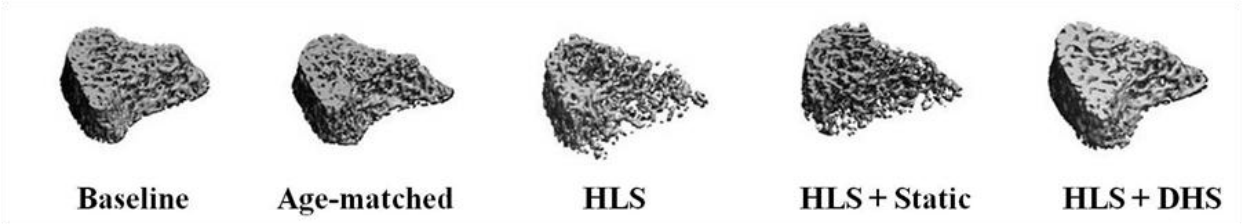

Figure 4.2. Representative 3D μCT images of proximal tibial trabecular bone. The proximal metaphysis of the tibiae were scanned for trabecular bone morphology using a high resolution μCT scanner with a spatial resolution of 30 μm. A 1500 μm region of trabeculae was analyzed in the proximal metaphysis, starting from 1800 μm distal to the growth plate.

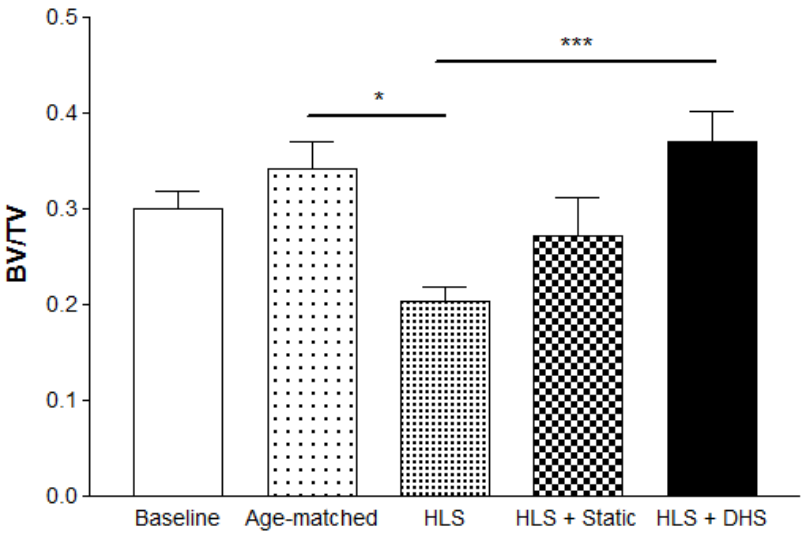

Figure 4.3. Graphs show mean±SD values for bone volume fraction (BV/TV, %). DHS at 2 Hz produced a significant change, compared with values obtained in 4-week HLS. *p<0.05; ***p<0.001.

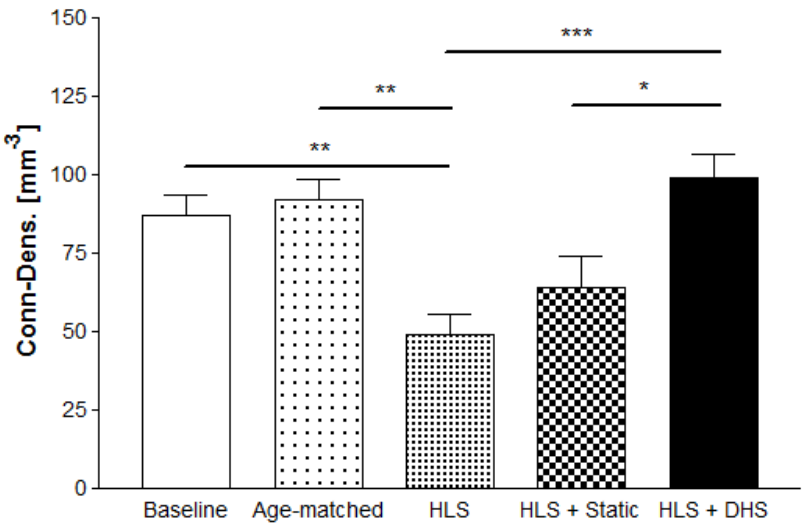

Figure 4.4. Graphs show mean±SD values for connectivity density (Conn.D, 1/mm^3). DHS at 2 Hz produced a significant change, compared with values obtained in 4-week HLS. *p<0.05; **p<0.01; ***p<0.001.

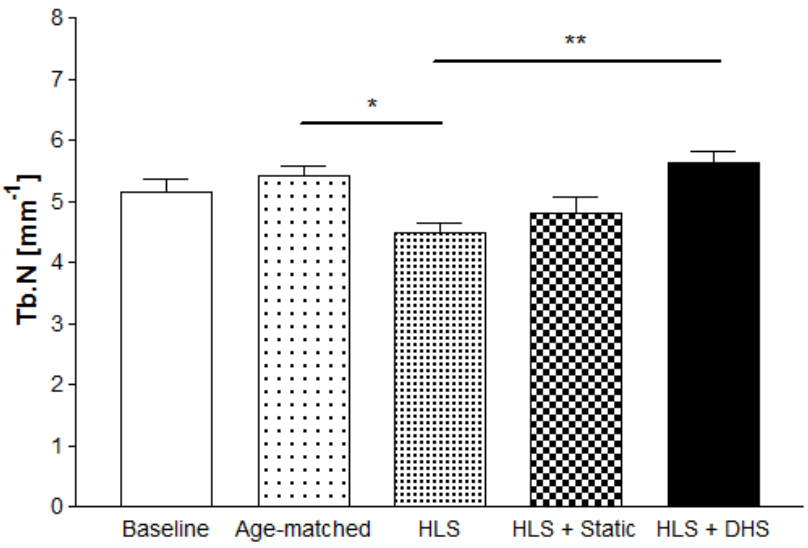

Figure 4.5. Graphs show mean±SD values for trabecular number (Tb.N, 1/mm). DHS at 2 Hz produced a significant change, compared with values obtained in 4-week HLS. *p<0.05; **p<0.01.

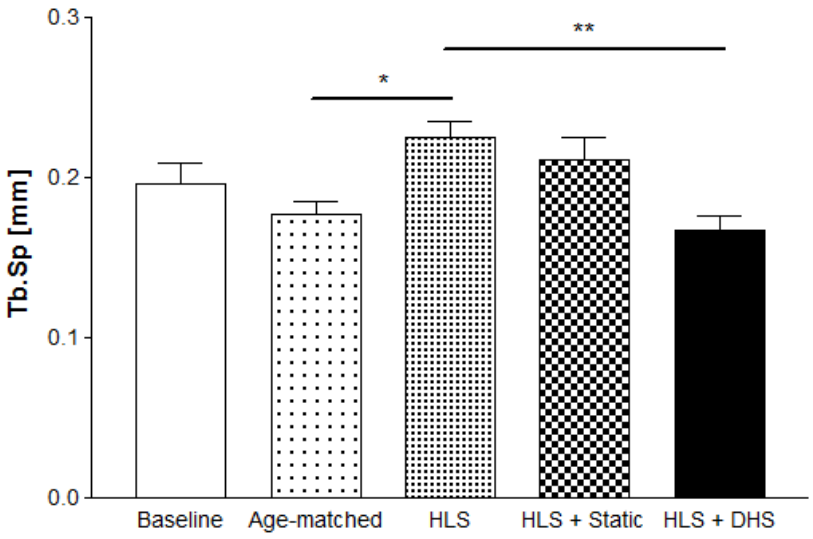

Figure 4.6. Graphs show mean±SD values for separation (Tb.Sp, mm). DHS at 2 Hz produced a significant change, compared with values obtained in 4-week HLS. *p<0.05; ** p<0.01.

	BV/TV (Histo, %)	MS/BS (%)	MAR (mm/day)	BFR/BS (mm^3/mm^2/day)	BFR/BV (mm^3/mm^3/day)
Age-matched	46.61±7.32	10.75±2.24	0.73±0.15	0.08±0.03	0.23±0.07
HLS	33.22±7.99*	4.12±0.84**	0.53±0.16*	0.02±0.01**	0.07±0.03**
HLS + Static	40.99±14.84	6.81±1.18**#	0.59±0.19	0.04±0.01**	0.12±0.03**
HLS + DHS	44.65±8.99#	9.09±2.94##	0.71±0.18	0.06±0.02##a	0.18±0.05##a

Table 4.1. Proximal tibia metaphysic histomorphometry. Trabecular bone histomorphological analyses on age-matched control, HLS, HLS+static, and HLS+DHS. Values are mean±SD. BV/TV, bone volume/tissue volume; MS/BS, mineralized surface/bone surface; MAR, mineral apposition rate; BFR/BS, bone formation rate/bone surface. *p<0.05 vs. age-matched; $^{\#}p$<0.05 vs. HLS; **p<0.001 vs. age-matched; $^{\#\#}p$<0.001 vs. HLS; ^{a}p<0.05 vs. HLS+static.

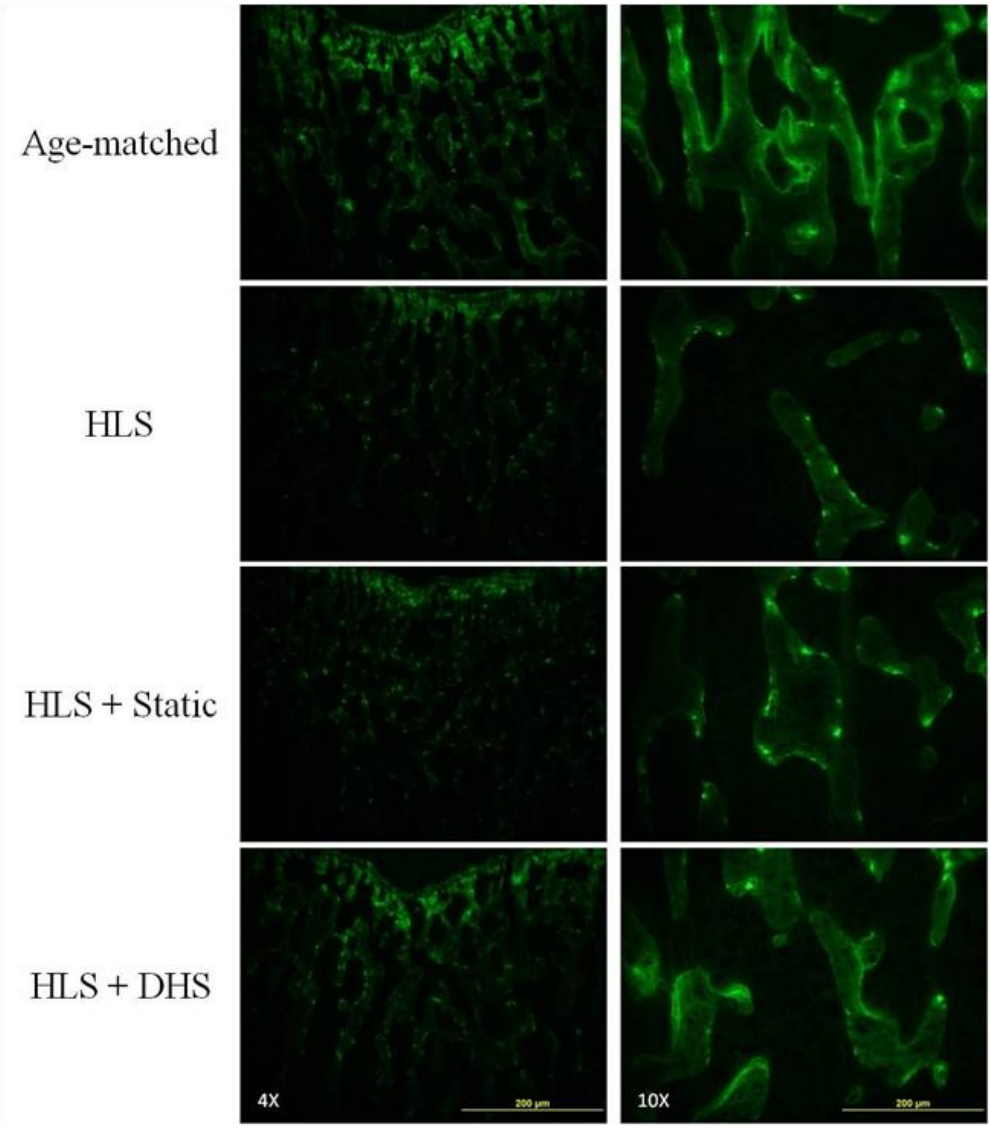

Figure 4.7. Representative 2D images of calcein (green) labeled trabecular bone histomorphometry in the proximal metaphyseal region of the tibia. The calcein (green marker) labeled the mineralizing bone surfaces. Trabecular bone formation was clearly indicated by the double calcein labels in the HLS+DHS group.

Chapter 5 – The Effects of Dynamic Hydraulic Stimulation on Bone Marrow Mesenchymal Stem Cell Population

Abstract

Osteoblasts are derived from mesenchymal stem cells (MSCs), and bone formation begins with MSC proliferation and condensation. New strategies for osteoporosis treatments have directed to control the fate of MSCs for skeletal phenotype. While studies have shown that functional disuse leads to decreased MSC growth potential and osteogenic potential, external mechanical signals have been shown to be able to increase MSC quantity and bias their differentiation toward osteoblastogenesis. Our group has recently introduced a novel, non-invasive dynamic hydraulic stimulation (DHS) and found its beneficial effects on mitigating trabecular bone loss in a rat hindlimb suspension (HLS) model. To further elucidate the downstream cellular effect of DHS as well as its potential mechanism underlying the bone quality enhancement, a longitudinal *in vivo* study was designed and aimed to evaluate the MSC populations in response to DHS over 3 days, 7 days, 14 days, and 21 days. Five-month old female Sprague Dawley rats were divided into three main groups for each time point: age-matched control, HLS, and HLS+DHS. DHS was delivered to the right mid-tibiae with a daily "10 min on - 5min off - 10min on" loading regime for 5 days per week. Rats in the 3-day group were stimulated for 2 days. At the animals' sacrifice at each time point, bone marrow MSCs of the stimulated and control tibiae were isolated through specific cell surface markers and then quantified by flow cytometry analysis. Interesting data indicated a time-dependent fashion of gradual bone marrow MSC inductions in response to DHS, which peaked on day 14. After 21 days, this effect of DHS was diminished. This study indicated that the MSC pool was positively influenced by the mechanical signals driven by DHS. Coincided with our previous findings of mitigation of disuse bone loss, DHS induced changes in MSC proliferation and may bias the

differentiation of the MSC population towards osteoblastogenesis, promoting bone formation under disuse condition.

Introduction

Bone loss due to functional disuse, classified as secondary osteoporosis [19], strikes the society with impacts of osteoporosis-related fractures and excessive medical costs [155, 156]. While millions of people are affected by such condition, patients subjected to prolonged immobility or bed-rest (e.g., due to spinal cord injury), as well as astronauts who participate in long-duration spaceflight missions are the common targets of disuse osteoporosis [19]. Subsequent health complications associated with the physiological and/or pathophysiological changes in the skeleton, such as increased risks of falls and fractures, often require long-term recovery. Unfortunately, a good understanding of the detailed mechanisms to facilitate the development of clinical treatments for osteoporosis is still lacking.

Mesenchymal stem cells (MSCs) are pluripotent cells defined by their abilities of self-renewal and potential differentiations into the cells that form different types of tissues such as bone [85]. MSCs can differentiate into osteoblasts, and bone formation begins with MSC proliferation and condensation [86, 87]. In addition to targeting the resident bone cell population, strategies of new treatments encountering osteoporosis have started to direct the design to regulate the fate of MSCs for skeletal phenotype [88-91]. Pharmacological agents, e.g., statins, have been shown to increase bone marrow osteogenesis [92]. On the other hand, a great amount of published work have pointed out that external mechanical signals are able to regulate osteogenesis of MSCs. The ability of different types of macro-level mechanical loading (e.g., fluid flow, tension, compression, hydrostatic pressure, etc.) to alter the differentiation patterns of

MSCs toward osteogenesis and chondrogenesis has been studied [87, 93]. Moreover, more complex 3D systems have been used by tissue engineers to explore the role of mechanical forces on MSC adhesion and differentiation, as well as promoting the growth of both bone and cartilage [94-100]. *In vivo* studies using mechanical stimulation, such as whole body vibration, have also demonstrated their effects on MSC proliferation and differentiation toward osteogenesis [101-103].

While mechanical signals direct MSCs toward osteoblastogenesis and are anabolic to bone, reduction in physical impacts on bone leads to adverse outcomes. *In vitro* simulated microgravity conditions, mimicking the reduced mechanical stress occurring in spaceflight and hindlimb suspension (HLS), could alter the expression of differentiation-associated genes in osteoblasts and pre-osteoblasts [104-108]. *Ex vivo* studies from HLS treatment in mice demonstrated a net consequence in suppressing the osteogenic gene expressions [108]. A similar study in rats showed that 28 days of HLS negatively affected the growth potential of MSCs, but this adverse effect was removed upon recovery of normal gravity. Decreased osteogenic potential of MSCs from HLS was even resulted under an *in vitro* osteogenic induction condition. Low levels of osteoblastic gene markers were observed in the cells induced from the MSCs of the HLS rats, which eventually led to a decrease of bone mass. However, re-exposure to normal gravity or centrifugal force was able to reverse such changes [109].

Our group has recently developed a novel, non-invasive dynamic hydraulic stimulation (DHS) as a countermeasure for osteoporosis in rats [127]. Demonstrating in a rat HLS model, DHS successfully mitigated trabecular bone loss under such disuse condition. The promising results suggested that DHS may potentially provide regulatory signals to osteoblast progenitors, which leads to phenotypic changes in bone structure. As this approach may provide a new

alternative mechanical intervention for future clinical treatment for osteoporosis, it is important to elucidate the downstream cellular effects of DHS and its potential mechanisms to enhance bone quality. Therefore, the current *in vivo* longitudinal study was designed and aimed to evaluate the responses of MSC populations to DHS over 3 days, 7 days, 14 days, and 21 days. It was hypothesized that mechanical signals derived from DHS may encounter the reduced bone marrow MSC growth under disuse condition, and it is in a time-dependent fashion.

Materials and Methods

Experimental Design

All experimental procedures were approved by the Institutional Animal Care and Use Committee (IACUC) at Stony Brook University. Ninety-three 5-month old female Sprague-Dawley virgin rats (Charles River, MA) were used to investigate the effects of DHS on *in vivo* bone marrow MSC proliferation. Standard rodent chow and water *ad libitum* were provided for the animals; and they were housed in 18”x18”x24” (LxWxH) stainless steel HLS cages. The animal room had a 12:12 hours light:dark cycle and was temperature-controlled. Animals were randomly divided into 12 groups: 1) age-matched – day 3 (n=8), 2) HLS – day 3 (n=8), 3) HLS+DHS – day 3 (n=8), 4) age-matched – day 7 (n=8), 5) HLS – day 7 (n=8), 6) HLS+DHS – day 7 (n=8), 7) age-matched – day 14 (n=8), 8) HLS – day 14 (n=6), 9) HLS+DHS – day 14 (n=8), 10) age-matched – day 21 (n=8), 11) HLS – day 21 (n=8), 12) HLS+DHS – day 21 (n=7). The HLS procedure, similar to the setup from Lam’s study [75], introduced functional disuse to the rat hindlimbs. Briefly, after cleaning with 70% alcohol, animal’s tail was lightly coated with tincture of benzoin. The dried and sticky tail was attached to a piece of surgical tape that formed a loop close to the end of the tail. Three strips of elastic adhesive bandage were used to secure

the surgical tape that was placed on the tail. A tail harness apparatus and a swivel hook suspended from the top of the cage were linked to the loop formed by the surgical tape. To have the hindlimbs about 2 cm above the cage bottom, the animals were suspended with an approximately 30° head-down tilt. The animal's forelimbs were allowed for full access to the entire cage. Throughout the entire study, animals' body weights and overall health were carefully monitored.

DHS Protocol

For the stimulated animals, daily DHS was applied in conjunction with HLS. The DHS setup was similar to the previous study [127]. Briefly, DHS was delivered through a costume-made inflatable cuff placed around the right hindlimb above the tibia. An oscillatory actuator-driven syringe, a force-controlled syringe and a pressure sensor were connected to the stimulation cuff. The actuator-driven syringe was controlled by a programmable 100 MHz waveform/signal generator (Model 395, Wavetek). The hydraulic pressure was monitored by the pressure sensor throughout the entire treatment. With a stimulation frequency of 2 Hz, the pressure stimulation magnitudes were 30 mmHg static pressure + 30 mmHg (peak-to-peak) dynamic pressure. Daily stimulation of the "10 min on – 5 min off – 10 min on" loading regime was applied to each stimulated animal while under anesthesia (isoflurane inhalation) for 5 days/week. The rats in groups 1 - 3 were stimulated for 2 days. The rats were euthanized in the end of the according time points.

MSC Quantification

At the end of each time point, animals were sacrificed and the bone marrow was extracted from the right tibia using MEM culture media. Red blood cells in the bone marrow extracts were removed by incubation with Pharmlyse (BD Bioscience) at room temperature for

10 min. MSCs were isolated from the bone marrow extracts and quantified using flow cytometry analysis. Appropriate antibodies (BD Bioscience) as positive and negative MSC surface markers (CD29+/CD49e+/CD90.1+/CD45-/CD11b-) were applied with suggested concentrations; and the cells were fixed at a final concentration of 1% formalin. Flow cytometry data were collected using FACS ARIA at Research Flow Cytometry Core Facility at Stony Brook University Medical Center.

Statistical Analyses

The MSC numbers of each time point were normalized to the according total cell numbers within the bone marrow extracts, followed by normalization to the age-matched values to obtain the MSC percentages. All the statistical analyses on the results were reported as mean±SD. GraphPad Prism 3.0 Software (GraphPad Software Inc., La Jolla, CA) was used to determine the differences between groups. One-way ANOVA with Tukey's post-hoc test were performed with normal equal variance. The level of significance was determined at $p<0.05$.

Results

Bone Marrow MSC Population – Day 3

Flow cytometry measurements indicated the MSC population as represented by cells positive for CD29, CD49e and CD90.1, and negative for CD45 and CD11b. Over 3 days, HLS started to lower the total MSC number in the bone marrow, although it was not statistically significant ($p>0.05$). At this stage, DHS has not shown any effects on the bone marrow MSC population under disuse condition (Figure 5.1).

Bone Marrow MSC Population – Day 7

By day 7, HLS reduced 67% of the total bone marrow MSCs compared to age-matched controls ($p<0.01$). On the other hand, DHS started to increase the MSC number within the bone marrow. Compared to the HLS group, this increase in bone marrow MSC number was up to 43% ($p>0.05$, Figure 5.2).

Bone Marrow MSC population – Day 14

By day 14, the trend of the changes in bone marrow MSC populations was more apparent. While HLS greatly reduced 39% of bone marrow MSCs compared to age-matched control, the increase in the bone marrow MSC number in response to DHS reached up to 55% compared to the HLS group ($p>0.05$, Figure 5.3).

Bone Marrow MSC Population – Day 21

Interesting results were observed by day 21. HLS continued to reduce the bone marrow MSC number for 78% compared to age-matched controls ($p<0.001$). The elevated bone marrow MSC number by DHS in conjunction with HLS was diminished. Significant reduction of the MSCs in the bone marrow was again observed in the HLS+DHS group, by 89% compared to the age-matched control ($p<0.001$, Figure 5.4).

Discussion

The present study focused on the mechanical contribution of DHS to the bone marrow cellular environment and indicated that non-invasive DHS was able to promote the number of MSCs residing in the bone marrow. The external DHS serves as a direct coupling with oscillatory marrow fluid pressure, which may lead to influences in the interstitial fluid flow in bone and regulate skeletal mechanotransductive mechanisms. Longitudinal bone marrow MSC

quantifications showed an interesting time-dependent manner of DHS to encounter the reduced MSC growth under disuse condition. The gradual changes of the MSC population size by DHS outlined the MSC activities and their contributions to the phenotypic changes in bone tissue.

To evaluate the changes in MSC population in response to DHS, flow cytometry analysis was employed to quantify the MSC cell counts of the bone marrow extracts. MSCs have been reported as expressing a series of surface markers, including CD90.1, CD29, and CD49e [157, 158]. CD45 is often used as a negative marker of MSCs to be isolated from hematopoetic stem cells (HSCs) [157, 159, 160]. CD11b is also often used as a negative marker of MSCs to isolate them from monocytes and macrophages [161]. To specifically isolate the MSCs, antibodies for CD90.1, CD29, CD49e, CD11b and CD45 were utilized.

The experiment reported here gave rise to data that support the growing body of evidence of how MSC growth potential and osteogenic potential respond to the mechanical environment. Gravity is a crucial factor for the differentiation and function of osteoblasts that are required for the maintenance of skeletal integrity. When exposed to normal gravity, MSCs are able to differentiate into osteoblasts followed by matrix mineralization under *in vitro* induction conditions [109, 162]. Previous *in vivo* studies showed a decreased osteogenesis in young rats treated with HLS, signifying the important role of osteogenesis in maintaining bone mass under disuse condition [163, 164]. Pan et al. found decreased *ex vivo* growth potential and osteogenesis of MSCs in the rat femurs subjected to HLS compared to the ones from the control rats [109]. Once again, the effects of unloading on MSC osteogenesis indicated its effects on osteoprogenitors, which are closely correlated to the observed changes in osteoblastic bone formation. Bone formation is initiated with stem cell proliferation and condensation [86, 87]. Changes in the mechanical environment, i.e., through low-magnitude mechanical loading, can

potentiate the number of MSCs that reside in the bone marrow. Furthermore, these load-driven mechanical signals have been shown to bias the MSC differentiation toward osteoblastogenesis over adipogenesis, promoting bone formation [101].

Therefore, as a novel form of low-magnitude external mechanical loading on bone, DHS serves great potential to encounter bone marrow MSC reduction due to disuse (e.g., HLS). Combining with previous findings on DHS's mitigation effects on disuse trabecular bone loss, it is suggesting that DHS may change the perfusion pressure that is associated with increased blood flow to the limbs [165], which mediates bone fluid flow (BFF) that alters the mechanical environment of bone marrow MSCs and further leads to the expression of osteogenic factors [166]. A limitation of the current study is that differentiation experiments on *ex vivo* MSCs were not included. However, our previous study has clearly showed the osteogenic adaptive response to DHS in a rat HLS model, indicating its osteogenic phenotypic outcome. This finding suggests that mechanical signals from DHS may have promoted the osteoblast differentiation from the MSC population in order to elicit the phenotypic osteogenic bone formation. This will also encourage our future investigations into the local cellular effects, e.g., osteoblasts and osteoclasts, in response to DHS.

One interesting finding in the present study is the non-linear time-dependent fashion of DHS in encountering the reduced MSC growth under disuse condition. The gradual changes on the MSC quantity in response to DHS suggest that the MSC growth activities seemed to take place within a certain time window (Figure 5.5). This once again supports our hypothesized mechanism that MSCs may respond to the DHS-derived mechanical signals, undergoing proliferation and differentiation into osteoblasts over time. These step-wise and highly coordinated activities may eventually contribute to the phenotypic change in bone tissue. As

observed in our previous work, bone growth was already accomplished by day 28. As an earlier event, it is reasonable to see enhanced MSC proliferation in response to the mechanical signals of DHS at earlier time points (7~14 days).

In summary, this study indicated that the MSC pool was positively influenced by the mechanical signals driven by DHS, which provided an important piece of information to elucidate the downstream cellular effects of mechanical signals and their contribution to enhance bone quality. DHS, as a novel and non-invasive intervention regulating skeletal adaptation, not only provides significant insights for future clinical applications, but also serves as an ideal tool to delineate the complex mechanotransductive mechanisms in the skeleton.

Figures

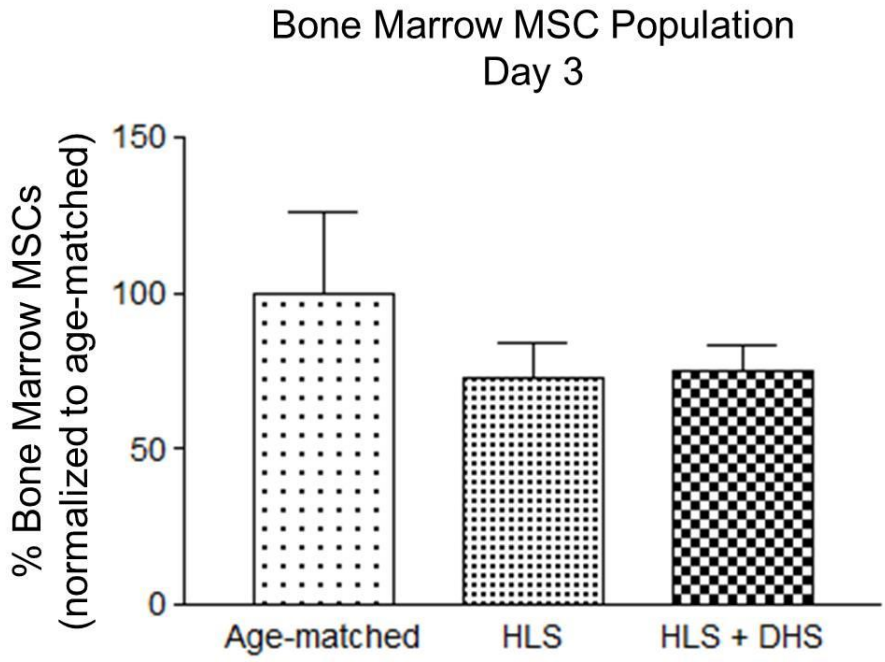

Figure 5.1. Bone marrow MSC population – day 3. Graphs show mean±SD. HLS reduced the total MSC number in the bone marrow, although it was not statistically significant (p>0.05). At this stage, DHS did not have any effect on the bone marrow MSC population under disuse condition.

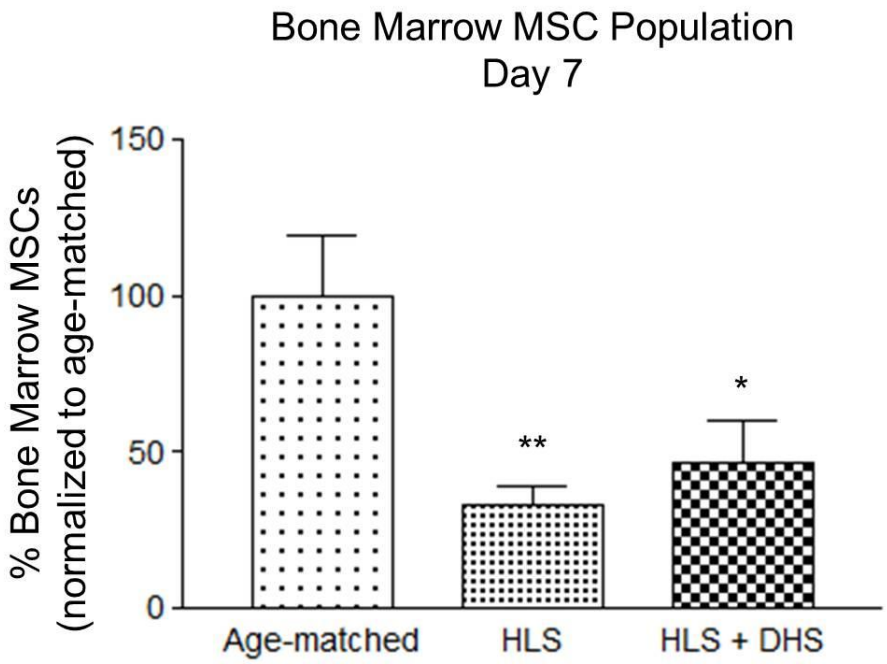

Figure 5.2. Bone marrow MSC population – day 7. Graphs show mean±SD. HLS significantly reduced the total bone marrow MSCs compared to age-matched control ($p<0.01$). By this day, DHS started to elevate the MSC number within the bone marrow ($p>0.05$). *$p<0.05$ vs. age-matched; **$p<0.01$ vs. age-matched.

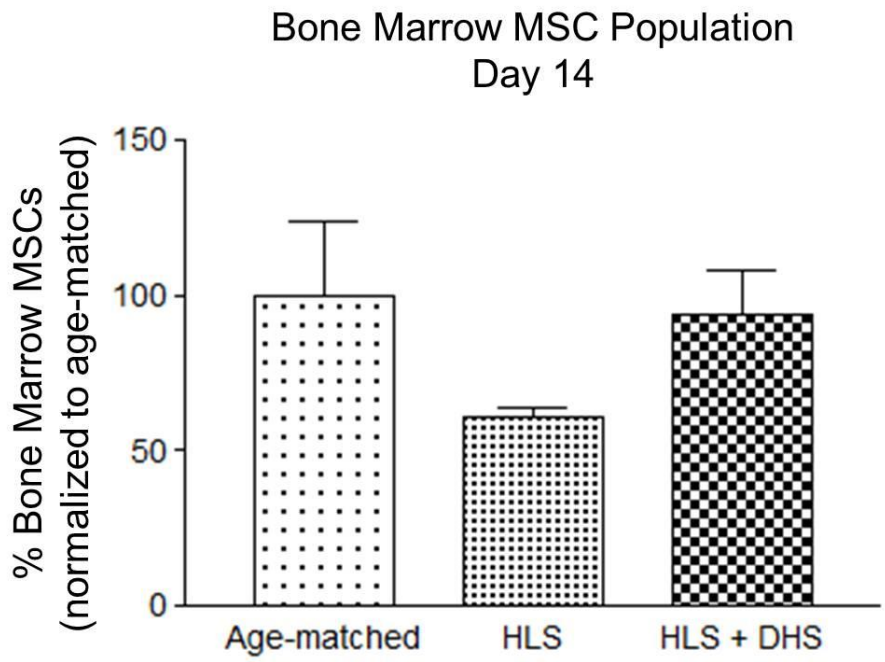

Figure 5.3. Bone marrow MSC population – day 14. Graphs show mean±SD. HLS greatly reduced the bone marrow MSCs compared to age-matched control (p>0.05). The increase of MSC number of the DHS-treated group became more apparent compared to HLS (p>0.05).

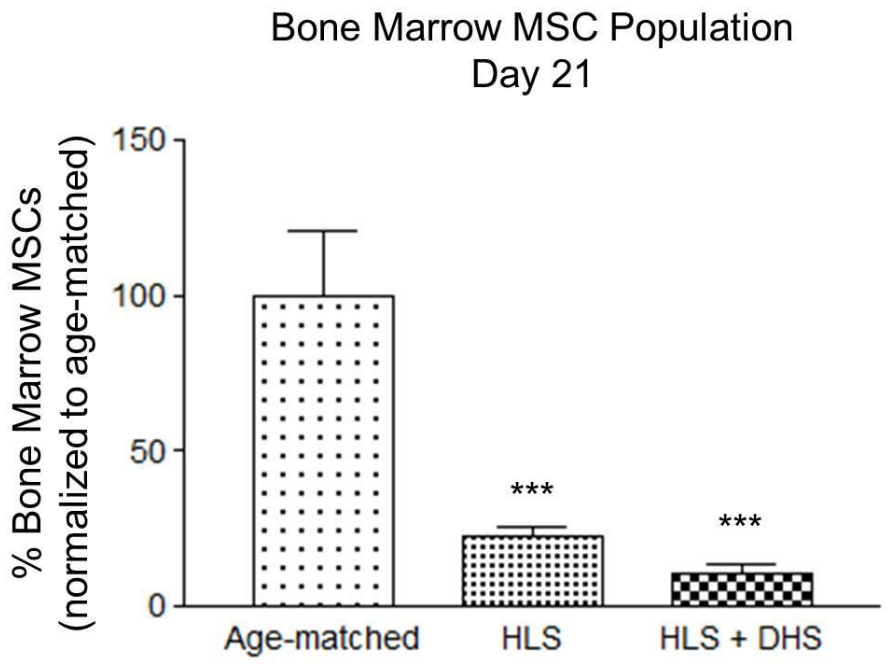

Figure 5.4. Bone marrow MSC population – day 21. Graphs show mean±SD. HLS continued to reduce the bone marrow MSC number (p<0.001). The previous elevated bone marrow MSC number by DHS in conjunction with HLS was diminished. Significant reduction of the MSCs within the bone marrow was again observed in the DHS-treated group compared to age-matched control (p<0.001). ***p<0.001 vs. age-matched.

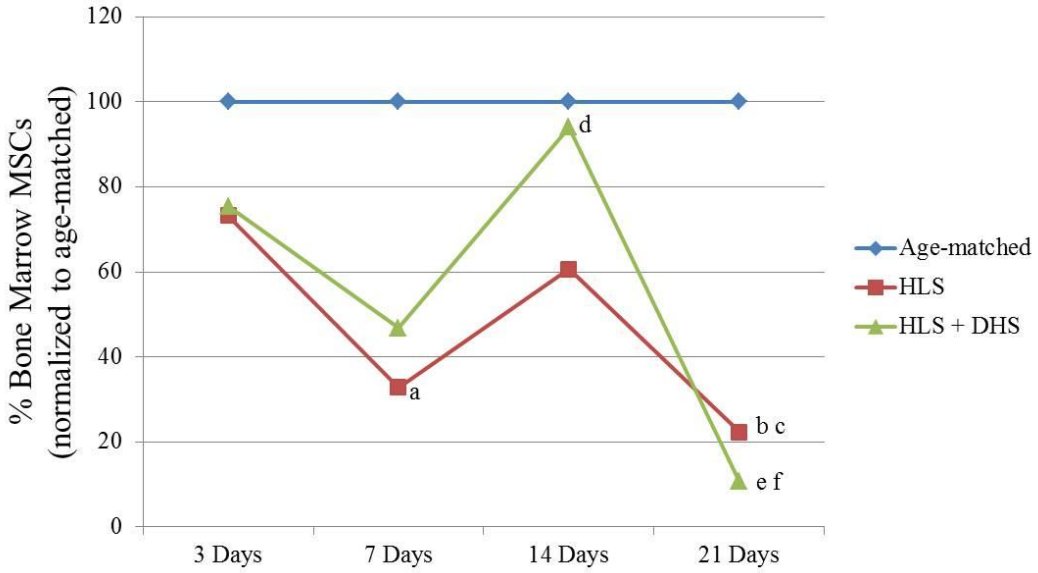

Figure 5.5. Summary of bone marrow MSC numbers of age-matched, HLS and HLS+DHS groups over 3 days, 7 days, 14 days, and 21 days. Normalized to age-matched, MSC numbers of HLS and HLS+DHS groups had similar trends of reductions, which the MSC numbers were greatly reduced by day 7, peaked on day 14, and diminished by 21 days. Compared to HLS, the induction of the MSC number in response to DHS gradually increased between 7 to 14 days. [a]$p<0.01$ vs. HLS – Day 3; [b]$p<0.01$ vs. HLS – Day 14; [c]$p<0.001$ vs. HLS – Day 3; [d]$p<0.05$ vs. HLS+DHS – Day 7; [e]$p<0.01$ vs. HLS+DHS – Day 3; [f]$p<0.001$ vs. HLS+DHS – Day 14.

Chapter 6 – The Alterations of the Gene Expressions of Osteogenic Growth Factors and Transcription Factors in Response to Dynamic Hydraulic Stimulation

Abstract

Mechanical stimulation serves as a key determinant to maintain and enhance skeletal mass and strength. Our group has recently developed a dynamic hydraulic stimulation (DHS) as a novel loading modality to induce anabolic responses in bone. Subsequent research should point to further investigation on the functional process of how DHS-derived mechanical signals act on bone cells to regulate bone metabolism. Therefore, the present study extended the previous findings of DHS and to evaluate the alterations of the gene expressions of osteogenic growth factors and transcription factors in response to DHS over time. Using a model system of 5-month old hindlimb suspended (HLS) female Sprague Dawley rats, DHS was applied to the right tibiae of the stimulated rats with a loading frequency of 2 Hz and a magnitude of 30 mmHg static pressure + 30 mmHg (peak-to-peak) dynamic pressure. The daily loading regime was set as "10 min on – 5 min off – 10 min on" over a time course of 3 days, 7 days, 14 days, and 21 days. Rats in the 3-day group were stimulated for 2 days; and the rats in the other groups were stimulated for 5 days/week. According to the time points, animals were sacrificed and the total RNA was isolated from the stimulated and control tibiae for quantitative real-time PCR analysis of the selected osteogenic genes (runx2, β-catenin, osteopontin, VEGF, BMP2, IGF-1, and TGF-β). Overall, interesting data indicated a time-dependent fashion of gradual changes in mRNA levels in response to DHS. Great reductions of the overall mRNA levels of the selected genes were observed in the HLS rats compared to age-matched controls. On the other hand, while DHS-driven fold changes of the mRNA levels remained low before day 7, the fold changes started to elevate by day 14 and then became less pronounced by day 21. This study indicated that the gene expressions of the selected osteogenic growth factors and transcription factors were altered in response to DHS. However, it was highly time-dependent. Together with our previous

observations of DHS-driven mitigation of phenotypic bone loss and reduction of MSC proliferation under disuse condition, this study further delineated the underlying molecular mechanism of DHS-derived mechanical signals. This allows us to better understand DHS's functions as a potential clinically applicable treatment for osteopenia/osteoporosis.

Introduction

Bone responds and adapts to its surrounding mechanical environment through the mechanotransduction process of bone cells, which involves the perception of extracellular stimuli and their conversion into downstream intracellular molecular events. This in turn transmits load-induced signals to the nucleus and the expressions of bone-related genes that further regulate bone metabolism [110]. Hence, amplified mechanical stimulation triggers biochemical signaling pathways that excite osteoblastic differentiation and proliferation, resulting in bone formation [114, 115]. Therefore, based on mechanical loading as a powerful anabolic stimulus for bone, interventional modalities delivering mechanical signals to the skeleton can provide an alternate non-pharmacological approach to treat disuse osteoporosis. However, the functional process of mechanical loading on mechano-sensing and adaptive response of bone cells requires a complex arrangement of growth factors as well as the activation of specific transcription factors for their target genes, which to determine the coordinated function of skeletal cells [116].

Dynamic hydraulic stimulation (DHS) is a recently developed, non-invasive modality as a potential countermeasure for osteopenia/osteoporosis. By using a hindlimb suspension (HLS) functional disuse rat model, DHS was shown to be able to mitigate tibial trabecular bone loss under such disuse condition [127]. Focusing on load-driven bone adaptation in the tibiae in

response to DHS and to follow up on our previous findings, the objective of the present study was to investigate the molecular mechanism of load-induced changes in the expressions of genes related to bone formation. The proposed mechanism may underlie the skeletal responses to the mechanical stimuli derived from DHS, i.e., eliciting downstream molecular responses. Mechanical signals derived from DHS may activate certain surface receptors of bone mechano-sensing cells, which in turn trigger signaling pathways that ultimately enhance the gene expressions of osteogenic growth factors and transcription factors.

Secretion of growth factors following mechanical stimulation aids to trigger bone regeneration. Some of the most potent growth factors include the transforming growth factor-β (TGF-β), the insulin-like growth factors (IGFs), the bone morphogenetic protein-2 (BMP-2) [116, 117], and vascular endothelial growth factor (VEGF) [116, 118]. Functions of these growth factors include enhancement of osteoprogenitor cells' and osteoblasts' proliferation during bone regeneration [117, 119], involvement in marrow stromal cells regulated osteoblast proliferation and osteoblastogenesis induction [117, 120], facilitation of the differentiation of mesenchymal stem cells (MSCs) to osteochondroblastic lineage [119, 121], and promotion of osteoblast differentiation and increases of mineralization of regenerated bone [118]. Intracellular signaling pathways are activated upon mechanical stimulation, which in turn converge with growth factors and activate transcription factors that promote bone formation [116]. Committed osteoprogenitor cells from MSCs further differentiate into osteoblasts, which then express osteoblast phenotypic genes once become mature and functional [122]. As a principal transcription factor, runx2 regulates osteoblast differentiation [123]. Downstream of runx2, β-catenin is a transcription factor that contributes to the control of osteoblastogenesis [124]. Other transcription factors, such

as osteopontin, modulate both osteoblastic and osteoclastic functions in response to cytokines and mechanical signals [125].

Bone formation progresses over time after the initiation of mechanical loading. Within 24 to 48 hours after mechanical loading starts, new osteoblasts lay on the bone surface and contribute to bone formation that is observed after 96 hours of loading. Bone formation follows a time-dependent manner, in which it increases between 5~12 days of loading and returns back to baseline levels after 6 weeks of loading. These data suggest that the whole cycle of bone formation, including osteoblast recruitment followed by matrix production, lasts for about 5 weeks before declining back to baseline levels [167]. Hence, the underlying molecular regulatory mechanism in bone following mechanical loading becomes an interesting research focus, yet it is not fully understood.

Knowing the phenotypic response of bone to DHS, the present study aimed to elucidate the alterations of the gene expressions of osteogenic growth factors and transcription factors in response to DHS over a time course. It was hypothesized that DHS activates the gene expressions of osteogenic growth factors and transcription factors that are involved in mechanotransduction and bone metabolism, in which the sequence of the events is time-dependent. In this study, we evaluated the DHS-induced expressions of selected osteogenesis related genes over a time course of 3 days, 7 days, 14 days, and 21 days.

Materials and Methods

Experimental Design

All experimental procedures were approved by Stony Brook University IACUC. Ninety-six 5-month old female Sprague Dawley virgin rats (Charles River, MA) were used to investigate

the alterations of the gene expressions of osteogenic growth factors and transcription factors in response to DHS. Housing in 18”x18”x24” (LxWxH) stainless steel HLS cages in animal room with a 12:12 hours light:dark cycle and temperature-control, the animals were provided with standard rodent chow and water *ad libitum*. The groups of the animals were: 1) age-matched – day 3 (n=8), 2) HLS – day 3 (n=8), 3) HLS+DHS – day 3 (n=8), 4) age-matched – day 7 (n=8), 5) HLS – day 7 (n=8), 6) HLS+DHS – day 7 (n=8), 7) age-matched – day 14 (n=8), 8) HLS – day 14 (n=8), 9) HLS+DHS – day 14 (n=8), 10) age-matched – day 21 (n=8), 11) HLS – day 21 (n=8), 12) HLS+DHS – day 21 (n=8). HLS was introduced to induce functional disuse to the rat hindlimbs. With the similar procedure as previous [127], animal’s tail was cleaned with 70% alcohol and then lightly coated with tincture of benzoin. A piece of surgical tape forming a loop was attached to the end of the tail. The surgical tape was secured by three strips of elastic adhesive bandage. The loop formed from the surgical tape was linked to a tail harness apparatus and a swivel hook suspended from the top of the cage. For an approximately 30° head-down tilt, the animals were suspended with the hindlimbs about 2 cm above the cage ground. Animals’ forelimbs were fully allowed for movements. Animals’ body weights were recorded regularly throughout the entire study; and their overall health were carefully monitored.

DHS Loading Protocol

Daily DHS was applied to the stimulated animals in conjunction with HLS. With the similar setup as in a previous study [127], DHS was delivered to the right tibia by placing a costume-made inflatable cuff around the right hindlimb over the tibia. Dynamic frequencies and magnitudes were controlled by an actuator-driven syringe connected to a programmable 100 MHz waveform/signal generator (Model 395, Wavetek). DHS was given with a stimulation

frequency of 2 Hz and a magnitude of 30 mmHg static pressure + 30 mmHg (peak-to-peak) dynamic pressures. Daily loading regime was set as "10 min on – 5 min off – 10 min on" over a time course of 3 days, 7 days, 14 days, and 21 days. Rats in the 3-day groups were stimulated for 2 days, and rats in the other groups were stimulated for 5 days/week. In the end, the rats were euthanized at the corresponding time points.

RNA Isolation

To determine mRNA levels of the selected genes, the stimulated right tibiae and the age-matched controls were harvested. The bone marrow within the tibiae was flushed out, and the surrounding soft tissues were dissected out from the bone samples. The bone tissue samples were then incubated immediately in RNAlater RNA Stabilization Reagent (Qiagen) and stored at -80ºC until ready for analysis. The frozen bone samples were ground with a mortar and pestle with RNeasy Plus lysis buffer while remain frozen. A QIA shredder spin column (Qiagen) was used to remove the tissue debris. Total RNA was collected using a standard procedure with an RNeasy plus mini kit (Qiagen) [168]. The total RNA samples were diluted down to 20ng/μl. By using the high capacity cDNA reverse transcription kits (Applied Biosystems), ~200ng of total RNA per sample was reverse transcribed into cDNA.

Quantitative Real-time PCR

Quantitative real-time PCR was conducted to examine the expressions of the selected genes (runx2, β-catenin, osteopontin, VEGF, BMP2, IGF-1, and TGF-β) along with a housekeeping gene GAPDH as an internal control (Gene Expression Assays, Applied Biosystems). The following quantitative real-time PCR was performed using TaqMan Gene Expression Master Mix Kit (Applied Biosystems) [168]. Following the calibration using the

GAPDH mRNA levels, the mRNA levels of the samples were normalized to the averaged mRNA levels of the age-matched control samples to derive the relative mRNA fold changes.

Statistical Analysis

Statistical outliers were excluded via Grubbs' test method with Alpha=0.05 significance level using GraphPad QuickCalcs Outlier Calculator. Values as mean±SD were used for the statistical analysis of the results, and the values were shown as mean±SE in the figures. Differences between groups were determined using GraphPad Prism 3.0 Software (GraphPad Software Inc., La Jolla, CA). One-way ANOVA with Tukey's post-hoc test was performed with normal equal variance to determine the differences among groups. The level of significance was established at $p<0.05$.

Results

mRNA Levels in the Tibiae – Day 3

After the first three days, HLS greatly reduced the mRNA levels of all the selected genes compared to age-matched controls (Figure 6.1). For instance, the fold changes of the HLS group were lowered by 51%, 89%, 87%, 61%, 70%, 47%, and 86% compared to age-matched controls, respectively to runx2, β-catenin, osteopontin, VEGF, BMP2, IGF-1, and TGF-β. At this stage, the effects of DHS were not obvious, where the mRNA levels in the DHS-treated group were similar to the HLS group for most of the selected genes, except for runx2. Interestingly, runx2 mRNA level of the DHS-treated group was 59% lower compared to the HLS group.

mRNA Levels in the Tibiae – Day 7

By day 7, the overall reductions of the mRNA levels in the HLS group compared to age-matched controls were lower than the day-3 data (Figure 6.2). At this stage, HLS reduced the

mRNA levels of the selected genes by 28%, 24%, 44%, 21%, 31%, 26%, and 21% compared to age-matched controls, respectively to runx2, β-catenin, osteopontin, VEGF, BMP2, IGF-1, and TGF-β. The mRNA levels of the DHS-treated group of all the selected genes remained low. For instance, the fold changes of the DHS-treated group were 0.06 (runx2), 0.04 (β-catenin), 0.54 (osteopontin), 0.07 (VEGF), 0.05 (BMP2), 0.05 (IGF-1), and 0.05 (TGF-β).

mRNA Levels in the Tibiae – Day 14

By day 14, the selected genes in the DHS-treated group were greatly upregulated. For instance, the fold changes of the DHS-treated group were 3.0 (runx2), 4.5 (β-catenin), 3.5 (osteopontin), 3.5 (VEGF), 3.7 (BMP2), 4.6 (IGF-1), and 3.2 (TGF-β). Comparing to the HLS, the DHS-driven fold changes increased by 64%, 94% 102%, 187%, 79%, 102%, and 44% respective to runx2, β-catenin, osteopontin, VEGF, BMP2, IGF-1, and TGF-β (Figure 6.3).

mRNA Levels in the Tibiae – Day 21

By day 21, the elevated mRNA levels of the DHS-treated group were slightly less pronounced compared to day-14's data. Specifically, the DHS-driven fold changes were 1.2 (runx2), 2.4 (β-catenin), 1.8 (osteopontin), 1.9 (VEGF), 2.5 (BMP2), 2.2 (IGF-1), and 2.4 (TGF-β). Comparing to the HLS, the DHS-driven fold changes increased by 110%, 80% 128%, 60%, -8%, 92%, and 14%, respectively to runx2, β-catenin, osteopontin, VEGF, BMP2, IGF-1, and TGF-β (Figure 6.4).

Discussion

The present study describes the molecular analyses of load-driven responses to a novel form of mechanical loading - DHS, in which its mitigation effect on disuse trabecular bone loss has been demonstrated in a previous study [127]. Real-time PCR analysis focused on the

mechanical contribution of DHS to the tibial bone mRNA levels of the selected osteogenic genes, which provided us a deeper understanding on the underlying mechanotransductive mechanism. The external DHS loading may directly couple with oscillatory marrow fluid pressure and further leads to influences in bone fluid flow (BFF), regulating skeletal mechanotransductive mechanisms that ultimately lead to bone formation. Longitudinal real-time PCR analysis of the selected osteogenesis-related genes showed an interesting time-dependent behavior of DHS loading of encountering these gene suppressions under disuse condition. The time-dependent changes of the expressions of the osteogenesis-related genes by DHS outlined their potential contributions to the phenotypic changes in bone tissue.

Bone formation by osteoblasts is one of the crucial steps of bone remodeling, which is an essential function for continuous bone renewal to maintain the structural integrity and metabolic capacity of the skeleton throughout one's lifetime [116]. Osteoblasts are originated from MSCs and form the bone multicellular unit with other bone-forming cells (e.g., osteocytes and bone-lining cells), bone-resorbing cells (e.g., osteoclasts), and their progenitor cells and associated cells (e.g., endothelial cells) [169-171]. The growth and differentiation of osteoblasts are determined by a complex array of growth factors and intracellular signaling [116].

Augmented external biomechanical stimulation, such as DHS in the present study, may trigger the recognition of mechanical signals by osteoblasts. The received signals then ultimately induce secretion of growth factors that act as local regulators for osteogenesis. Potent growth factors, including IGF, TGF-β, BMP and VEGF, strongly modulate the osteoblastic activities as well as other bone growth regulators [116]. These genes play critical roles in the fate of osteoblastogenesis, which is crucial for bone formation. *In vitro* mechanical loading induced TFG-β production in osteoblasts, as well as in MSCs [172-174]. *In vitro* and *in vivo* mechanical

loading enhanced IGF gene expression in MSCs [175] and human osteoblasts [176]. Mechanical stimulation of osteoblasts resulted in upregulation of BMP-2 mRNA [177]. VEGF gene expression was upregulated in osteoblasts [178] and in bone marrow MSCs [174] in response to *in vitro* mechanical stimulation. In the current study, amplifications of the expressions of these genes were observed upon DHS over 14 days, strongly indicating the anabolic effect of DHS in bone.

Studies have shown that significantly altered gene expressions of 140 osteogenesis-related genes, including runx2 in 2T3 preosteoblasts, were observed under weightlessness condition. Specifically, only 3 days of unloading decreased the mRNA levels of ALP, runx2, and PTHR1 by 5, 2, and 5 folds, respectively [105, 179]. Similar observations were seen in our present study. By day 3 of HLS, unloaded tibial bones showed greatly reduced mRNA levels of the selected osteogenesis-related genes. This observed reduction continued over 21 days.

On the other hand, studies of mechanical loading have demonstrated the effects of mechanostimulation on the expression levels of growth factors and transcription factors. For instance, *in vitro* cyclic and static stretching of osteoblasts (MC3T3-E1) was shown to increase IGF-mediated signaling, leading to differentiation of late osteoblasts and early osteocytes [117, 180]. Mechanical strains of 2000 με on human osteoblast-like cells (SaOS-2) induced bone-forming indices, whereas strains of 200,000~300,000 με led to reductions [176, 181, 182]. Inductions of BMP-mediated upregulations of runx2 and smad1 phosphorylation were observed in human SaOS in response to compression force. BMP mRNA level was elevated by *in vitro* sinusoidal cyclic stretch on human spinal ligament cells [117, 183, 184]. In cultured osteoblasts, load-driven upregulations of ALP and runx2 were reported [104, 179, 185]. Our present study showed mechanical loading-dependent upregulations of the mRNA levels of the selected genes

in an *in vivo* setting. After 14 days, pronounced increases in the mRNA levels of the selected genes were shown in the DHS-treated group compared to the HLS group. This increase of gene expressions continued but started to diminish by day 21. Our group previously presented a longitudinal study of bone marrow MSC quantification under DHS in a rat HLS model, where MSC number was greatly increased in response to DHS by day 14 and diminished by day 21. MSCs may have completed proliferation and begin to differentiate toward osteoblastogenesis at this stage. In the meantime, the induced mRNA levels of the selected genes that we observed in the present study may couple the process of transforming MSC proliferation and differentiation into osteoblasts, which may commit to the subsequent bone formation. Strong mitigation effect of DHS on disuse trabecular bone loss has been demonstrated in our previous published work. Altogether, the *in vivo* study of the phenotypic change in bone tissue as well as the longitudinal studies of bone marrow MSC quantification and mRNA levels of osteogenesis-related genes compile these events as a sequential pathway of how DHS exerts its mechanical signals to bone cells. How bone cells respond to such stimuli contributes to the phenotypic change in bone.

At the earlier time points, i.e., 3 days and 7 days, DHS did not induce the mRNA levels of the selected genes compared to the according HLS groups (Figure 6.5). By incorporating the longitudinal bone marrow MSC quantification data, bone marrow MSCs seemed to start proliferating and the total MSC number increased compared to HLS group during the first 7 days. However, the mRNA levels of the selected osteogenesis-related genes remained low by day 7. Based on the sequential events of MSC proliferation and differentiation, it may be suggesting that the MSCs were still undergoing the proliferation activity. Since the differentiation process had not begun yet, expressions of the osteogenesis-related genes were inactive.

In summary, this study indicated that the mRNA levels of the selected osteogenesis-related genes were positively influenced by the mechanical signals derived from DHS, which provides important understanding of the downstream molecular mechanism of DHS in bone adaptation. DHS is not only a novel, non-invasive intervention for regulating skeletal adaptation, it also serves as a unique tool to study the molecular mechanotransduction process in response to the fluid flow stimuli in bone.

Figures

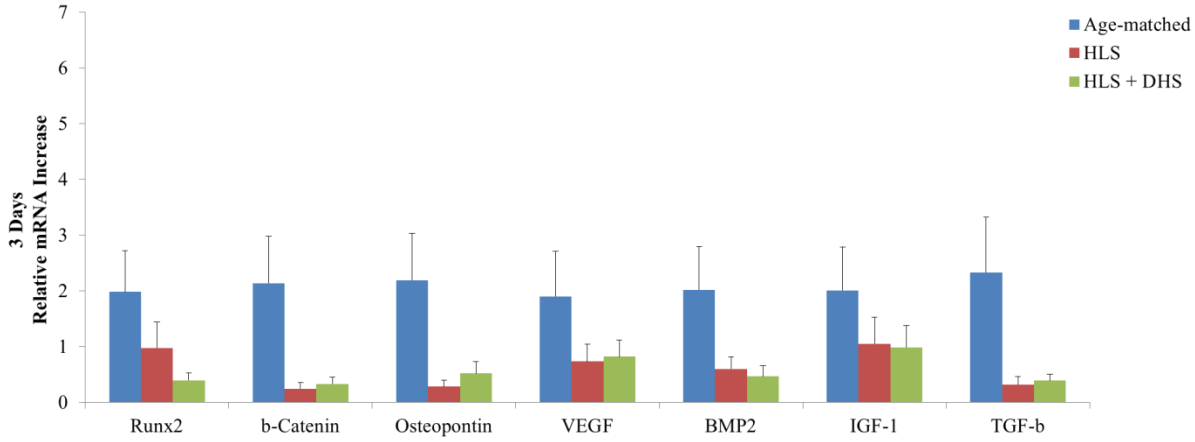

Figure 6.1. mRNA levels in the tibiae – day 3. Graphs show mean±SE. HLS greatly reduced the mRNA levels of all the selected genes compared to age-matched controls. The effect of DHS was not obvious, where the mRNA levels in the DHS-treated group were similar to the HLS group for most of the selected genes, except for runx2.

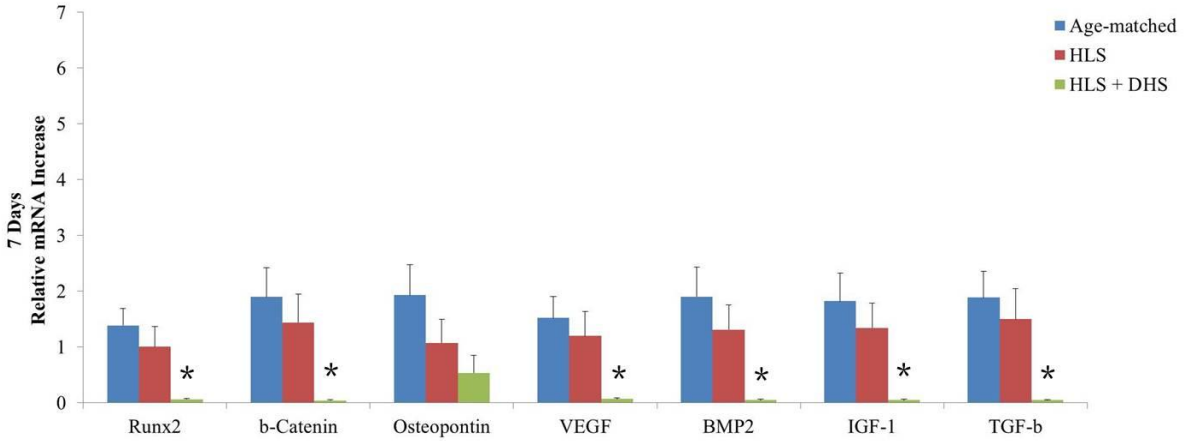

Figure 6.2. mRNA levels in the tibiae – day 7. Graphs show mean±SE. The overall reductions of the mRNA levels in the HLS group compared to age-matched controls were lower than day-3's data. Interestingly, the mRNA levels of DHS-treated group of all the selected genes remained low. *p<0.05 vs. HLS.

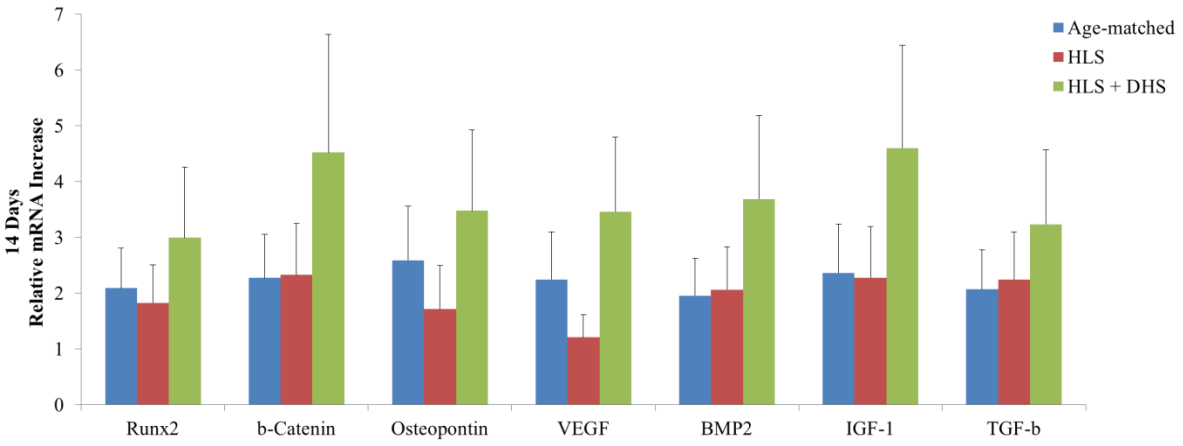

Figure 6.3. mRNA levels in the tibiae – day 14. Graphs show mean±SE. The selected genes in the DHS-treated group were greatly upregulated. For instance, the fold changes of the DHS-treated group were 3.0 (runx2), 4.5 (β-catenin), 3.5 (osteopontin), 3.5 (VEGF), 3.7 (BMP2), 4.6 (IGF-1), and 3.2 (TGF-β).

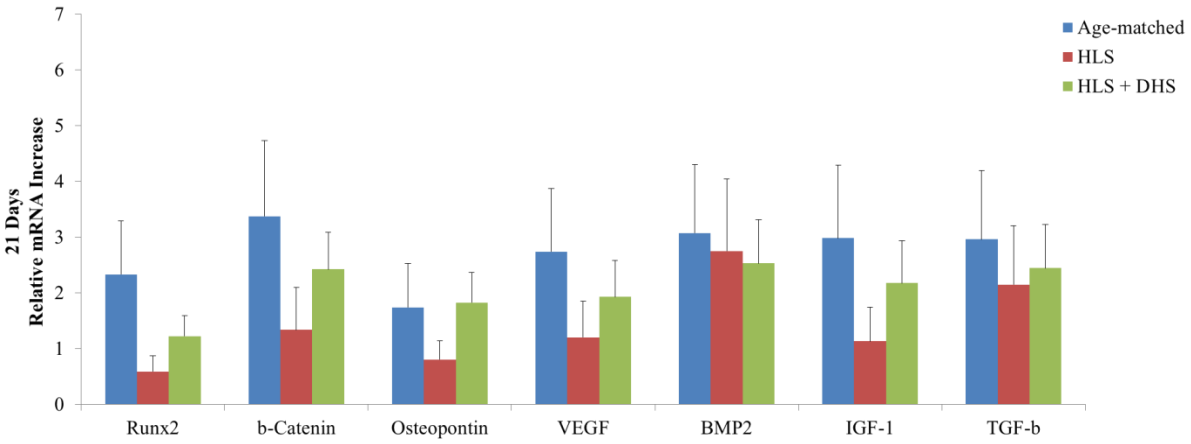

Figure 6.4. mRNA levels in the tibiae – day 21. Graphs show mean±SE. The elevated mRNA levels of the DHS-treated group were slightly less pronounced compared to day-14's data. Specifically, the DHS-driven fold changes were 1.2 (runx2), 2.4 (β-catenin), 1.8 (osteopontin), 1.9 (VEGF), 2.5 (BMP2), 2.2 (IGF-1), and 2.4 (TGF-β).

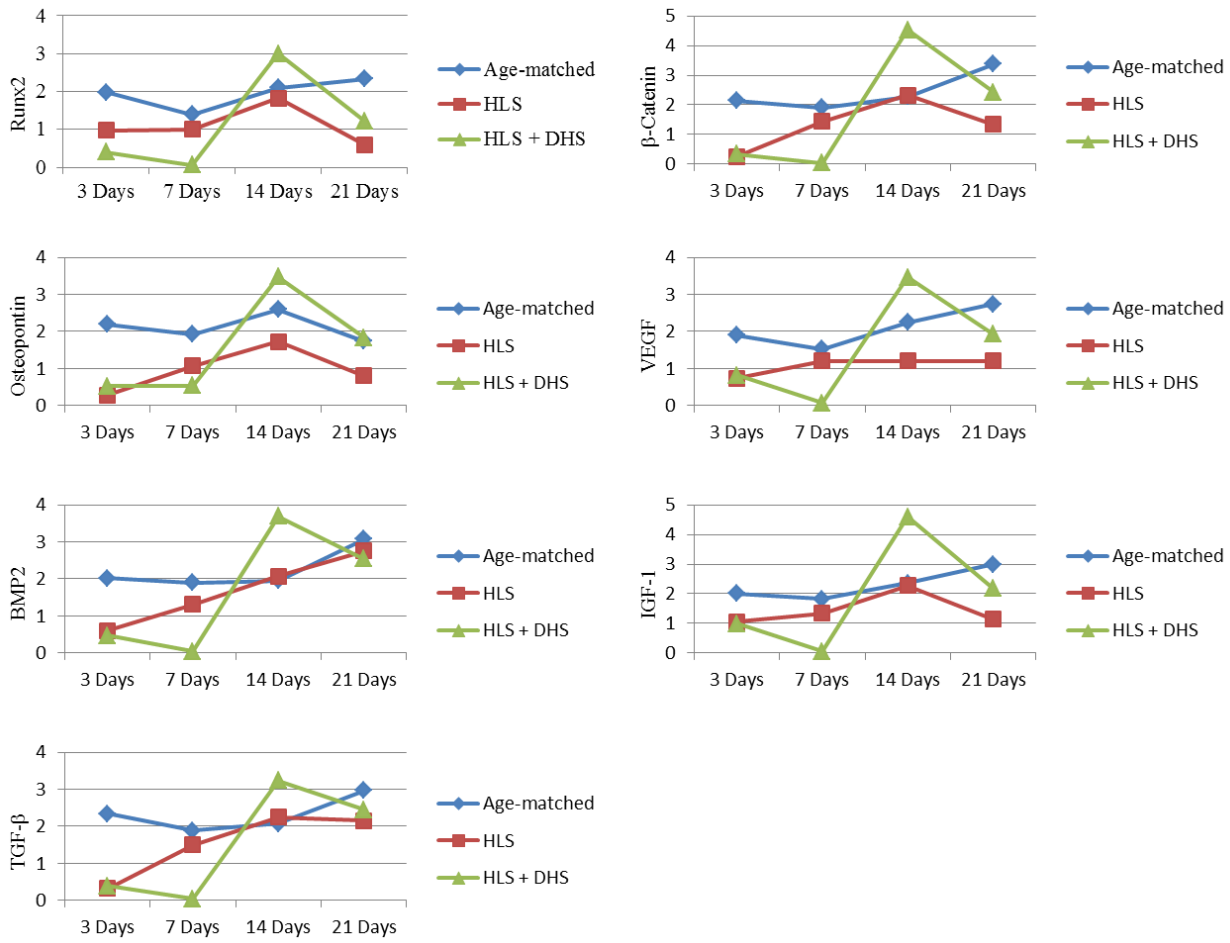

Figure 6.5. Summary of mRNA fold changes of the selected osteogenesis related genes over the 21-day time course. In general, the mRNA levels of the selected genes in the HLS groups attempted to catch up to the according age-matched levels. However, the mRNA levels of these genes in the HLS+DHS groups did not elevate until day 14.

Chapter 7 - Overall Discussion

The regulatory potentials of a novel, non-invasive dynamic hydraulic stimulation (DHS) on skeletal responses at the tissue, cellular, and molecular levels were investigated in this dissertation. It was hypothesized that DHS mediates intramedullary pressure (ImP)-induced regulation of bone fluid flow (BFF) and promotes osteogenic adaptation, which in turn mitigates bone deterioration under disuse condition. The hypothesis was tested via four specific aims, in which the ability of DHS to induce ImP, the effects of DHS on skeletal tissue under disuse condition, the effects of DHS on bone marrow mesenchymal stem cell (MSC) population, and the alterations of the gene expressions of osteogenic growth factors and transcription factors in response to DHS were investigated. The results from this study indicated that DHS can induce ImP and trigger cellular and molecular responses in bone, leading to successful mitigation of disuse bone loss. In particular, the degree of DHS-mediated ImP induction was highly dependent on the loading frequency; and the cellular and molecular responses to DHS were suggested to be time-dependent. Based on these studies, four major conclusions can be drawn:

1. Direct ImP and bone strain measurements on rats showed noticeable ImP induction by oscillatory DHS in the stimulated tibiae. Over the range of DHS loading frequencies, the observed ImP (peak-to-peak) values were induced in a nonlinear fashion and peaked at 2 Hz. On the other hand, minimal bone strain (<8 με) was detected upon oscillatory DHS on the tibiae at various loading frequencies. We did not see noticeable induction of ImP or bone strain in the un-stimulated femur.
2. Demonstrating in a hindlimb suspension (HLS) functional disuse rat model, trabecular bone quantity and microarchitecture were significantly improved by the application of DHS loading. Increases of 83% BV/TV and 25% Tb.N, as well as a decrease of 26% in Tb.Sp compared to the HLS were observed via μCT analysis. Histomorphometry analysis

of trabecular mineralization further confirmed the μCT data, in which DHS loading yielded increases of histomorphometric BV/TV, MS/BS, BFR/BS, and BFR/BV compared to HLS.

3. The *in vivo* longitudinal study evaluated the bone marrow MSC quantifications in response to DHS over 3 days, 7 days, 14 days, and 21 days. The results indicated a time-dependent fashion of gradual bone marrow MSC inductions in response to DHS, which peaked on day 14. This study indicated that the bone marrow MSC proliferation was positively influenced by the mechanical signals derived from DHS.
4. In the same *in vivo* longitudinal study over the time course (3 days, 7 days, 14 days, and 21 days), RNA was isolated from the stimulated and control tibiae for quantitative real-time PCR analysis on the selected osteogenesis-related genes (runx2, β-catenin, osteopontin, VEGF, BMP2, IGF-1, and TGF-β). Overall, the data indicated a time-dependent fashion of gradual changes of the mRNA levels in response to DHS. DHS-driven fold changes of the mRNA levels started to elevate by day 14 and became less pronounced by 21 days. This study indicated that the gene expressions of the selected osteogenic growth factors and transcription factors were altered in response to DHS, yet it was highly time-dependent.

Altogether, these data strongly suggest that oscillatory DHS may regulate the skeletal tissue fluid dynamics, which serves critically in bone adaptation. Demonstrating at the tissue, cellular, and molecular levels, DHS was shown to be able to mediate ImP and promote osteogenic adaptation, which in turn mitigates bone deterioration under disuse condition. The results from this dissertation clearly imply DHS's ability as an effective, non-invasive intervention for potential osteopenia and osteoporosis treatments.

The importance of dynamic mechanobiology and cyclic load-induced signaling on skeletal health has long been recognized, in which mechanical signals play a critical role in strong anabolic potential and naturally gauge bone strength [18]. BFF, a communication media between an external load and bone cells, serves as a potent regulator in bone remodeling [76-81]. Regulatory factors such as strain and ImP are potential determinants to alter BFF, mediating bone adaptation under normal and disuse conditions. While several *in vivo* studies using invasive methods have shown that BFF altered by ImP with no bone strain can drive bone remodeling, isolating these two factors non-invasively is still challenging.

A large body of strong evidence has pointed out that BFF can be altered by external muscular activities through various mechanisms [133, 134]. The muscle pump theory describes that when skeletal muscle contracts, the within blood vessels are compressed, which then leads to the propagation of an arteriovascular pressure gradient that further increases the hydraulic pressure in veins and amplifies the capillary filtration in bone [8-10]. Meanwhile, increased vessel pressure can directly increase ImP within the marrow cavity and further drives BFF [11].

The study in Chapter 3 of this dissertation demonstrated the ability of oscillatory DHS to isolate ImP from bone strain in a rodent model. It was indicated that oscillatory DHS was able to generate local ImP in bone with simultaneously minimal bone strain. The observed ImP inductions in response to DHS were in a nonlinear fashion over the loading spectrum between 0.5 Hz and 10 Hz, in which peaked at 2 Hz. The direct tibial ImP measurements between DHS loading at 1.5 Hz and 5 Hz showed significant increases compared to the baseline level. The effective DHS-driven ImP inductions were at a relatively lower frequency range. The loads at high frequencies could be quickly damped because of the characteristics of tissue material, e.g., viscoelastic nature of the surrounding soft tissues. The direct bone fluid coupling through DHS

may influence bone adaptation in a physiological frequency range, where normal heart rate is 360 times per minute (~6 Hz). Based on these results, DHS was suggested to have potential to produce high dynamic fluid pressure within the local bone marrow cavity. As one of the key determinants of BFF, oscillatory DHS-induced fluid pressure (ImP) in bone, if loaded at optimal frequencies, may serve strong potentials in attenuating disuse bone loss.

To evaluate the effects of DHS on mitigation of trabecular bone loss, a DHS protocol was designed to apply this novel modality with the optimized frequency of 2 Hz to the *in vivo* hindlimb suspended rats for 4 weeks (Chapter 4). DHS loading at frequency of 2 Hz was successful to attenuate disuse trabecular bone loss under such disuse condition, in which trabecular bone BV/TV in the tibia was increased by 83% compared to HLS. This *in vivo* study suggested strong phenotypic bone adaptation in response to DHS, indicating the effectiveness of this non-invasive modality as a novel countermeasure for disuse osteoporosis/osteopenia in rats. By circular dynamic compressions around the diaphysis region of the loaded bone, DHS was able to exert its anabolic/anti-catabolic effects to the trabecular bone within the metaphyseal region. This strongly supports the ImP-induced BFF mechanism. The trabecular network with high surface area exposes to the altered fluid pressure, leading to the responsive adaptation of the trabecular bone to DHS.

Loading frequency is one of the parameters determining effective bone adaptation to mechanical loading. Various studies have demonstrated a positive correlation between them [128-130], which was shown in a nonlinear relationship [145, 146, 153, 154]. Furthermore, various loading modalities seem to have different effective loading frequencies [74, 128, 129]. Higher frequencies (>30 Hz) are more effective for whole-body vibrations. However, ulna axial loading on mice was more responsive to lower frequencies (5 Hz and 10 Hz) [69]. Similarly,

relatively lower frequencies (5 Hz and/or 10 Hz) were found to be effective in BFF-induced bone adaptation in the femur [83] and tibia [74], respectively. While it is important to select an optimal loading regimen with the best loading frequency specific to the modality, one limitation of this study is that various frequencies were not tested in the *in vivo* experiment (Chapter 4) to discover the highest skeletal adaptive response. Moreover, parameters such as loading magnitude and duration can also be included to define the most optimal loading regime of DHS in bone.

The exciting interventional aspect of DHS is that its oscillatory signals can non-invasively induce ImP with minimal bone deformation. Direct bone strain measurements in Chapter 3 showed a <8 με of bone strain at all loading frequencies of oscillatory DHS. Although previous studies have used various methods to isolate the ImP and bone strain factors *in vivo* [82, 83], this present investigation introduced a non-invasive *in vivo* loading method to successfully eliminate bone deformation. Furthermore, the site-specific effect of DHS was demonstrated, in which DHS only induced ImP of the stimulated bone but not others simultaneously.

To further delineate the downstream cellular and molecular mechanisms of DHS in bone adaptation, longitudinal studies were conducted to evaluate the bone marrow MSC population and expressions of osteogenesis-related genes in response to DHS, which were described in Chapter 5 and Chapter 6, respectively. These two studies indicated a time-dependent manner of induced MSC proliferation and amplified mRNA levels of the selected genes upon DHS. These cellular and molecular events contribute greatly to the DHS-induced phenotypic change in bone.

The growth potential and osteogenic potential of MSC respond greatly to their mechanical environment. While bone formation is initiated with stem cell proliferation and condensation [86, 87], changes in the mechanical environment, e.g., through low magnitude mechanical signals, can potentiate the number of bone marrow MSCs. Further, these mechanical

signals bias the MSC differentiation toward osteoblastogenesis, and subsequently promote bone formation [101]. Results from Chapter 5 of this dissertation showed that DHS, as a low-magnitude external mechanical loading, could serve a great potential to encounter bone marrow MSC reduction due to disuse. Changes in perfusion pressure, which is associated with increased blood flow to the limbs, may act upon DHS [165], mediating BFF that alters the bone marrow mechanical environment of MSCs and then further leads to the osteogenic gene expressions [166].

Therefore, the study in Chapter 6 aimed to delineate the underlying molecular mechanism in bone in response to the mechanical signals derived from DHS. The alterations of the gene expressions of osteogenic growth factors and transcription factors were measured. Similar to the MSC study, the longitudinal real-time PCR analysis of the selected osteogenesis-related genes showed a time-dependent fashion over the 21-day time course. Together with the observations from the induced bone marrow MSC proliferation, it is believed that the external DHS loading can directly couple with ImP-regulated BFF, which then regulates MSC proliferation and differentiation toward osteoblastogenesis. These are crucial events prior to the phenotypic changes in bone tissue, which were observed by day 28 [127]. Furthermore, the observations over time signified the sequence of the events including MSC proliferation, osteogenic differentiation, and phenotypic bone formation. Combining the data from Chapters 4, 5, and 6 of this dissertation, it is suggested that the MSC proliferation process started from day 7 and peaked on day 14, followed by osteogenic differentiation that may start between day 7 to day 14 and peaked on day 14. Both of these events started to diminish by day 21, which was the most likely time point that the phenotypic bone formation begun (observed by day 28). These step-wise and highly coordinated activities may eventually contribute to the phenotypic changes in bone tissue.

Future studies may include more close time points to evaluate the detailed sequence of cellular and molecular events underlying the bone adaptation in response to DHS. Other cellular analysis, such as *ex vivo* MSC differentiation experiments, may also be included. Furthermore, the positive effects of DHS on bone, whether it is due to increased anabolic or decreased catabolic regulations, have not been fully dissected. Further molecular studies may look into osteoclastogenesis related genes.

The signal transduction pathways activated by mechanical stimuli are known as complex events (Figure 1.5). It would be a great value to pursue a future investigation to further delineate the underlying signal transduction pathways activated by the mechanical signals derived from DHS. As indicated by the results from Chapter 6, genes of growth factors including VEGF, BMP2, IGF-1, and TGF-β were expressed in response to DHS. It would then be interesting to further delineate the signaling pathways that are downstream of their receptors upon DHS loading. Studies using various types of mechanical loadings have shown the involvements of these signaling pathways. *In vitro* mechanical stimulation enhanced the pro-angiogenic capacity of early human haematomas, which is crucial for bone healing and dependent on VEGF signaling [186]. Coordinated BMP2 signaling and mechanical forces were shown to affect efficient osteogenic differentiation [187]. IGF-1 receptor signaling in osteoblasts was enhanced by mechanical loading of fluid shear stress, which was found to be in a PKCzeta-dependent manner [188]. Through PI3K/Akt, Bcl-2, and phospho-Bad signaling, TGF-β was found to prevent skeletal unloading-induced osteoblast apoptosis. Together, signaling pathways of VEGF, BMP2, IGF-1, and TGF-β serve great potentials to transduce the mechanical signals to activate osteoblastic gene expressions. Future studies may extend the investigation into these molecular events under DHS.

As novel modalities with strong translational potential to prevent osteoporosis are urgently called for, direct ImP-coupled BFF can provide new insights to develop non-pharmacological treatments for osteopenia/osteoporosis. This dissertation introduced a novel, non-invasive oscillatory DHS that was shown to be able to induce ImP with minimal bone deformation. The promising effects of DHS on mitigation of trabecular bone loss were demonstrated in a rat functional disuse model. Oscillatory DHS may regulate the tissue fluid dynamics, which serves critically in bone adaptation. The further longitudinal evaluations on bone marrow MSC population and osteogenic gene expressions outlined the cellular and molecular mechanisms underlying DHS, which may contribute greatly to the phenotypic bone formation. Therefore, DHS not only provides significant insights for future clinical applications, but can also serve as an ideal tool to delineate the complex mechanotransductive mechanisms in the skeleton.

References

1. Clarke, B., *Normal bone anatomy and physiology.* Clin J Am Soc Nephrol, 2008. **3 Suppl 3**: p. S131-9.
2. Kelly, P.J., *Anatomy, physiology, and pathology of the blood supply of bones.* J Bone Joint Surg Am, 1968. **50**(4): p. 766-83.
3. Aarden, E.M., E.H. Burger, and P.J. Nijweide, *Function of osteocytes in bone.* J Cell Biochem, 1994. **55**(3): p. 287-99.
4. Raisz, L.G., *Physiology and pathophysiology of bone remodeling.* Clin Chem, 1999. **45**(8 Pt 2): p. 1353-8.
5. *Disturbed balance in bone remodeling*. Available from: http://www.roche.com/pages/facets/11/ostedefe.htm.
6. Fritton, S.P. and S. Weinbaum, *Fluid and Solute Transport in Bone: Flow-Induced Mechanotransduction.* Annu Rev Fluid Mech, 2009. **41**: p. 347-374.
7. Rubin, C.T., K.J. McLeod, and S.D. Bain, *Functional strains and cortical bone adaptation: epigenetic assurance of skeletal integrity.* J Biomech, 1990. **23 Suppl 1**: p. 43-54.
8. Winet, H., *A bone fluid flow hypothesis for muscle pump-driven capillary filtration: II. Proposed role for exercise in erodible scaffold implant incorporation.* Eur Cell Mater, 2003. **6**: p. 1-10; discussion 10-1.
9. Otter, M.W., et al., *Does bone perfusion/reperfusion initiate bone remodeling and the stress fracture syndrome?* Med Hypotheses, 1999. **53**(5): p. 363-8.
10. Laughlin, M.H., *The muscle pump: what question do we want to answer?* J Appl Physiol, 2005. **99**(2): p. 774.

11. Qin, Y.X., et al., *Dynamic skeletal muscle stimulation and its potential in bone adaptation.* J Musculoskelet Neuronal Interact, 2010. **10**(1): p. 12-24.

12. *Osteoporosis prevention, diagnosis, and therapy.* NIH Consens Statement, 2000. **17**(1): p. 1-45.

13. Aaseth, J., G. Boivin, and O. Andersen, *Osteoporosis and trace elements--an overview.* J Trace Elem Med Biol, 2012. **26**(2-3): p. 149-52.

14. Reginster, J.Y. and N. Burlet, *Osteoporosis: a still increasing prevalence.* Bone, 2006. **38**(2 Suppl 1): p. S4-9.

15. Riggs, B.L. and L.J. Melton, 3rd, *The worldwide problem of osteoporosis: insights afforded by epidemiology.* Bone, 1995. **17**(5 Suppl): p. 505S-511S.

16. *NIH Consensus Development Panel on Osteoporosis Prevention, Diagnosis, and Therapy, March 7-29, 2000: highlights of the conference.* South Med J, 2001. **94**(6): p. 569-73.

17. Becker, D.J., M.L. Kilgore, and M.A. Morrisey, *The societal burden of osteoporosis.* Curr Rheumatol Rep, 2010. **12**(3): p. 186-91.

18. Schwab, P. and R.F. Klein, *Nonpharmacological approaches to improve bone health and reduce osteoporosis.* Curr Opin Rheumatol, 2008. **20**(2): p. 213-7.

19. Lau, R.Y. and X. Guo, *A review on current osteoporosis research: with special focus on disuse bone loss.* J Osteoporos, 2011. **2011**: p. 293808.

20. Lewiecki, E.M. and J.L. Borges, *Bone density testing in clinical practice.* Arq Bras Endocrinol Metabol, 2006. **50**(4): p. 586-95.

21. Seeman, E. and J.A. Eisman, *7: Treatment of osteoporosis: why, whom, when and how to treat. The single most important consideration is the individual's absolute risk of fracture.* Med J Aust, 2004. **180**(6): p. 298-303.

22. Ullom-Minnich, P., *Prevention of osteoporosis and fractures.* Am Fam Physician, 1999. **60**(1): p. 194-202.

23. Mitchner, N.A. and S.T. Harris, *Current and emerging therapies for osteoporosis.* J Fam Pract, 2009. **58**(7 Suppl Osteoporosis): p. S45-9.

24. Fritton, S.P., K.J. McLeod, and C.T. Rubin, *Quantifying the strain history of bone: spatial uniformity and self-similarity of low-magnitude strains.* J Biomech, 2000. **33**(3): p. 317-25.

25. Rubin, C.T., *Skeletal strain and the functional significance of bone architecture.* Calcif Tissue Int, 1984. **36 Suppl 1**: p. S11-8.

26. Rubin, C.T., et al., *Inhibition of osteopenia by low magnitude, high-frequency mechanical stimuli.* Drug Discov Today, 2001. **6**(16): p. 848-858.

27. Rubin, C., S. Judex, and Y.X. Qin, *Low-level mechanical signals and their potential as a non-pharmacological intervention for osteoporosis.* Age Ageing, 2006. **35 Suppl 2**: p. ii32-ii36.

28. Buckwalter, J.A. and R.R. Cooper, *Bone structure and function.* Instr Course Lect, 1987. **36**: p. 27-48.

29. Duan, Y., et al., *Structural and biomechanical basis of sexual dimorphism in femoral neck fragility has its origins in growth and aging.* J Bone Miner Res, 2003. **18**(10): p. 1766-74.

30. Khosla, S., et al., *Relationship of serum sex steroid levels to longitudinal changes in bone density in young versus elderly men.* J Clin Endocrinol Metab, 2001. **86**(8): p. 3555-61.

31. Modlesky, C.M., et al., *Trabecular bone microarchitecture is deteriorated in men with spinal cord injury.* J Bone Miner Res, 2004. **19**(1): p. 48-55.

32. Riggs, B.L., S. Khosla, and L.J. Melton, 3rd, *A unitary model for involutional osteoporosis: estrogen deficiency causes both type I and type II osteoporosis in postmenopausal women and contributes to bone loss in aging men.* J Bone Miner Res, 1998. **13**(5): p. 763-73.

33. Robling, A.G., A.B. Castillo, and C.H. Turner, *Biomechanical and molecular regulation of bone remodeling.* Annu Rev Biomed Eng, 2006. **8**: p. 455-98.

34. McCarthy, I., *The physiology of bone blood flow: a review.* J Bone Joint Surg Am, 2006. **88 Suppl 3**: p. 4-9.

35. de Saint-Georges, L. and S.C. Miller, *The microcirculation of bone and marrow in the diaphysis of the rat hemopoietic long bones.* Anat Rec, 1992. **233**(2): p. 169-77.

36. Collin-Osdoby, P., *Role of vascular endothelial cells in bone biology.* J Cell Biochem, 1994. **55**(3): p. 304-9.

37. Parfitt, A.M., *The mechanism of coupling: a role for the vasculature.* Bone, 2000. **26**(4): p. 319-23.

38. Villanueva, J.E. and M.E. Nimni, *Promotion of calvarial cell osteogenesis by endothelial cells.* J Bone Miner Res, 1990. **5**(7): p. 733-9.

39. Gerber, H.P., et al., *VEGF couples hypertrophic cartilage remodeling, ossification and angiogenesis during endochondral bone formation.* Nat Med, 1999. **5**(6): p. 623-8.

40. Dudley-Javoroski, S. and R.K. Shields, *Muscle and bone plasticity after spinal cord injury: review of adaptations to disuse and to electrical muscle stimulation.* J Rehabil Res Dev, 2008. **45**(2): p. 283-96.

41. Lazo, M.G., et al., *Osteoporosis and risk of fracture in men with spinal cord injury.* Spinal Cord, 2001. **39**(4): p. 208-14.

42. Vestergaard, P., et al., *Fracture rates and risk factors for fractures in patients with spinal cord injury.* Spinal Cord, 1998. **36**(11): p. 790-6.

43. Eser, P., et al., *Relationship between the duration of paralysis and bone structure: a pQCT study of spinal cord injured individuals.* Bone, 2004. **34**(5): p. 869-80.

44. Frey-Rindova, P., et al., *Bone mineral density in upper and lower extremities during 12 months after spinal cord injury measured by peripheral quantitative computed tomography.* Spinal Cord, 2000. **38**(1): p. 26-32.

45. Heaney, R.P., *Pathophysiology of osteoporosis.* Endocrinol Metab Clin North Am, 1998. **27**(2): p. 255-65.

46. Ingram, R.R., R.K. Suman, and P.A. Freeman, *Lower limb fractures in the chronic spinal cord injured patient.* Paraplegia, 1989. **27**(2): p. 133-9.

47. Szollar, S.M., et al., *Bone mineral density and indexes of bone metabolism in spinal cord injury.* Am J Phys Med Rehabil, 1998. **77**(1): p. 28-35.

48. Holick, M.F., *Perspective on the impact of weightlessness on calcium and bone metabolism.* Bone, 1998. **22**(5 Suppl): p. 105S-111S.

49. Vico, L., et al., *Effects of long-term microgravity exposure on cancellous and cortical weight-bearing bones of cosmonauts.* Lancet, 2000. **355**(9215): p. 1607-11.

50. Lang, T.F., et al., *Adaptation of the proximal femur to skeletal reloading after long-duration spaceflight.* J Bone Miner Res, 2006. **21**(8): p. 1224-30.

51. Lang, T., et al., *Cortical and trabecular bone mineral loss from the spine and hip in long-duration spaceflight.* J Bone Miner Res, 2004. **19**(6): p. 1006-12.

52. Collet, P., et al., *Effects of 1- and 6-month spaceflight on bone mass and biochemistry in two humans.* Bone, 1997. **20**(6): p. 547-51.

53. Wilmet, E., et al., *Longitudinal study of the bone mineral content and of soft tissue composition after spinal cord section.* Paraplegia, 1995. **33**(11): p. 674-7.

54. Morey-Holton, E.R. and R.K. Globus, *Hindlimb unloading of growing rats: a model for predicting skeletal changes during space flight.* Bone, 1998. **22**(5 Suppl): p. 83S-88S.

55. Morey-Holton, E.R. and R.K. Globus, *Hindlimb unloading rodent model: technical aspects.* J Appl Physiol, 2002. **92**(4): p. 1367-77.

56. Cann, C.E. and R.R. Adachi, *Bone resorption and mineral excretion in rats during spaceflight.* Am J Physiol, 1983. **244**(3): p. R327-31.

57. Jee, W.S., et al., *Effects of spaceflight on trabecular bone in rats.* Am J Physiol, 1983. **244**(3): p. R310-4.

58. Vico, L., et al., *Histomorphometric analyses of cancellous bone from COSMOS 2044 rats.* J Appl Physiol, 1993. **75**(5): p. 2203-8.

59. Morey-Holton, E., et al., *The hindlimb unloading rat model: literature overview, technique update and comparison with space flight data.* Adv Space Biol Med, 2005. **10**: p. 7-40.

60. Lafage-Proust, M.H., et al., *Space-related bone mineral redistribution and lack of bone mass recovery after reambulation in young rats.* Am J Physiol, 1998. **274**(2 Pt 2): p. R324-34.

61. Allen, M.R. and S.A. Bloomfield, *Hindlimb unloading has a greater effect on cortical compared with cancellous bone in mature female rats.* J Appl Physiol, 2003. **94**(2): p. 642-50.

62. Bloomfield, S.A., et al., *Site- and compartment-specific changes in bone with hindlimb unloading in mature adult rats.* Bone, 2002. **31**(1): p. 149-57.

63. David, V., et al., *Two-week longitudinal survey of bone architecture alteration in the hindlimb-unloaded rat model of bone loss: sex differences.* Am J Physiol Endocrinol Metab, 2006. **290**(3): p. E440-7.

64. Sessions, N.D., et al., *Bone response to normal weight bearing after a period of skeletal unloading.* Am J Physiol, 1989. **257**(4 Pt 1): p. E606-10.

65. Hefferan, T.E., et al., *Effect of gender on bone turnover in adult rats during simulated weightlessness.* J Appl Physiol, 2003. **95**(5): p. 1775-80.

66. Pedersen, E.A., et al., *Bone response to in vivo mechanical loading in C3H/HeJ mice.* Calcif Tissue Int, 1999. **65**(1): p. 41-6.

67. Kameyama, Y., et al., *Bone response to mechanical loading in adult rats with collagen-induced arthritis.* Bone, 2004. **35**(4): p. 948-56.

68. Li, J., D.B. Burr, and C.H. Turner, *Suppression of prostaglandin synthesis with NS-398 has different effects on endocortical and periosteal bone formation induced by mechanical loading.* Calcif Tissue Int, 2002. **70**(4): p. 320-9.

69. Warden, S.J. and C.H. Turner, *Mechanotransduction in the cortical bone is most efficient at loading frequencies of 5-10 Hz.* Bone, 2004. **34**(2): p. 261-70.

70. Hsieh, Y.F., et al., *Mechanical loading of diaphyseal bone in vivo: the strain threshold for an osteogenic response varies with location.* J Bone Miner Res, 2001. **16**(12): p. 2291-7.

71. Tanaka, S.M., H.B. Sun, and H. Yokota, *Bone formation induced by a novel form of mechanical loading on joint tissue.* Biol Sci Space, 2004. **18**(2): p. 41-4.

72. Yokota, H. and S.M. Tanaka, *Osteogenic potentials with joint-loading modality.* J Bone Miner Metab, 2005. **23**(4): p. 302-8.

73. Zhang, P., et al., *Knee loading dynamically alters intramedullary pressure in mouse femora.* Bone, 2007. **40**(2): p. 538-43.

74. Zhang, P., et al., *Frequency-dependent enhancement of bone formation in murine tibiae and femora with knee loading.* J Bone Miner Metab, 2007. **25**(6): p. 383-91.

75. Lam, H. and Y.X. Qin, *The effects of frequency-dependent dynamic muscle stimulation on inhibition of trabecular bone loss in a disuse model.* Bone, 2008. **43**(6): p. 1093-100.

76. Pollack, S.R., et al., *Stress-generated potentials in bone: effects of collagen modifications.* J Biomed Mater Res, 1977. **11**(5): p. 677-70.

77. Montgomery, R.J., et al., *Interstitial fluid flow in cortical bone.* Microvasc Res, 1988. **35**(3): p. 295-307.

78. Reich, K.M., C.V. Gay, and J.A. Frangos, *Fluid shear stress as a mediator of osteoblast cyclic adenosine monophosphate production.* J Cell Physiol, 1990. **143**(1): p. 100-4.

79. Rubin, J., et al., *Pressure regulates osteoclast formation and MCSF expression in marrow culture.* J Cell Physiol, 1997. **170**(1): p. 81-7.

80. Jacobs, C.R., et al., *Differential effect of steady versus oscillating flow on bone cells.* J Biomech, 1998. **31**(11): p. 969-76.

81. Burger, E.H. and J. Klein-Nulend, *Mechanotransduction in bone--role of the lacuno-canalicular network.* FASEB J, 1999. **13 Suppl**: p. S101-12.

82. Qin, Y.X., et al., *Fluid pressure gradients, arising from oscillations in intramedullary pressure, is correlated with the formation of bone and inhibition of intracortical porosity.* J Biomech, 2003. **36**(10): p. 1427-37.

83. Kwon, R.Y., et al., *Microfluidic enhancement of intramedullary pressure increases interstitial fluid flow and inhibits bone loss in hindlimb suspended mice.* J Bone Miner Res, 2010. **25**(8): p. 1798-807.

84. Qin, Y.X. and H. Lam, *Intramedullary pressure and matrix strain induced by oscillatory skeletal muscle stimulation and its potential in adaptation.* J Biomech, 2009. **42**(2): p. 140-5.

85. Lu, X., S. Li, and J. Cheng, *[Bone marrow mesenchymal stem cells: progress in bone/cartilage defect repair]*. Sheng Wu Yi Xue Gong Cheng Xue Za Zhi, 2002. **19**(1): p. 135-9.

86. Karsenty, G. and E.F. Wagner, *Reaching a genetic and molecular understanding of skeletal development.* Dev Cell, 2002. **2**(4): p. 389-406.

87. Kelly, D.J. and C.R. Jacobs, *The role of mechanical signals in regulating chondrogenesis and osteogenesis of mesenchymal stem cells.* Birth Defects Res C Embryo Today, 2010. **90**(1): p. 75-85.

88. Cheng, S.L., et al., *MSX2 promotes osteogenesis and suppresses adipogenic differentiation of multipotent mesenchymal progenitors.* J Biol Chem, 2003. **278**(46): p. 45969-77.

89. David, V., et al., *Mechanical loading down-regulates peroxisome proliferator-activated receptor gamma in bone marrow stromal cells and favors osteoblastogenesis at the expense of adipogenesis.* Endocrinology, 2007. **148**(5): p. 2553-62.

90. Krishnan, V., H.U. Bryant, and O.A. Macdougald, *Regulation of bone mass by Wnt signaling.* J Clin Invest, 2006. **116**(5): p. 1202-9.

91. Menuki, K., et al., *Climbing exercise enhances osteoblast differentiation and inhibits adipogenic differentiation with high expression of PTH/PTHrP receptor in bone marrow cells.* Bone, 2008. **43**(3): p. 613-20.

92. Akune, T., et al., *PPARgamma insufficiency enhances osteogenesis through osteoblast formation from bone marrow progenitors.* J Clin Invest, 2004. **113**(6): p. 846-55.

93. Castillo, A.B. and C.R. Jacobs, *Mesenchymal stem cell mechanobiology.* Curr Osteoporos Rep, 2010. **8**(2): p. 98-104.

94. Holtorf, H.L., J.A. Jansen, and A.G. Mikos, *Flow perfusion culture induces the osteoblastic differentiation of marrow stroma cell-scaffold constructs in the absence of dexamethasone.* J Biomed Mater Res A, 2005. **72**(3): p. 326-34.

95. Datta, N., et al., *In vitro generated extracellular matrix and fluid shear stress synergistically enhance 3D osteoblastic differentiation.* Proc Natl Acad Sci U S A, 2006. **103**(8): p. 2488-93.

96. Bjerre, L., et al., *Flow perfusion culture of human mesenchymal stem cells on silicate-substituted tricalcium phosphate scaffolds.* Biomaterials, 2008. **29**(17): p. 2616-27.

97. Duty, A.O., M.E. Oest, and R.E. Guldberg, *Cyclic mechanical compression increases mineralization of cell-seeded polymer scaffolds in vivo.* J Biomech Eng, 2007. **129**(4): p. 531-9.

98. Emans, P.J., et al., *Differential cell viability of chondrocytes and progenitor cells in tissue-engineered constructs following implantation into osteochondral defects.* Tissue Eng, 2006. **12**(6): p. 1699-709.

99. LeBaron, R.G. and K.A. Athanasiou, *Ex vivo synthesis of articular cartilage.* Biomaterials, 2000. **21**(24): p. 2575-87.

100. Bryant, S.J., et al., *Crosslinking density influences chondrocyte metabolism in dynamically loaded photocrosslinked poly(ethylene glycol) hydrogels.* Ann Biomed Eng, 2004. **32**(3): p. 407-17.

101. Luu, Y.K., et al., *Mechanical stimulation of mesenchymal stem cell proliferation and differentiation promotes osteogenesis while preventing dietary-induced obesity.* J Bone Miner Res, 2009. **24**(1): p. 50-61.

102. Sen, B., et al., *Mechanical signal influence on mesenchymal stem cell fate is enhanced by incorporation of refractory periods into the loading regimen.* J Biomech, 2011. **44**(4): p. 593-9.

103. Sen, B., et al., *Mechanical strain inhibits adipogenesis in mesenchymal stem cells by stimulating a durable beta-catenin signal.* Endocrinology, 2008. **149**(12): p. 6065-75.

104. Patel, M.J., et al., *Identification of mechanosensitive genes in osteoblasts by comparative microarray studies using the rotating wall vessel and the random positioning machine.* J Cell Biochem, 2007. **101**(3): p. 587-99.

105. Pardo, S.J., et al., *Simulated microgravity using the Random Positioning Machine inhibits differentiation and alters gene expression profiles of 2T3 preosteoblasts.* Am J Physiol Cell Physiol, 2005. **288**(6): p. C1211-21.

106. Carmeliet, G., et al., *Gene expression related to the differentiation of osteoblastic cells is altered by microgravity.* Bone, 1998. **22**(5 Suppl): p. 139S-143S.

107. Zayzafoon, M., W.E. Gathings, and J.M. McDonald, *Modeled microgravity inhibits osteogenic differentiation of human mesenchymal stem cells and increases adipogenesis.* Endocrinology, 2004. **145**(5): p. 2421-32.

108. Visigalli, D., et al., *Hind limb unloading of mice modulates gene expression at the protein and mRNA level in mesenchymal bone cells.* BMC Musculoskelet Disord, 2010. **11**: p. 147.

109. Pan, Z., et al., *Effects of hindlimb unloading on ex vivo growth and osteogenic/adipogenic potentials of bone marrow-derived mesenchymal stem cells in rats.* Stem Cells Dev, 2008. **17**(4): p. 795-804.

110. Papachristou, D.J., et al., *Signaling networks and transcription factors regulating mechanotransduction in bone.* Bioessays, 2009. **31**(7): p. 794-804.

111. Huang, H., R.D. Kamm, and R.T. Lee, *Cell mechanics and mechanotransduction: pathways, probes, and physiology.* Am J Physiol Cell Physiol, 2004. **287**(1): p. C1-11.

112. Iqbal, J. and M. Zaidi, *Molecular regulation of mechanotransduction.* Biochem Biophys Res Commun, 2005. **328**(3): p. 751-5.

113. Liedert, A., et al., *Signal transduction pathways involved in mechanotransduction in bone cells.* Biochem Biophys Res Commun, 2006. **349**(1): p. 1-5.

114. Schriefer, J.L., et al., *Cellular accommodation and the response of bone to mechanical loading.* J Biomech, 2005. **38**(9): p. 1838-45.

115. Ng, A.F., et al., *Factors regulating condylar cartilage growth under repeated load application.* Front Biosci, 2006. **11**: p. 949-54.

116. Papachroni, K.K., et al., *Mechanotransduction in osteoblast regulation and bone disease.* Trends Mol Med, 2009. **15**(5): p. 208-16.

117. Bikle, D.D., *Integrins, insulin like growth factors, and the skeletal response to load.* Osteoporos Int, 2008. **19**(9): p. 1237-46.

118. Zelzer, E. and B.R. Olsen, *Multiple roles of vascular endothelial growth factor (VEGF) in skeletal development, growth, and repair.* Curr Top Dev Biol, 2005. **65**: p. 169-87.

119. Lieberman, J.R., A. Daluiski, and T.A. Einhorn, *The role of growth factors in the repair of bone. Biology and clinical applications.* J Bone Joint Surg Am, 2002. **84-A**(6): p. 1032-44.

120. Zhang, R.W., et al., *Contribution of marrow stromal cells to the regulation of osteoblast proliferation in rats: evidence for the involvement of insulin-like growth factors.* Bone Miner, 1991. **13**(3): p. 201-15.

121. Gautschi, O.P., S.P. Frey, and R. Zellweger, *Bone morphogenetic proteins in clinical applications.* ANZ J Surg, 2007. **77**(8): p. 626-31.

122. Harada, S. and G.A. Rodan, *Control of osteoblast function and regulation of bone mass.* Nature, 2003. **423**(6937): p. 349-55.

123. Ziros, P.G., E.K. Basdra, and A.G. Papavassiliou, *Runx2: of bone and stretch.* Int J Biochem Cell Biol, 2008. **40**(9): p. 1659-63.

124. Marie, P.J., *Transcription factors controlling osteoblastogenesis.* Arch Biochem Biophys, 2008. **473**(2): p. 98-105.

125. Ishijima, M., et al., *Resistance to unloading-induced three-dimensional bone loss in osteopontin-deficient mice.* J Bone Miner Res, 2002. **17**(4): p. 661-7.

126. Xie, L., C. Rubin, and S. Judex, *Enhancement of the adolescent murine musculoskeletal system using low-level mechanical vibrations.* J Appl Physiol, 2008. **104**(4): p. 1056-62.

127. Hu, M., J. Cheng, and Y.X. Qin, *Dynamic hydraulic flow stimulation on mitigation of trabecular bone loss in a rat functional disuse model.* Bone, 2012. **51**(4): p. 819-25.

128. Turner, C.H., I. Owan, and Y. Takano, *Mechanotransduction in bone: role of strain rate.* Am J Physiol, 1995. **269**(3 Pt 1): p. E438-42.

129. Hsieh, Y.F. and C.H. Turner, *Effects of loading frequency on mechanically induced bone formation.* J Bone Miner Res, 2001. **16**(5): p. 918-24.

130. Rubin, C.T. and K.J. McLeod, *Promotion of bony ingrowth by frequency-specific, low-amplitude mechanical strain.* Clin Orthop Relat Res, 1994(298): p. 165-74.

131. Wang, L., et al., *On bone adaptation due to venous stasis.* J Biomech, 2003. **36**(10): p. 1439-51.

132. Wang, L., et al., *Delineating bone's interstitial fluid pathway in vivo.* Bone, 2004. **34**(3): p. 499-509.

133. Stevens, H.Y., D.R. Meays, and J.A. Frangos, *Pressure gradients and transport in the murine femur upon hindlimb suspension.* Bone, 2006. **39**(3): p. 565-72.

134. Valic, Z., J.B. Buckwalter, and P.S. Clifford, *Muscle blood flow response to contraction: influence of venous pressure.* J Appl Physiol, 2005. **98**(1): p. 72-6.

135. Sornay-Rendu, E., et al., *Cortical and trabecular architecture are altered in postmenopausal women with fractures.* Osteoporos Int, 2009. **20**(8): p. 1291-7.

136. Cowin, S.C., *Wolff's law of trabecular architecture at remodeling equilibrium.* J Biomech Eng, 1986. **108**(1): p. 83-8.

137. Rubin, C., et al., *Prevention of postmenopausal bone loss by a low-magnitude, high-frequency mechanical stimuli: a clinical trial assessing compliance, efficacy, and safety.* J Bone Miner Res, 2004. **19**(3): p. 343-51.

138. Nilsson, B.E. and N.E. Westlin, *Bone density in athletes.* Clin Orthop Relat Res, 1971. **77**: p. 179-82.

139. Jones, H.H., et al., *Humeral hypertrophy in response to exercise.* J Bone Joint Surg Am, 1977. **59**(2): p. 204-8.

140. Judex, S. and R.F. Zernicke, *High-impact exercise and growing bone: relation between high strain rates and enhanced bone formation.* J Appl Physiol, 2000. **88**(6): p. 2183-91.

141. Donaldson, C.L., et al., *Effect of prolonged bed rest on bone mineral.* Metabolism, 1970. **19**(12): p. 1071-84.

142. Rubin, C.T. and L.E. Lanyon, *Kappa Delta Award paper. Osteoregulatory nature of mechanical stimuli: function as a determinant for adaptive remodeling in bone.* J Orthop Res, 1987. **5**(2): p. 300-10.

143. Sugiyama, T., et al., *Mechanical loading enhances the anabolic effects of intermittent parathyroid hormone (1-34) on trabecular and cortical bone in mice.* Bone, 2008. **43**(2): p. 238-48.

144. Judex, S., S. Gupta, and C. Rubin, *Regulation of mechanical signals in bone.* Orthod Craniofac Res, 2009. **12**(2): p. 94-104.

145. Rubin, C., et al., *Anabolism. Low mechanical signals strengthen long bones.* Nature, 2001. **412**(6847): p. 603-4.

146. Xie, L., et al., *Low-level mechanical vibrations can influence bone resorption and bone formation in the growing skeleton.* Bone, 2006. **39**(5): p. 1059-66.

147. Bloomfield, S.A., *Cellular and molecular mechanisms for the bone response to mechanical loading.* Int J Sport Nutr Exerc Metab, 2001. **11 Suppl**: p. S128-36.

148. Chow, J.W., *Role of nitric oxide and prostaglandins in the bone formation response to mechanical loading.* Exerc Sport Sci Rev, 2000. **28**(4): p. 185-8.

149. Rubin, J., C. Rubin, and C.R. Jacobs, *Molecular pathways mediating mechanical signaling in bone.* Gene, 2006. **367**: p. 1-16.

150. Qin, Y.X., W. Lin, and C. Rubin, *The pathway of bone fluid flow as defined by in vivo intramedullary pressure and streaming potential measurements.* Ann Biomed Eng, 2002. **30**(5): p. 693-702.

151. Johnson, D.L., T.N. McAllister, and J.A. Frangos, *Fluid flow stimulates rapid and continuous release of nitric oxide in osteoblasts.* Am J Physiol, 1996. **271**(1 Pt 1): p. E205-8.

152. Kasten, T.P., et al., *Potentiation of osteoclast bone-resorption activity by inhibition of nitric oxide synthase.* Proc Natl Acad Sci U S A, 1994. **91**(9): p. 3569-73.

153. Midura, R.J., C.J. Dillman, and M.D. Grabiner, *Low amplitude, high frequency strains imposed by electrically stimulated skeletal muscle retards the development of osteopenia in the tibiae of hindlimb suspended rats.* Med Eng Phys, 2005. **27**(4): p. 285-93.

154. Qin, Y.X., C.T. Rubin, and K.J. McLeod, *Nonlinear dependence of loading intensity and cycle number in the maintenance of bone mass and morphology.* J Orthop Res, 1998. **16**(4): p. 482-9.

155. Turner, A.S., *Animal models of osteoporosis--necessity and limitations.* Eur Cell Mater, 2001. **1**: p. 66-81.

156. Garnero, P. and P.D. Delmas, *Contribution of bone mineral density and bone turnover markers to the estimation of risk of osteoporotic fracture in postmenopausal women.* J Musculoskelet Neuronal Interact, 2004. **4**(1): p. 50-63.

157. Zangi, L., et al., *High-yield isolation, expansion, and differentiation of rat bone marrow-derived mesenchymal stem cells with fibrin microbeads.* Tissue Eng, 2006. **12**(8): p. 2343-54.

158. Harting, M., et al., *Immunophenotype characterization of rat mesenchymal stromal cells.* Cytotherapy, 2008. **10**(3): p. 243-53.

159. Wang, C., et al., *[Isolation and culturation, phenotype detection of rat bone marrow mesenchymal stem cells]*. Xi Bao Yu Fen Zi Mian Yi Xue Za Zhi, 2007. **23**(5): p. 466-8.

160. P, M., et al., *Adult mesenchymal stem cells and cell surface characterization - a systematic review of the literature.* Open Orthop J, 2011. **5**(Suppl 2): p. 253-60.

161. Marcus, A.J., et al., *Isolation, characterization, and differentiation of stem cells derived from the rat amniotic membrane.* Differentiation, 2008. **76**(2): p. 130-44.

162. Phinney, D.G., et al., *Donor variation in the growth properties and osteogenic potential of human marrow stromal cells.* J Cell Biochem, 1999. **75**(3): p. 424-36.

163. Barou, O., et al., *Hindlimb unloading in rat decreases preosteoblast proliferation assessed in vivo with BrdU incorporation.* Am J Physiol, 1998. **274**(1 Pt 1): p. E108-14.

164. Basso, N., C.G. Bellows, and J.N. Heersche, *Effect of simulated weightlessness on osteoprogenitor cell number and proliferation in young and adult rats.* Bone, 2005. **36**(1): p. 173-83.

165. Raitakari, M., et al., *Relationship between limb and muscle blood flow in man.* J Physiol, 1996. **496 (Pt 2)**: p. 543-9.

166. Kreke, M.R., W.R. Huckle, and A.S. Goldstein, *Fluid flow stimulates expression of osteopontin and bone sialoprotein by bone marrow stromal cells in a temporally dependent manner.* Bone, 2005. **36**(6): p. 1047-55.

167. Mantila Roosa, S.M., C.H. Turner, and Y. Liu, *Regulatory mechanisms in bone following mechanical loading.* Gene Regul Syst Bio, 2012. **6**: p. 43-53.

168. Zhang, P., C.H. Turner, and H. Yokota, *Joint loading-driven bone formation and signaling pathways predicted from genome-wide expression profiles.* Bone, 2009. **44**(5): p. 989-98.

169. Abdallah, B.M. and M. Kassem, *Human mesenchymal stem cells: from basic biology to clinical applications.* Gene Ther, 2008. **15**(2): p. 109-16.

170. Heino, T.J. and T.A. Hentunen, *Differentiation of osteoblasts and osteocytes from mesenchymal stem cells.* Curr Stem Cell Res Ther, 2008. **3**(2): p. 131-45.

171. Frost, H.M., *Bone's mechanostat: a 2003 update.* Anat Rec A Discov Mol Cell Evol Biol, 2003. **275**(2): p. 1081-101.

172. Neidlinger-Wilke, C., et al., *Human osteoblasts from younger normal and osteoporotic donors show differences in proliferation and TGF beta-release in response to cyclic strain.* J Biomech, 1995. **28**(12): p. 1411-8.

173. Gonzalez, O., et al., *Fluid shear stress magnitude, duration, and total applied load regulate gene expression and nitric oxide production in primary calvarial osteoblast cultures.* Plast Reconstr Surg, 2008. **122**(2): p. 419-28.

174. Sharp, L.A., Y.W. Lee, and A.S. Goldstein, *Effect of low-frequency pulsatile flow on expression of osteoblastic genes by bone marrow stromal cells.* Ann Biomed Eng, 2009. **37**(3): p. 445-53.

175. Hamrick, M.W., et al., *Loss of myostatin (GDF8) function increases osteogenic differentiation of bone marrow-derived mesenchymal stem cells but the osteogenic effect is ablated with unloading.* Bone, 2007. **40**(6): p. 1544-53.

176. Cillo, J.E., Jr., et al., *Growth factor and cytokine gene expression in mechanically strained human osteoblast-like cells: implications for distraction osteogenesis.* Oral Surg Oral Med Oral Pathol Oral Radiol Endod, 2000. **90**(2): p. 147-54.

177. Rath, B., et al., *Compressive forces induce osteogenic gene expression in calvarial osteoblasts.* J Biomech, 2008. **41**(5): p. 1095-103.

178. Thi, M.M., et al., *Fluid shear stress upregulates vascular endothelial growth factor gene expression in osteoblasts.* Ann N Y Acad Sci, 2007. **1117**: p. 73-81.

179. Zhang, P., K. Hamamura, and H. Yokota, *A brief review of bone adaptation to unloading.* Genomics Proteomics Bioinformatics, 2008. **6**(1): p. 4-7.

180. Tang, L.L., C.Y. Xian, and Y.L. Wang, *The MGF expression of osteoblasts in response to mechanical overload.* Arch Oral Biol, 2006. **51**(12): p. 1080-5.

181. Ahdjoudj, S., et al., *Transforming growth factor beta2 inhibits adipocyte differentiation induced by skeletal unloading in rat bone marrow stroma.* J Bone Miner Res, 2002. **17**(4): p. 668-77.

182. Ito, Y. and K. Miyazono, *RUNX transcription factors as key targets of TGF-beta superfamily signaling.* Curr Opin Genet Dev, 2003. **13**(1): p. 43-7.

183. Zhao, G., et al., *Targeted overexpression of insulin-like growth factor I to osteoblasts of transgenic mice: increased trabecular bone volume without increased osteoblast proliferation.* Endocrinology, 2000. **141**(7): p. 2674-82.

184. Duncan, R.L., *Transduction of mechanical strain in bone.* ASGSB Bull, 1995. **8**(2): p. 49-62.

185. Kanno, T., et al., *Mechanical stress-mediated Runx2 activation is dependent on Ras/ERK1/2 MAPK signaling in osteoblasts.* J Cell Biochem, 2007. **101**(5): p. 1266-77.

186. Groothuis, A., et al., *Mechanical stimulation of the pro-angiogenic capacity of human fracture haematoma: involvement of VEGF mechano-regulation.* Bone, 2010. **47**(2): p. 438-44.

187. Kopf, J., et al., *BMP2 and mechanical loading cooperatively regulate immediate early signalling events in the BMP pathway.* BMC Biol, 2012. **10**: p. 37.

188. Triplett, J.W., et al., *Mechanical loading by fluid shear stress enhances IGF-1 receptor signaling in osteoblasts in a PKCzeta-dependent manner.* Mol Cell Biomech, 2007. **4**(1): p. 13-25.